String Stability of Interconnected Vehicles Network-aware Modelling, Analysis & Experiments Sinan Öncü

String Stability of Interconnected Vehicles

Network-aware Modelling, Analysis & Experiments

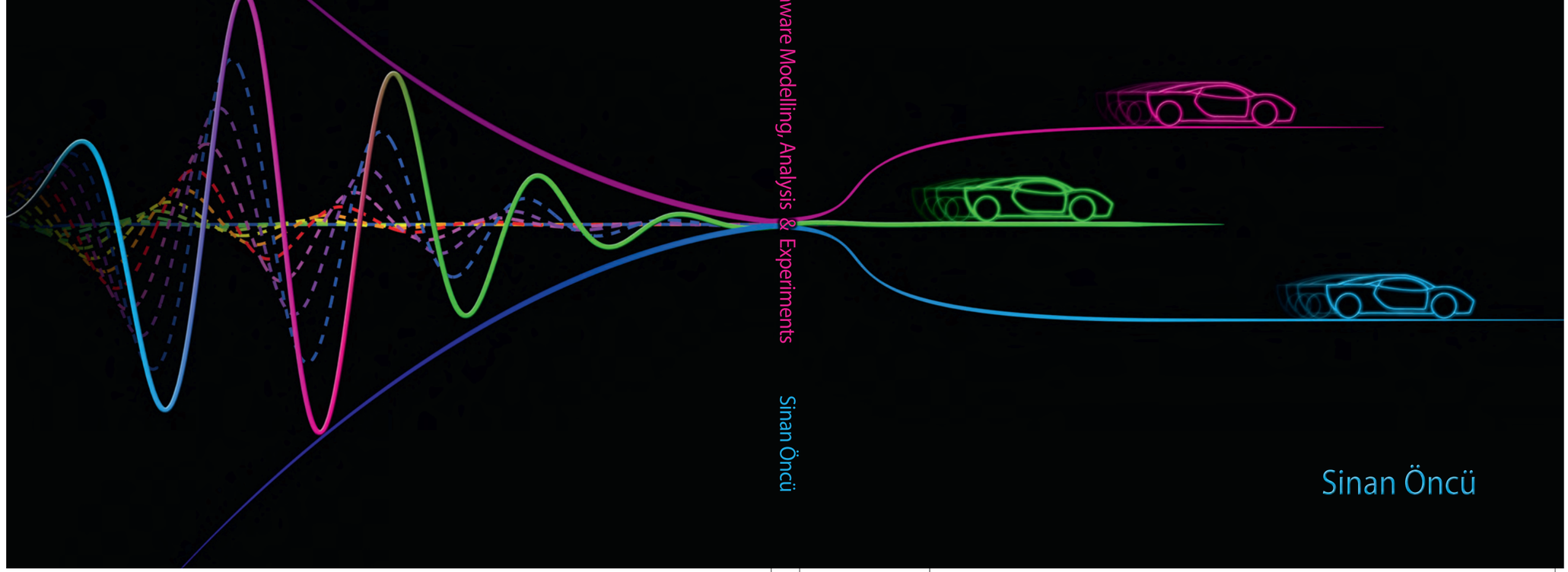

Sinan Öncü

Uitnodiging

Tot het bijwonen van de openbare verdediging van mijn proefschrift

String Stability of Interconnected Vehicles

Network-aware Modelling, Analysis & Experiments

op maandag

13 januari 2014

om 16:00 uur

Sinan Öncü

sinan.oncu@gmail.com

String Stability of Interconnected Vehicles:
Network-aware Modelling, Analysis and Experiments

This work was supported by HTAS (High Tech Automotive Systems) Connect & Drive Project, the European 7th Framework Network of Excellence: Highly-complex and networked control systems (HYCON2) (grant agreement no. 257462), and the Innovational Research Incentives Scheme under the VICI grant Wireless control systems: A new frontier in automation (No. 11382) awarded by NWO (The Netherlands Organization for Scientific Research) and STW (Dutch Science Foundation).

A catalog record is available from the Eindhoven University of Technology Library.
ISBN: 978-90-386-3543-9

Typeset by the author using LaTeX 2_ε

Reproduction: Ipskamp Drukkers, Enschede, The Netherlands.
Cover Design: Sinan Öncü, Ceylan Çölmekçi Öncü, and Nick Bauer.

String Stability of Interconnected Vehicles:
Network-aware Modelling, Analysis and Experiments

PROEFSCHRIFT

ter verkrijging van de graad van doctor
aan de Technische Universiteit Eindhoven, op gezag van de
rector magnificus, prof.dr.ir. C.J. van Duijn, voor een
commissie aangewezen door het College voor
Promoties in het openbaar te verdedigen
op maandag 13 januari 2014 om 16.00 uur

door

Sinan Öncü

geboren te Manisa, Turkije

Dit proefschrift is goedgekeurd door de promotoren en de samenstelling van de promotiecommissie is als volgt:

voorzitter:	prof.dr. L.P.H. de Goey
1^e promotor:	prof.dr. H. Nijmeijer
2^e promotor:	prof.dr.ir. W.P.M.H. Heemels
copromotor:	dr.ir. N. van de Wouw
leden:	prof.dr. L. Güvenç (Okan University)
	dr. C. Canudas-de-Wit (Polytechnique de Grenoble)
	prof.dr.ir. B. de Schutter (Delft University of Technology)
	prof.dr.ir. P.P.J. van den Bosch

Contents

Nomenclature

List of Symbols

a_i	acceleration of the i-th vehicle
C_a	aerodynamic friction coefficient
C_r	rolling friction coefficient
C_s	static friction coefficient
d	actual distance
d_i	actual distance of the i-th vehicle to its predecessor
d_r	desired distance
$d_{r,i}$	desired distance of the i-th vehicle to its predecessor
e	distance error
e_i	distance error of the i-th vehicle
F_f	total friction force
F_w	desired wheel force
$h_{d,i}$	headway-time constant
i	vehicle index
$k_{p,i}$	proportional gain
$k_{d,i}$	derivative gain
L_i	length of the i-th vehicle
n	number of vehicles in a string
q_i	vehicle position
r_i	desired inter-vehicle spacing at standstill
r_f	final drive ratio
r_g	gear ratio
r_w	wheel radius
T	sampling interval
T_e	engine torque
$T_\%$	engine torque command
u_i	total control command to the i-th vehicle

$u_{fb,i}$	feedback control command
$u_{ff,i}$	feedforward control command
u_r	reference input
v_i	vehicle velocity
v_p	velocity of the preceding vehicle
x_i	state vector of the i-th vehicle
$\tilde{x}_i$	extended state vector with Padé approximations
$\bar{x}_n$	lumped state vector of an n-vehicle string
κ	order of the Padé approximation
τ	time delay
τ_k	time delay at the k-th sampling interval
$\tau_{a,i}$	actuator delay
$\omega_{c,i}$	controller bandwidth
$\omega_{g,i}$	vehicle bandwidth

Abbreviations

ACC	adaptive cruise control
CACC	cooperative adaptive cruise control
CAN	controller area network
CPU	central processing unit
DFFT	discrete fast Fourier transform
EBS	electronic braking system
ECU	electronic control unit
FRF	frequency response function
GCDC	grand cooperative driving challenge
HMI	human machine interface
IEEE	Institute of Electrical and Electronics Engineers
ITS	intelligent transportation systems
LMI	linear matrix inequality
LAN	local area network
MAD	maximum allowable delay
MATI	maximum allowable transmission interval
ML	maximum likelihood
NCS	networked control system
PMC	power management control
RR	round-robin
RT	real time
SD	sampled-data
TOD	try-once-discard
TNO	Dutch Organization for Applied Scientific Research
V2I	vehicle to infrastructure

V2V	vehicle to vehicle
ZOH	zero order hold

Chapter 1

Introduction

The ever increasing demand for mobility in today's life brings additional burden on the existing ground transportation infrastructure for which a feasible solution in the near future lies in more efficient use of currently available means of transportation. For this purpose, the development of Intelligent Transportation Systems (ITS) technologies that contribute to improved traffic flow stability, throughput, fuel economy and safety are needed. Cooperative Adaptive Cruise Control (CACC), being one of the promising ITS technologies, extends the currently available Adaptive Cruise Control (ACC) technology with the addition of information exchange between vehicles through Vehicle-to-Vehicle (V2V) and Vehicle-to-Infrastructure (V2I) wireless communication [81]. CACC can contribute to improving these aspects by realizing a better synchronised traffic flow and therewith overcoming excessive variations in cruising speeds of vehicles even when vehicles are driving at reduced inter-vehicle distances.

In today's traffic, limited human perception of traffic conditions and human reaction characteristics constrain the lower limits of achievable safe inter-vehicle distances. Besides, erroneous human driving characteristics may cause traffic flow instabilities which result in so-called shockwaves. In dense traffic conditions, a single driver overreacting to a momentary disturbance (e.g. a slight deceleration of the predecessor) can trigger a chain of reactions in the backward chain of follower vehicles. The amplification of such a disturbance can bring the traffic

to a full stop kilometers away from the disturbance source and cause traffic jams for no apparent reason. For this reason, the attenuation of disturbances across the vehicle string, which is covered by the notion of *string stability*, is an essential requirement for vehicle platooning. ACC operated vehicles which rely merely on line of sight measurements (which are obtained via a radar or lidar) also suffer from the same reaction limitations as human drivers. Wireless information exchange between vehicles provides the means for overcoming sensory limitations of human or ACC operated vehicles and, therefore, can contribute significantly to improving the traffic flow, especially on highways [81, 72].

1.1 Vehicular Platooning

One of the earliest studies towards regulating inter-vehicle distances to achieve improved traffic flow dates back to the 60's in which the authors formulated the problem in an optimal control design framework [41]. A solution to this problem, formulated as an optimal regulation problem, was provided in a centralized control structure in [46]. Ever since, the ITS-control community has shown considerable interest in the automatic longitudinal control of moving vehicles due to its potential benefits for improving traffic throughput and has addressed many of the technical specifications for the deployment of such systems [72]. Many practical issues regarding a successful implementation were addressed especially in the scope of the California PATH program [73, 28] such as different inter-vehicle spacing strategies [80, 79], information flow structures [66, 77], heterogeneous traffic conditions [71], communication delays [42], and actuator limitations [34].

A centralized control structure as in [41, 46] is infeasible for realistic traffic conditions since this would require extensive central computational power and information exchange to/from every individual vehicle forming the platoon [17]. Another drawback of such a centralized control structure is its susceptibility to node (vehicle) malfunctioning. Therefore, more practical solutions have been investigated. One solution, on the opposite side of centralized schemes, are fully decentralized implementations, where every individual vehicle relies merely on its own sensory information, and are therefore named *autonomous vehicle-follower systems*. Adaptive Cruise Control (ACC) technology is such an autonomous vehicle-follower system that has now already become commercially available. Although it has been shown that an increase in traffic throughput could also be achieved with the use of ACC systems [35], the line of sight sensing limitations (achieved by a radar or lidar) of these vehicle-follower systems fail to reveal the potential benefits of vehicular platooning to the full extent.

The general objective of vehicular platooning is to pack the driving vehicles together as tightly as possible in order to increase traffic throughput while preventing amplification of disturbances throughout the string, the latter of which is known as *string instability* [78, 77]. These are two conflicting objectives when conventional methods are considered, since reducing inter-vehicle distances re-

sults in shockwaves (due to string instability) which adversely affect the global traffic flow. Studies for improving string stability properties of ACC operated vehicles have suggested the use of non-identical controllers for individual vehicles with linearly increasing gains as the platoon size increases [36]. However, this is not feasible in practice due to vehicle dynamics and actuator limitations and it compromises ride quality [64]. Therefore, ACC systems are considered more as a comfort enhancing Advanced Driver Assistance Systems (ADAS) technology.

Cooperative Adaptive Cruise Control technology can overcome the drawbacks of ACC systems by making use of information exchange between vehicles (even with those that may be occluded from direct line of sight). Inter-vehicle communication can support the increase of traffic flow by reducing inter-vehicle distances while improving the ride quality [64] and preventing amplifications of disturbances along the vehicle string. Most CACC schemes are neither fully centralized nor fully decentralized. Computations are executed in a decentralized fashion in each individual vehicle, but implemented control strategies rely on shared information from other vehicles, and hence are named *cooperative vehicle-follower systems*. Control strategies arising from different information flow structures have been investigated for CACC systems in terms of their effects on string stability [66, 77].

The interconnections arising from control laws that make use of shared information between dynamic agents (e.g. vehicles) has also been a popular research subject in closely related fields of flight formation control [5, 19], cooperative control [16, 47], and decentralized /distributed control [75, 76, 58, 38, 12]. Stankovic and Siljak [75, 76, 74] approached the problem from a large-scale systems perspective and used the inclusion principle to decompose the interconnected vehicle string into subsystems with overlapping states for which decentralized controllers were designed. In [16], algebraic graph theory was used to model the interconnection structure of vehicle formations to inspect the effect of communication topology on formation stability. Some research has focused on making use of underlying interconnection structures to derive scalable system theoretic properties for this type of platoon systems and designing controllers using distributed control methods [12, 39, 38]. These results are mostly applicable either to infinite length vehicle strings with *spatially invariant* interconnections or their finite-extensions with certain spatial symmetry properties.

CACC Technology

A CACC system as illustrated in Fig. 1.1 utilizes information exchange between vehicles through wireless communication besides local sensor measurements that are available in an ACC system. With this additional information, a CACC-equipped vehicle is able to react faster to the behaviour of the surrounding vehicles and, therewith, achieves a better synchronised traffic flow while avoiding string instability at smaller inter-vehicle distances. Besides the obvious increase

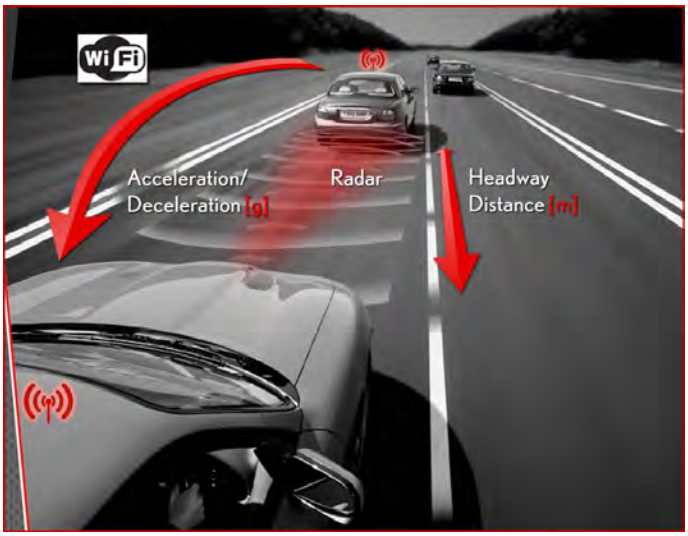

Figure 1.1: CACC concept.

in traffic throughput that is achieved by densely packing driving vehicles, another major benefit of CACC is the ability to attenuate the propagation of disturbances throughout the vehicle string. Such amplifications not only result in excessive acceleration/braking but also impair the traffic flow in general. All together, CACC is able to increase traffic flow, improve ride comfort, reduce travel times and achieve improved fuel economy.

Reduced inter-vehicle distances that can be achieved with CACC can be also beneficial for reducing the fuel consumption of platooning heavy-duty trucks. This benefit in terms of fuel economy is especially apparent for heavy-duty trucks due to the fact that the aerodynamic drag of a truck is high due to the flat frontal surface. Therefore, close distance driving will result in a significant fuel reduction [3, 4, 45, 24]. Experimental results have shown that fuel reduction for both the follower and the leading truck can be achieved, respectively, as much as 20% and 6% [8]. In [10], the inter-vehicle distance between two heavy-duty trucks is varied between 3 - 10 m resulting in a fuel reduction of $10 - 12\%$ for the following truck and a fuel reduction of $5 - 10\%$ for the leading truck.

More recently, proof-of-concept demonstrations with CACC vehicles were performed with homogeneous vehicle strings [61] and also with heterogeneous vehicle strings in a multi-vendor setting [62, 52, 27]. These implementations have shown the feasibility of CACC implementations and that significant improvements over existing ACC technology can be achieved already with relatively simple control algorithms and communication structures. However, given the safety-critical nature of the application, implementation for real traffic con-

ditions requires consideration of the constraints imposed by the wireless communication needed to implement CACC. On the one hand, control over a wireless communication network is the enabling technology that makes CACC realizable; on the other hand, very few studies consider the imperfections that are introduced by the network [42]. This is mainly due to the fact that systematic analysis and design tools for NCS arose relatively recently. In [42], a continuous-time transfer function based analysis of the effects of constant time delays on string stability was carried out.

The research incorporated in this thesis has been published in [55, 54, 53]; therein, a Networked Control Systems (NCS) approach is adopted for the analysis of string stability properties of CACC systems. For the purpose of such analysis, we develop a novel modelling method which can be used for the analysis of string stability for vehicle platooning while taking into account the effect of network-induced imperfections. In [55], a discretisation-based NCS modelling and analysis approach is adopted which also incorporates the effects of the sampling and the zero-order-hold in addition to constant wireless communication delays. These results have been extended in [53] with experiments. In [54], string stability conditions are provided on the uncertain and time-varying sampling/transmission intervals, delays, and scheduling constraints (requiring network protocols) induced by the wireless communication between vehicles. A brief overview of research in the field of NCS, relevant in the scope of vehicular platooning, will be presented next.

1.2 Networked Control Systems

In the field of NCS, one considers the control of systems over a communication network [87, 7]. Communication and control over a shared network has received an increasing attention over the recent years, see e.g., the overview papers [32, 89, 87, 30]. Such control systems, in which the sensor data and control commands are transmitted over a wired or wireless network, are called Networked Control Systems (NCSs). A typical example of a network employed in the scope of control is the widely used Controller Area Network (CAN) in the automotive industry [40]. Compared to a traditional control system, which uses end-to-end wired connections between the sensors, actuators and controllers, NCSs make use of a shared medium to exchange information. The primary advantages of an NCS are ease of troubleshooting, maintenance and installation. Moreover, NCSs offer a large flexibility, since they can be easily modified and reconfigured by adding sensors, actuators, and controllers without the need of making major changes to the overall structure of the system. A particular benefit of employing wireless networks is avoiding the need for wired connections, which are infeasible in many situations including vehicular platooning applications for obvious reasons. However, the usage of (wireless) networked communication introduces new challenges related to the occurrence of time-varying sampling intervals, delays,

and communication constraints. The impact of such network-induced effects on the control system requires a careful analysis and tradeoffs need to be made between control properties, such as stability and performance, and network-related properties such as delays, scheduling, bandwidth limitations etc. [7].

Network-induced Imperfections

The use of a communication network in the control loop makes the analysis and design of an NCS more complicated than a traditional (non-networked) control loop. Indeed, next to the presence of constraints and uncertainties, disturbances, and measurement noise, which already occur in traditional control loops, in NCSs, additional challenges arise that must be overcome before the advantages NCSs offer can be fully exploited. In particular, the design of an NCS has to deal with network-induced communication imperfections and constraints, which can be categorized into five types [7]:

i) **Variable sampling/transmission intervals**. If there is no synchronised clock for all nodes, the sampling/transmission intervals are uncertain and time varying. This phenomenon is also known as *clock jitter* in the literature [13].

ii) **Variable transmission delays**. In NCSs, transmission of data over a network takes a finite amount of time. Furthermore, if multiple nodes share a network, the network might be occupied for an uncertain period before the current nodes can send their data; this effect causes so-called contention delays. Therefore, the transmission delays are often uncertain and time varying.

iii) **Communication constraints**. NCSs have multiple sensors and actuators, which are grouped into nodes which all communicate over a shared network. Due to a shared communication medium, it is not possible that all these nodes transmit their data simultaneously. Therefore, a scheduling protocol is needed which orchestrates access of these nodes to the network for transmitting their data.

iv) **Packet dropouts**. Another difference between NCSs and a traditional plant-controller setup (in which end-to-end communication is employed) is the occurrence of packet dropouts, i.e., the possibility that data is lost during transmissions. Packet dropouts can result from collisions, unreliability of the network channel or congestion.

v) **Sampling effects**. In any practical implementation, the control system is implemented in a digital environment and can only transmit data that are digitized by using sampling.

In this thesis, the effects of such NCS imperfections on string stability properties of vehicular platoons are analysed. In Section 4.2, the analysis of the effects of (constant) transmission delays (ii), and sampling (v) is pursued; in Section 4.3, the effects of variable transmission intervals (i), transmission delays (ii) and communication constraints (iii) are studied.

NCS modelling and analysis approaches

To analyse the effects of these network-induced imperfections on stability and performance of the NCS, a model that encompasses these imperfections is required. In the NCS literature, three different approaches towards modelling and stability analysis for NCSs have been considered:

i) **Modelling approach based on discrete-time parameter varying systems**. This approach is based on constructing a discrete-time representation of the sampled-data NCS system. The uncertain network parameters can then be captured by polytopic embeddings (overapproximations) in order to construct a model suitable for stability analysis. We refer to [31, 11, 63, 14, 82, 84, 83, 21, 23, 33, 67, 89, 88] for an overview of discretisation-based approaches for NCS. The resulting discrete-time polytopic models can then be analysed by using robust stability analysis methods. Note that, using a discrete-time approach, one can typically prove stability at the sampling instants; however, the sampled-data control system is evolving in continuous-time between these sampling times. Consequently, the final step in this approach is to guarantee that the intersample behaviour is also stable in order to prove stability of the continuous-time sampled-data system.
A property of this modelling approach is that it allows to consider discrete-time controllers, which is favorable since controllers are typically implemented on a digital computer. Note that for linear systems, this discretisation can be done exactly. Therefore, this approach mainly focusses on linear systems. Recently, extensions towards nonlinear systems, see e.g. [84, 83], have also been developed.

ii) **Modelling approach based on impulsive/hybrid systems**. In this approach, stability analysis techniques are proposed based on a hybrid model of the sampled-data NCS. This approach is applicable to a large class of NCSs (both linear as well as nonlinear) [51, 29, 50]. However, some drawbacks of this approach are that only continuous-time (non)linear controllers can be considered (due to the fact that this approach is emulation based). Moreover, it has been shown, e.g. in [14], that the modelling and analysis approach is more conservative than the discrete-time approach for linear systems. Another drawback is that it is limited to small delays (delays smaller than the transmission interval).

iii) **Modelling approach based on delayed (impulsive) differential equations**. In this approach, the NCS is modeled based on delay (impulsive) differential equations [48, 82]. This approach allows to consider discrete-time controllers and nonlinear plants. However, the stability analysis is based on Lyapunov Krasovskii or Lyapunov Razumikhin methods, which makes stability analysis intricate.

Most works on NCS focus on the stability analysis of closed-loop NCS consisting of a plant and controller interconnected by a (wireless) network [32, 11, 22, 33, 20, 14, 88]. Relatively few works consider sensitivity of NCS to perturbations, see e.g. [29, 82]. In the context of CACC, the latter aspect is highly relevant as, firstly, wireless communications take place between controlled vehicles and, secondly, string stability relates to the attenuation of disturbances along the string, and not just stability (of an equilibrium). This work will address the effects of aforementioned wireless communication imperfections on the string stability properties of vehicular platoons by using both a discretisation-based modelling approach (i) and the hybrid system modelling approach (ii).

1.3 Main Contributions

Recent implementations of CACC have demonstrated that significant improvements over existing ACC technology can be achieved already with relatively simple control algorithms and communication structures. However, the implementation for real traffic conditions requires consideration of the constraints imposed by the wireless communication needed to implement CACC. Therefore, the focus in this thesis is on the design of CACC systems from a Networked Control System (NCS) perspective. The main contributions of the thesis can be summarized as follows:

I) **Network-aware modelling of CACC vehicle strings.** A novel NCS modelling framework for interconnected vehicle strings is presented. The interconnected vehicle string model arises from the dynamical coupling of a cascade of CACC vehicles, each of which is controlled to maintain a desired distance to its predecessor. In this model, two types of data employed in the CACC controller are distinguished according to the way they are being transferred, i.e. either locally sensed or wirelessly communicated information. This approach allows to cast the interconnected system dynamics with wireless communication constraints into an NCS model that incorporates the effects of sample-and-hold, transmission frequency and network delays. The framework is set up in a general manner such that the inclusion of scheduling constraints induced by the wireless communication between vehicles can be incorporated as well.

II) **Network-aware string stability analysis.** The modelling framework is

extended with analysis tools for string stability in the presence of network effects. These analyses can provide the designer with guidelines for making multidisciplinary tradeoffs between control and network specifications and support the design of CACC systems that are robust to uncertainties introduced by wireless communication. Using these analysis tools, the dependency of string stability on network-induced effects is studied. The analyses provide bounds on the maximum allowable transmission intervals (MATI) and maximum allowable delays (MAD) while string stability is still guaranteed.

III) **Experimental validation/demonstration.** Moreover, the validity of the presented analysis framework is demonstrated via experiments performed with CACC-equipped prototype passenger vehicles in a homogeneous string. Experimental results show that the developed NCS modelling framework captures the dependency of string stability on network-induced effects and confirm the string stable operation conditions obtained by model-based analyses.

Furthermore, the CACC algorithm was implemented on a heavy-duty truck and tested during the Grand Cooperative Driving Challenge (GCDC) in a multi-vendor setting where participating teams tested their CACC-equipped vehicle and benchmarked it to the CACC vehicles of other competitors [85, 2, 52]. These tests show improved string stable behaviour of the truck within a heterogeneous vehicle string. These experiments address the effects of wireless communication losses and vehicle dynamics limitations on string stability properties of heavy-duty vehicles.

1.4 Outline of the Thesis

This thesis is divided into six main chapters (in addition to this introduction). The outline of the thesis is as follows.

Chapter 2: Model Description

In this chapter, the interconnected vehicle string model that will be used in the rest of the thesis will be constructed. This interconnected vehicle string model arises from the dynamical coupling of a cascade of CACC-equipped vehicles. One of the general control objectives, namely the *vehicle following objective* is introduced which relates to the objective of following the preceding vehicle at a desired distance (the latter of which depends on the so-called spacing policy).

We cast the interconnected vehicle string dynamics in a form amendable for the network-aware analysis that will be carried out in Chapter 4. Hereto, two types of data employed in the CACC controller are distinguished according to their way of being transferred: either as locally sensed information or as

wirelessly communicated information. This allows us to consider the feedback of local sensor measurements as internal dynamics of the interconnected system and to focus on the effects of network imperfections on the wirelessly communicated data separately. As an ideal case, we also introduce a Network-Free(NF)-CACC model, which is obtained when the wireless communication imperfections are not considered and which will be used in Chapter 3 for investigating *string stability* properties of *interconnected systems* and serves as a reference for the evaluation of the networked system performance in terms of string stability in Chapter 4.

Chapter 3: String Stability of Interconnected Vehicles

In addition to the vehicle following objective that is described in Chapter 2, another important requirement in a CACC vehicle platooning system is to avoid amplification of the effect of disturbances throughout the string as the vehicle index increases (i.e. string instability). As already indicated before, the amplification of such disturbances not only poses risks on safe and reliable operation of the individual vehicle following controllers but also compromises traffic flow stability, fuel economy and throughput. In this chapter, *string stability* properties of interconnected vehicle strings are discussed by using the models that were developed throughout Chapter 2. The Network-Free(NF)-CACC model forms the basis for the string stability analysis of this particular type of interconnected vehicle strings. First, the string (in)-stability phenomenon is illustrated by time simulations and the effects of amplification of certain signals along the vehicle string on realizing the control objectives are discussed. Then, we present frequency-domain based and dissipation-based conditions for string stability. The tools and methods presented in this chapter will be exploited in Chapter 4 where both frequency-domain and dissipation-based conditions for string stability will be employed for the analysis of networked CACC models.

Chapter 4: Network-aware Cooperative Adaptive Cruise Control

The impact of wireless communication imperfections on string stability requires a careful analysis to support the making of tradeoffs between CACC performance and network specifications. In this chapter, a network-aware modelling and analysis framework is built on the basis of the interconnected vehicle string model that is constructed in Chapter 2 and by using the string stability analysis tools presented in Chapter 3. Based on this network-aware modelling approach, the string stability analysis techniques presented in Chapter 3 are extended to study the *string stability* properties of the interconnected vehicle string when wireless communication imperfections are present.

These analyses can be used to investigate tradeoffs between CACC performance (string stability) and network specifications (such as delays) which are essential in the multi-disciplinary design of CACC-based platooning systems. The main purpose of this chapter is to emphasize the necessity for considering

CACC in a Networked Control Systems (NCS) framework by studying the effects of wireless communication on the performance of an existing CACC controller in terms of string stability. Moreover, we also show how these string stability analyses can provide the designer with guidelines for making the tradeoffs between control and network specifications.

Chapter 5: Experimental Validation

In this chapter, the validity of the network-aware modelling and string stability analysis framework, that was developed in Chapter 4, is demonstrated in practice by experiments performed with prototype vehicles equipped with Cooperative Adaptive Cruise Control (CACC). The main goal of these experiments is to test string stability properties for a range of time headways and communication delays in order to validate the model-based analyses that are obtained by using the Networked Control Systems (NCS) methods in Chapter 4. We obtain string stable operation conditions for the prototype passenger vehicles by using the network-aware modelling and string stability analysis method presented in Chapter 4 which incorporates the effects of the sampling and zero-order-hold (ZOH) in addition to constant wireless communication delays. Herewith, we obtain maximum allowable time delays for a range of headway times and sampling intervals for which the boundary of string stability will be revealed and, therewith, find appropriate settings for which experiments will be carried out. The CACC-related components instrumented in the test vehicles and the implementation of the CACC system are explained in detail. For the validation of the model-based string stability analyses presented in Chapter 4, experiments have been carried out at representative operating points with different time headway values where the (constant) wireless communication delay was regulated at different levels in order to support the experimental analysis of string stability for different delay magnitudes. These experimental results show how string stability is compromised by wireless communication delays and demonstrate the reliability and practical validity of the network-aware modelling and string stability analysis method presented in Chapter 4 in practice.

Chapter 6: Cooperative Driving with a Heavy-Duty Truck in Mixed Traffic: Experimental Results

This chapter describes the implementation and testing of a Cooperative Adaptive Cruise Control (CACC) strategy on a heavy-duty truck. The adopted control strategy utilizes additional information exchange through wireless communication to improve the vehicle following behaviour achieved by the underlying Adaptive Cruise Controller (ACC). The control method is evaluated in a mixed traffic condition. It is shown that the truck can perform smooth predecessor following in most of the test scenarios even for small inter-vehicle distances. Furthermore,

the results demonstrate how string stability is affected by wireless communication imperfections and ac-(de)celeration limitations of the heavy-duty truck in a heterogeneous platoon.

Chapter 7: Conclusions and Recommendations:

This chapter summarizes the main conclusions and provides recommendations for future research based on the findings in this thesis.

Chapter 2

Model Description

The general objective of a Cooperative Adaptive Cruise Control (CACC) system is to pack the driving vehicles together as tightly as possible in order to increase traffic throughput while preventing amplification of the effect of disturbances throughout the string, the latter of which is known as *string instability* [77, 78]. These are two conflicting objectives when conventional methods are considered, since reducing inter-vehicle distances results in shockwaves (due to string instability) which adversely affect the global traffic flow. In CACC, wireless information exchange between vehicles provides the means for overcoming sensory limitations of human or ACC operated vehicles and, therefore, can contribute significantly to improving the traffic flow, especially on highways. Significant improvements over existing ACC technology can be achieved already with relatively simple control algorithms and communication structures but implementation for real traffic conditions requires consideration of the constraints imposed by the wireless communication needed to implement CACC. For this matter, a network-aware modelling is needed. Such an approach is developed

in this thesis, which allows to study the effects of wireless communication imperfections on the performance and string stability properties of CACC-based platooning strategies.

In this chapter, the interconnected vehicle string model that will be used in the rest of the thesis will be constructed. This interconnected vehicle string model arises from the dynamical coupling of a cascade of CACC-equipped vehicles, each of which is controlled to maintain a desired distance to its predecessor. In Section 2.1, we introduce one of the general control objectives, namely the *vehicle following objective*. The other important control objective being string stability will be addressed in more detail in Chapter 3. Vehicle following relates to the objective of following the preceding vehicle at a desired distance (the latter of which depends on the so-called spacing policy). In Section 2.2, the underlying longitudinal vehicle dynamics is presented. In Section 2.3, the ACC and CACC structures are presented which together with the longitudinal vehicle dynamics form the closed-loop CACC vehicle model, which is given in Section 2.4. We use this closed-loop CACC vehicle model to derive the interconnected vehicle string model in Section 2.5. Here, we cast the interconnected vehicle string dynamics in a form amendable for the network-aware analysis that will be carried out in Chapter 4. Hereto, we distinguish two types of data employed in the CACC controller according to their way of being transferred: either as locally sensed information or as wirelessly communicated information. This allows us:

- to consider the feedback of local sensor measurements as internal dynamics of the interconnected system and,
- to focus on the effects of network imperfections on the wirelessly communicated data.

In Section 2.6, we also introduce a Network-Free(NF)-CACC model which is obtained when the wireless communication imperfections are not considered. This model will be used in Chapter 3 for investigating *string stability* properties of *interconnected systems* and serves as a reference for the evaluation of the networked system performance in Chapter 4.

2.1 Vehicle Following Objective

The vehicles forming the platoon as shown in Fig. 2.1 are interconnected by means of control in order to meet the vehicle following objective. This vehicle following objective relates to the fact that each vehicle is desired to follow its predecessor while maintaining a desired, but not necessarily constant, distance. Here, we consider a constant time headway spacing policy, where the desired spacing ($d_{r,i}$) between the front bumper of i-th vehicle to its predecessor's ($(i-1)$-th vehicle) rear bumper is given by

$$d_{r,i} = r_i + h_{d,i} v_i. \tag{2.1}$$

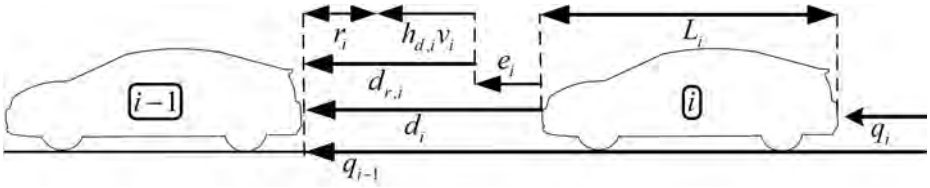

Figure 2.1: Subsequent vehicles driving in a platoon formation.

Herein, i is the vehicle index, r_i is a constant term that forms the desired gap between consecutive vehicles at standstill, $h_{d,i}$ is the headway time constant representing the (desired) time that it will take the i-th vehicle to arrive at the same position as its predecessor when $r_i = 0$ and v_i is the vehicle velocity. For the sake of simplicity, $r_i = 0$ is taken in the rest of this thesis since it does not affect the dynamics of the system in the scope of the presented work. For similar reasons, the car length (L_i) will also be taken as zero. The actual distance between two consecutive vehicles (d_i) is

$$d_i = q_{i-1} - (q_i + L_i) = q_{i-1} - q_i, \tag{2.2}$$

where q_i is the absolute position of the i-th vehicle in global coordinates. The local control objective, referred to as *vehicle following*, can now be defined as regulating the error

$$e_i = d_i - d_{r,i}, \tag{2.3}$$

to zero asymptotically.

Next, the underlying longitudinal vehicle dynamics and the control structure are presented, respectively, in Sections 2.2 and 2.3, which together form the CACC vehicle model (Section 2.4). Subsequently, we use this CACC vehicle model to construct the interconnected vehicle string model in Section 2.5.

2.2 Longitudinal Vehicle Dynamics Model

We use the following linearized third-order state-space representation of the longitudinal dynamics for each vehicle in the string:

$$\begin{aligned} \dot{q}_i(t) &= v_i(t), \\ \dot{v}_i(t) &= a_i(t), \\ \dot{a}_i(t) &= -\eta_i^{-1} a_i(t) + \eta_i^{-1} u_i(t), \end{aligned} \tag{2.4}$$

where $q_i(t), v_i(t), a_i(t)$ are the absolute position, velocity, and acceleration, respectively, at time $t \in \mathbb{R}_{\geq 0}$, η_i represents a parameter characterising the internal actuator dynamics and $u_i(t)$ is the desired acceleration for the i-th vehicle. This

model is widely used in the literature as a basis for analysis [42, 75, 49, 61, 54]. Equivalently, by using Laplace transforms, $\mathcal{L}(q_i(t)) =: Q_i(s)$ and $\mathcal{L}(u_i(t)) =: U_i(s)$, the vehicle model for vehicle i can be represented by the transfer function

$$G_i(s) = \frac{Q_i(s)}{U_i(s)} = \frac{1}{s^2(\eta_i s + 1)}, s \in \mathbb{C}. \tag{2.5}$$

Note that the conventional usage of small letters for time-domain signals and capital letters for their Laplace- or frequency-domain counterparts will be adopted throughout the rest of this thesis.

Longitudinal Vehicle Dynamics with Actuator Delay

In practical implementations of longitudinal control of the vehicle dynamics, the underlying low-level controllers that regulate the engine, transmission, and driveline dynamics to realize the desired acceleration (u_i) introduce an additional actuation delay. In order to account for such delays in the throttle actuation, we extend the model in (2.4) with an additional constant actuation delay ($\tau_{a,i}$) between the desired acceleration (u_i) and the commanded acceleration, thereby replacing the longitudinal dynamics for the i-th vehicle in (2.4) by

$$\begin{aligned} \dot{q}_i(t) &= v_i(t), \\ \dot{v}_i(t) &= a_i(t), \\ \dot{a}_i(t) &= -\eta_i^{-1} a_i(t) + \eta_i^{-1} \tilde{u}_i(t) \end{aligned} \tag{2.6}$$

with

$$\tilde{u}_i(t) = u_i(t - \tau_{a,i}). \tag{2.7}$$

An equivalent Laplace-domain representation of this vehicle model can be obtained by using Laplace transforms, $\mathcal{L}(q_i(t)) =: Q_i(s)$ and $\mathcal{L}(u_i(t)) =: U_i(s)$, as before. This leads to the transfer function

$$G_i(s) = \frac{Q_i(s)}{U_i(s)} = \frac{1}{s^2(\eta_i s + 1)} e^{-\tau_{a,i} s}, s \in \mathbb{C}. \tag{2.8}$$

Padé approximations of the Actuator Delay

Note that the function $e^{-\tau_{a,i} s}$ in (2.8) of the actuator delay in (2.7) is non-rational and renders the model infinite-dimensional. In Chapter 4, we will pursue a discrete-time modelling approach for the modelling of the *networked* CACC controlled vehicle string relying on finite-dimensional models of the vehicle dynamics. To support this approach, we approximate the delay transfer function $e^{-\tau_{a,i} s}$ by a rational transfer function based on Padé approximations [26]. This

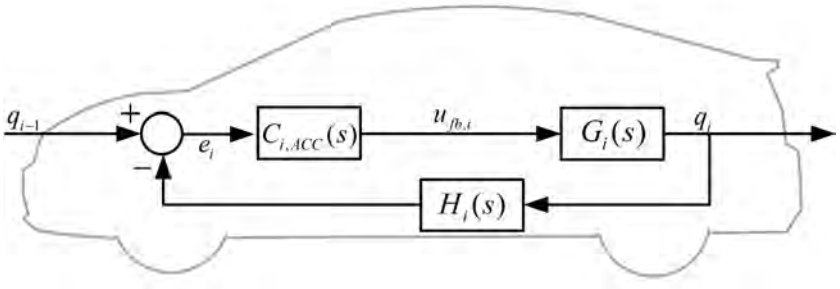

Figure 2.2: Control structure block diagram of ACC-equipped vehicle i.

leads to the following state-space representation of the κ-th order Padé approximation of the actuator delay:

$$\begin{aligned} \dot{\tilde{p}}_i &= A_{p,i}\tilde{p}_i + B_{p,i}u_i \\ \tilde{u}_i &= C_{p,i}\tilde{p}_i + D_{p,i}u_i \end{aligned} \tag{2.9}$$

with $\tilde{p}_i = [p_{i,1}\ p_{i,2}\dots p_{i,\kappa}]^T \in \mathbb{R}^\kappa$.

2.3 C-ACC Control Structure

The vehicle following controller consists of an Adaptive Cruise Controller (ACC) in addition to which cooperative action is introduced in a feedforward fashion. In this section, both the ACC and CACC control structures will be presented.

2.3.1 Adaptive Cruise Controller (ACC)

The control structure block diagram of the ACC controller for vehicle i is shown in Fig. 2.2. The signal conditioning block $H_i(s) = 1 + h_{d,i}s$ is used to implement the spacing strategy given in (2.1). The feedback controller $C_{i,ACC}(s)$, which constitutes the ACC part, is a PD-type controller that acts on locally sensed data (e.g. obtained using radar or lidar) to achieve the vehicle following objective. This ACC controller is given in the Laplace domain as

$$U_{fb,i}(s) = C_{i,ACC}(s)E_i(s) = \omega_{c,i}(\omega_{c,i} + s)E_i(s), \tag{2.10}$$

where $E_i(s) := \mathcal{L}(e_i(t))$, $U_{fb,i}(s) := \mathcal{L}(u_{fb,i}(t))$, and $\omega_{c,i}$ is the bandwidth of the controller which is chosen such that $\omega_{c,i} \ll \omega_{g,i} := \frac{1}{\eta_i}$ in order to prevent

actuator saturation. The time-domain equivalent of (2.10) is obtained by using (2.3) with (2.1) and (2.2), which leads to:

$$\begin{aligned} u_{fb,i} &= \omega_{c,i}^2 e_i + \omega_{c,i}\dot{e}_i, \\ &= \omega_{c,i}^2 e_i + \omega_{c,i}(v_{i-1} - v_i - h_{d,i}a_i), \\ &= k_{p,i}e_i + k_{d,i}(v_{i-1} - v_i - h_{d,i}a_i), \end{aligned} \tag{2.11}$$

where for notational convenience, the definitions $k_{p,i} := \omega_{c,i}^2$ and $k_{d,i} := \omega_{c,i}$ are used. Note that $k_{p,i}$ and $k_{d,i}$ represent, respectively, the proportional and derivative gains of the ACC controller in the remainder of this thesis. This controller uses the relative distance $(q_i - q_{i-1})$ and relative velocity $(v_i - v_{i-1})$ between the host and the directly preceding vehicle which are available as sensed measurements through a radar unit that is mounted at the front of the vehicle (i) and local measurements of velocity (v_i) and acceleration (a_i) of the host vehicle i. This ACC controller achieves the vehicle following objective (i.e. regulating e_i to zero in (2.3)) when the vehicle platoon drives with a constant speed in steady state (i.e. $u_r = 0$).

2.3.2 Cooperative Adaptive Cruise Controller (CACC)

The control structure for a single CACC equipped vehicle (vehicle i) is shown in Fig. 2.3. Additional feedforward action is utilized to improve vehicle following and string stability performance and forms the CACC part of the controller ($C_{i,CACC}(s)$ in Fig. 2.3). CACC operation is introduced as an addition to the underlying ACC controller $C_{i,ACC}(s)$ in a feedforward fashion by the CACC controller $C_{i,CACC}(s)$. Following the design guidelines in [49], the feedforward filter is given as

$$U_{ff,i}(s) = C_{i,CACC}(s)A_{i-1}(s) = \frac{1}{H_i(s)G_i(s)s^2}A_{i-1}(s), \tag{2.12}$$

and achieves zero steady-state vehicle following error (e_i in (2.3)). Now, using $A_{i-1}(s) = s^2Q_{i-1}(s) = s^2G_{i-1}(s)U_{i-1}(s)$, (2.12) can be rewritten as

$$U_{ff,i}(s) = \frac{1}{H_i(s)G_i(s)}G_{i-1}(s)U_{i-1}(s). \tag{2.13}$$

Remark 2.1. For heterogeneous vehicle strings, this particular implementation of the CACC algorithm as in (2.13) requires the dynamics of the preceding vehicle (i.e. $G_{i-1}(s)$) to be known by the i-th vehicle. ◁

For a homogeneous vehicle string (i.e. identical vehicles, and thus $G_i(s) = G_{i-1}(s)$, for all $i \in \mathbb{N}_{\geq 1}$) (2.13) reduces to

$$U_{ff,i}(s) = \frac{1}{H_i(s)}U_{i-1}(s) = \frac{1}{1 + h_{d,i}s}U_{i-1}(s). \tag{2.14}$$

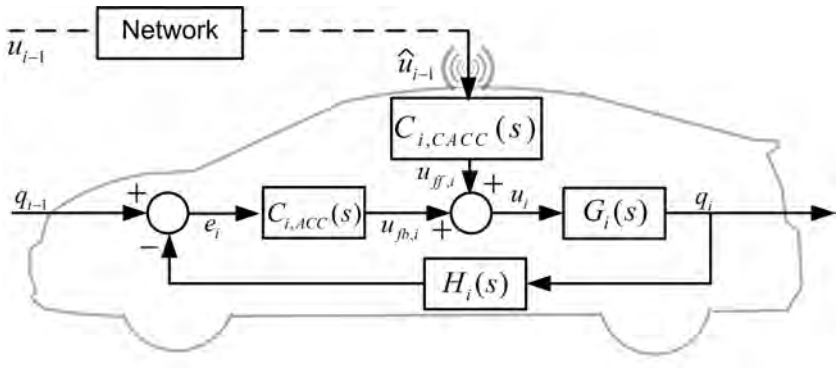

Figure 2.3: Control structure block diagram of CACC-equipped vehicle i.

Here, it can be seen that additional dynamics is introduced in the controller due to the velocity-dependent spacing policy in (2.1), which gives the following time-domain representation for the CACC feedforward filter in (2.14):

$$\dot{u}_{ff,i} = -h_{d,i}^{-1} u_{ff,i} + h_{d,i}^{-1} u_{i-1}. \tag{2.15}$$

The time-domain representations of the CACC controller given in (2.11) and (2.15) together constitute the total control command u_i, given by

$$u_i = u_{fb,i} + u_{ff,i}, \tag{2.16}$$

which will be used in the state-space representation of the closed-loop CACC vehicle model presented next.

2.4 Closed-Loop CACC Model

The general form of the closed-loop CACC vehicle model is obtained by combining the vehicle longitudinal dynamics in (2.4) with the distance error equation in (2.3), the feedback control law (2.11), the feedforward control law (2.15), and the total control command in (2.16). In doing so, we replace u_{i-1} by $\hat{u}_{i-1}$, where $\hat{u}_{i-1}$ denotes the fact that u_{i-1} is transmitted over a shared wireless communication network, see Figure 2.3. Note that $\hat{u}_{i-1}$ typically differs from u_{i-1} due to network-induced phenomena such as sample-and-hold effects and transmission delays. This leads to the following equation for the CACC filter:

$$\dot{u}_{ff,i} = -h_{d,i}^{-1} u_{ff,i} + h_{d,i}^{-1} \hat{u}_{i-1}. \tag{2.17}$$

By choosing the state variables as $x_i^T = [e_i \; v_i \; a_i \; u_{ff,i}] \in \mathbb{R}^{n_x}$ with $n_x = 4$, and by combining (2.6) and (2.17), the i-th CACC equipped vehicle dynamics,

($i \in \mathbb{N}_{[2,n]}$, where $\mathbb{N}_{[2,n]}$ is used to denote the set of natural numbers in the interval $[2, n]$), in an n-vehicle string is described by

$$\dot{x}_i = A_{i,i}x_i + A_{i,i-1}x_{i-1} + B_{s,i}\tilde{u}_i + \underbrace{B_{c,i}\hat{u}_{i-1}}_{CACC},$$

$$A_{i,i} = \begin{bmatrix} 0 & -1 & -h_{d,i} & 0 \\ 0 & 0 & 1 & 0 \\ 0 & 0 & -\eta_i^{-1} & 0 \\ 0 & 0 & 0 & -h_{d,i}^{-1} \end{bmatrix}, B_{s,i} = \begin{bmatrix} 0 \\ 0 \\ \eta_i^{-1} \\ 0 \end{bmatrix},$$

$$A_{i,i-1} = \begin{bmatrix} 0 & 1 & 0 & 0 \\ 0 & 0 & 0 & 0 \\ 0 & 0 & 0 & 0 \\ 0 & 0 & 0 & 0 \end{bmatrix}, B_{c,i} = \begin{bmatrix} 0 \\ 0 \\ 0 \\ h_{d,i}^{-1} \end{bmatrix}, \tag{2.18}$$

where $B_{s,i}$ is the input vector corresponding to the total control input $\tilde{u}_i$ to vehicle i and $B_{c,i}$ is the input vector for the additional CACC input $\hat{u}_{i-1}$, which is sent to the i-th vehicle through the wireless network and is therefore subject to network effects.

A time-domain representation of the CACC feedback/feedforward control input with the given spacing policy is given below:

$$\begin{aligned} u_i &= u_{fb,i} + u_{ff,i}, \qquad i \in \mathbb{N}_{[1,n]}, \\ &= K_{i,i-1}x_{i-1} + K_{i,i}x_i, \end{aligned} \tag{2.19}$$

$$K_{i,i-1} = \begin{bmatrix} 0 \\ k_{d,i} \\ 0 \\ 0 \end{bmatrix}^T, K_{i,i} = \begin{bmatrix} k_{p,i} \\ -k_{d,i} \\ -k_{d,i}h_{d,i} \\ \nu_i \end{bmatrix}^T,$$

where $\nu_i = 1$ corresponds to an operational CACC, and $\nu_i = 0$ gives only ACC. For more details on the CACC setup, see [49, 61].

The longitudinal vehicle dynamics with actuator delay is obtained by using the augmented state vector $\tilde{x}_i^T = [x_i^T \ \tilde{p}_i^T]$ in (2.18) together with (2.9) to obtain the total vehicle dynamics model given by

$$\dot{\tilde{x}}_i = \tilde{A}_{i,i}\tilde{x}_i + \tilde{A}_{i,i-1}\tilde{x}_{i-1} + \tilde{B}_{s,i}u_i + \tilde{B}_{c,i}\hat{u}_{i-1}, \qquad i \in \mathbb{N}_{[2,n]},$$

$$\tilde{A}_{i,i} = \begin{bmatrix} A_{i,i} & B_{s,i}C_{p,i} \\ 0 & A_{p,i} \end{bmatrix}, \tilde{B}_{s,i} = \begin{bmatrix} B_{s,i}D_{p,i} \\ B_{p,i} \end{bmatrix},$$

$$\tilde{A}_{i,i-1} = \begin{bmatrix} A_{i,i-1} & 0 \\ 0 & 0 \end{bmatrix}, \tilde{B}_{c,i} = \begin{bmatrix} B_{c,i} \\ 0 \end{bmatrix}. \tag{2.20}$$

This closed-loop CACC model serves as the basic building block of the interconnected vehicle string as shown in Fig. 2.4.

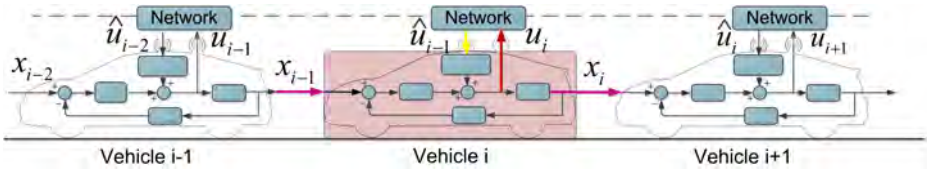

Figure 2.4: Basic building block of the interconnected vehicle string.

Next, the interconnected vehicle string model will be presented which is defined as a finite-dimensional interconnection of these basic building blocks in (2.20) (i.e. single CACC-controlled vehicle) which are dynamically coupled through their states and inputs via the underlying vehicle following controllers. This model also forms the basis for the discussions in Section 3.4 on so-called *string stability* properties of the interconnected system.

2.5 Interconnected Vehicle String Model

In this section, the closed-loop CACC model for the individual vehicle as proposed in the previous section is employed to construct the total interconnected vehicle string model for the entire platoon. In order to do so, a reference vehicle (denoted by index $i = 0$ and with state x_0) is introduced which represents a trajectory generator in the lead vehicle in case there are no preceding vehicles in front of it. The dynamics of the reference vehicle, without actuator delay, is described by

$$\begin{aligned} \dot{x}_0 &= A_0 x_0 + B_{s,0} u_r, \\ A_0 &= \begin{bmatrix} 0 & 0 & 0 & 0 \\ 0 & 0 & 1 & 0 \\ 0 & 0 & -\eta_0^{-1} & 0 \\ 0 & 0 & 0 & 0 \end{bmatrix}, \; B_{s,0} = \begin{bmatrix} 0 \\ 0 \\ \eta_0^{-1} \\ 0 \end{bmatrix}, \end{aligned} \tag{2.21}$$

where $x_0 = [e_0,\ v_0,\ a_0,\ u_{ff,0}]^T$, and u_r is the reference acceleration profile. In (2.21), the state variables are chosen in accordance with those for the real vehicles in the string in (2.18). Consequently, redundant states exist in (2.21) (i.e. $e_0, u_{ff,0}$), but nevertheless, we opt for this representation as it results in a uniform representation for the upcoming vehicle string model.

The lead ($i = 1$) vehicle (with state x_1) in the string also requires special consideration. The CACC input u_r is locally available to this vehicle without any network-induced imperfections since it is generated by this vehicle. By considering these two special cases for the reference ($i = 0$) and the lead ($i = 1$) vehicles and using the CACC vehicle model in (2.20) for each operational CACC subsystem ($i \in \mathbb{N}_{[2,n]}$), we obtain the following equations for an n-vehicle string as shown in Fig. 2.5:

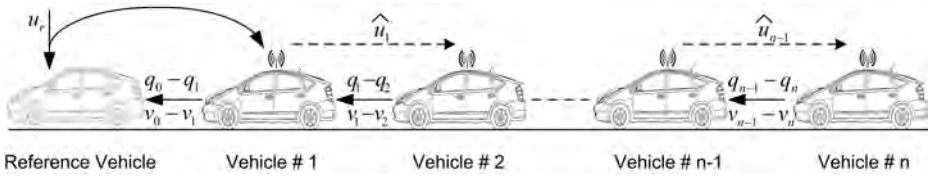

Figure 2.5: Schematic representation of the n-vehicle string.

$$
\begin{aligned}
\dot{\tilde{x}}_0 &= \tilde{A}_0\tilde{x}_0 + B_{s,0}u_r,\\
\dot{\tilde{x}}_1 &= \tilde{A}_{1,1}\tilde{x}_1 + \tilde{A}_{1,0}\tilde{x}_0 + \tilde{B}_{s,1}u_1 + \tilde{B}_{c,1}u_r,\\
\dot{\tilde{x}}_2 &= \tilde{A}_{2,2}\tilde{x}_2 + \tilde{A}_{2,1}\tilde{x}_1 + \tilde{B}_{s,2}u_2 + \tilde{B}_{c,2}\hat{u}_1,\\
&\vdots\\
\dot{\tilde{x}}_n &= \tilde{A}_{n,n}\tilde{x}_n + \tilde{A}_{n,n-1}\tilde{x}_{n-1} + \tilde{B}_{s,n}u_n + \tilde{B}_{c,n}\hat{u}_{n-1},
\end{aligned}
\tag{2.22}
$$

where extended state vectors $\tilde{x}_i, i \in \mathbb{N}_{[0,n]}$, are used here indicating the inclusion of Padé approximations for the actuator delay in the vehicles if needed (see (2.20)). By defining a new state vector $\bar{x}_n = [\tilde{x}_0^T\ \tilde{x}_1^T\ \tilde{x}_2^T\ \cdots\ \tilde{x}_n^T]^T$, we lump n vehicle subsystems together with the reference model ($\tilde{x}_0$) and use the input of the reference vehicle model (u_r) as the exogenous input to the cascaded system which can now be represented as

$$\dot{\bar{x}}_n = \bar{A}_n\bar{x}_n + \bar{B}_{s,n}\bar{u}_n + \bar{B}_{c,n}\hat{\bar{u}}_n + B_r u_r \tag{2.23}$$

with,

$$
\bar{A}_n = \begin{bmatrix} \tilde{A}_0 & 0 & 0 & \cdots & 0\\ \tilde{A}_{1,0} & \tilde{A}_{1,1} & 0 & \cdots & 0\\ 0 & \tilde{A}_{2,1} & \tilde{A}_{2,2} & \cdots & 0\\ \vdots & & \ddots & \ddots & \vdots\\ 0 & \cdots & 0 & \tilde{A}_{n,n-1} & \tilde{A}_{n,n} \end{bmatrix}, \bar{B}_{s,n} = \begin{bmatrix} 0 & \cdots & \cdots & 0\\ \tilde{B}_{s,1} & 0 & \cdots & 0\\ 0 & \tilde{B}_{s,2} & & \vdots\\ \vdots & & \ddots & 0\\ 0 & \cdots & 0 & \tilde{B}_{s,n} \end{bmatrix},
$$

$$
\bar{B}_{c,n} = \begin{bmatrix} 0 & \cdots & 0 & 0\\ 0 & \cdots & 0 & 0\\ \tilde{B}_{c,2} & \cdots & 0 & 0\\ \vdots & \ddots & \vdots & \vdots\\ 0 & \cdots & \tilde{B}_{c,n} & 0 \end{bmatrix}, \quad B_r = \begin{bmatrix} \tilde{B}_{s,0}\\ \tilde{B}_{c,1}\\ 0\\ \vdots\\ 0 \end{bmatrix},
$$

and $\hat{\bar{u}}_n = \left[\hat{u}_1\hat{u}_2\ldots\hat{u}_n\right]^T$ with $\bar{u}_n = [u_1\ u_2\ \ldots\ u_n]^T$. The control law in (2.19), i.e. $u_i = [K_{i,i-1}\ K_{i,i}][x_{i-1}^T\ x_i^T]^T$, for each sub-system $i \in \mathbb{N}_{[1,n]}$, can now be

incorporated in (2.23) by using

$$\bar{u}_n = \bar{K}_n \bar{x}_n \tag{2.24}$$

with

$$\bar{K}_n = \begin{bmatrix} K_{1,0} & K_{1,1} & 0 & \cdots & 0 \\ 0 & K_{2,1} & K_{2,2} & \cdots & 0 \\ \vdots & & \ddots & \ddots & \vdots \\ 0 & \cdots & & K_{n,n-1} & K_{n,n} \end{bmatrix}. \tag{2.25}$$

In the resulting interconnected vehicle string model (2.23), (2.24), the wirelessly communicated control commands $\hat{\bar{u}}_n$ are kept separate for future analysis.

Let us now formulate the closed-loop CACC vehicle string model (2.23)-(2.24) in a more compact form. Above, the interconnected vehicle string was formulated such that the control inputs (namely $\bar{u}_n$ and $\hat{\bar{u}}_n$) are kept separate according to their way of being acquired by the host vehicle (i.e. through direct measurement or through wireless communication, respectively). Also, the model permits to express the CACC control commands, which are actually feedforward signals from one vehicle to the next, as state feedback control laws. Now, we adopt the realistic assumption that a much higher sampling rate is employed for the locally sensed data used for the ACC functionality than for the wirelessly communicated CACC commands (which is also the case in the experimental CACC-vehicle setup presented in Chapter 5). Hence, we can model the ACC vehicle following controller as an inherently continuous-time dynamic coupling between vehicles. This results in the following compact model reformulation which allows us to analyse in detail the effects of wireless communication inputs:

$$\begin{aligned} \dot{\bar{x}}_n &= (\bar{A}_n + \bar{B}_{s,n}\bar{K}_n)\bar{x}_n + \bar{B}_{c,n}\hat{\bar{u}}_n + B_r u_r, \\ &= A_{\bar{x}_n}^{ACC}\bar{x}_n + \bar{B}_{c,n}\hat{\bar{u}}_n + B_r u_r, \end{aligned} \tag{2.26}$$

where $A_{\bar{x}_n}^{ACC} := \bar{A}_n + \bar{B}_{s,n}\bar{K}_n$, u_r is the exogenous input, and

$$\bar{z}_i = C_{z,i}\bar{x}_n, \tag{2.27}$$

is the particular output of interest whose propagation throughout the string is the subject of discussions on *string stability* in Chapters 3 and 4. Note that by setting either $\nu_i = 0$ or $\nu_i = 1$ for individual vehicles ($i \in \mathbb{N}_{[1,n]}$) in the C-ACC control law in (2.19), this interconnected vehicle string model can be used to study the string stability properties of mixed (C-)ACC vehicle strings as well.

2.6 Network-Free CACC Model

In the previous section, the wirelessly communicated control commands $\hat{\bar{u}}_n$ have been kept separate for future analysis in Chapter 4. As an ideal case, the

Network-free(NF)-CACC model is obtained by assuming that the CACC control inputs are perfectly transmitted (i.e. no network effects are introduced) and therefore, $\hat{\bar{u}}_n = \bar{u}_n = \bar{K}_n \bar{x}_n$ can also be incorporated in (2.26) to yield

$$\begin{aligned} \dot{\bar{x}}_n &= (\bar{A}_n + (\bar{B}_{s,n} + \bar{B}_{c,n})\bar{K}_n)\bar{x}_n + B_r u_r, \\ &= A_{\bar{x}_n}^{NF} \bar{x}_n + B_r u_r, \end{aligned} \tag{2.28}$$

where $A_{\bar{x}_n}^{NF} := \bar{A}_n + (\bar{B}_{s,n} + \bar{B}_{c,n})\bar{K}_n$, and

$$\bar{z}_i = C_{z,i} \bar{x}_n \tag{2.29}$$

is the output of the system.

In Chapter 3, we will use this NF-CACC model for investigating *string stability* properties of such systems when the wireless communication imperfections are absent. These analyses will serve as a reference for the evaluation of the networked system performance in Chapter 4.

2.7 Conclusions

The interconnected vehicle string model, constructed in this chapter, arises from the dynamical coupling of a cascade of CACC vehicles, each of which is controlled to maintain a desired distance to its predecessor (vehicle following) and to ensure string stability. In order to construct this overall model, the vehicle longitudinal dynamics and the vehicle following controller were presented that together constitute the closed-loop CACC vehicle models. These closed-loop CACC vehicle models form the basic building blocks of the overall interconnected vehicle string model and will be used for discussions on the string stability properties of these types of interconnected systems in Chapter 3. In this overall vehicle string model, two types of data employed in the CACC controller are distinguished according to the way they are being transferred, i.e. either locally sensed or wirelessly communicated information. This approach allows to cast the interconnected system dynamics with wireless communication constraints into a Networked Control System (NCS) model that incorporates the effects of sample-and-hold, transmission frequency and network delays (see Chapter 4). In turn, this modelling approach permits us to pursue a string stability analysis that takes these effects of wireless communication into account in Chapter 4. As a special case, the Network-Free(NF)-CACC model has been also introduced where the imperfections induced by the wireless communication are assumed to be negligible. This model will serve as a basis for the *string stability* properties of interconnected systems in Chapter 3, and the analyses obtained therewith serve as a reference for the evaluation of the networked system performance in Chapter 4.

Chapter 3

String Stability of Interconnected Vehicles

3.1 Introduction

In addition to realizing the vehicle following objective that is described in the previous chapter in Section 2.1, another important requirement in a CACC vehicle platooning system is to avoid amplification of the effect of disturbances throughout the string as the vehicle index increases. The amplification of such disturbances not only poses risks on safe and reliable operation of the individual vehicle following controllers but also compromises traffic flow stability and throughput. Hence, stability should not only be studied in the time domain, but also in the spatial domain, such as in so-called mesh stability [56]. For spatially 1-D systems, this property is called *string stability*. For the evaluation of string stability, one considers the amplification of variables such as the distance error, the velocity, the acceleration or the control effort along the vehicle string [77, 49, 61].

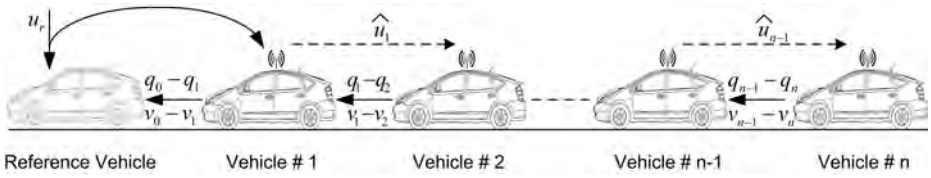

Figure 3.1: Schematic representation of the n-vehicle string.

In this chapter, we will discuss *string stability* properties of interconnected vehicle strings by using the models that were developed throughout Chapter 2. The Network-Free(NF)-CACC model presented in Section 2.6 forms the basis for the string stability analysis of this particular type of interconnected vehicle strings. First, in Section 3.2, we use this interconnected vehicle string model for the illustration of the string (in)-stability phenomenon by time simulations and the discussion of the effects of amplification of certain signals along the vehicle string on realizing the control objectives. In Section 3.3, we present frequency-domain based conditions for string stability. In Section 3.4, we present dissipation-based counterparts of these conditions for string stability. In these analyses, we will assume (for now) that the wirelessly exchanged CACC control commands are perfectly transmitted; therefore, wireless communication imperfections such as sampling, delays, and losses are not yet considered in this chapter. A network-aware modelling and string stability analysis framework, where these imperfections are taken account, will be pursued in Chapter 4. These results will exploit the tools and methods presented in this chapter. In Chapter 4, both frequency-domain and dissipation-based conditions for string stability will be employed.

Before we proceed with the analysis of string stability properties in the next sections, we will concisely recapitulate the network-free CACC platooning model.

Network-Free CACC Model

The vehicle platoon shown in Fig. 3.1 is modelled by using the NF-CACC model for an n-vehicle string in (2.28) to model the interconnection of n-vehicles together with the reference model (vehicle $i = 0$). We use the input of the reference vehicle model (u_r) as the exogenous input to the resulting cascaded system

$$\begin{aligned} \dot{\bar{x}}_n &= f(\bar{x}_n, u_r) := A^{NF}_{\bar{x}_n} \bar{x}_n + B_r u_r, \\ \bar{z}_i &= C_{z,i} \bar{x}_n, \end{aligned} \tag{3.1}$$

where $A^{NF}_{\bar{x}_n} := \bar{A}_n + (\bar{B}_{s,n} + \bar{B}_{c,n})\bar{K}_n$, and $\bar{x}_n = [x_0^T \; x_1^T \; x_2^T \; \cdots \; x_n^T]^T$ are the lumped states of the vehicles ($i \in \mathbb{N}_{[0,n]}$) in the vehicle string depicted in Fig. 3.1. Here, we presume that the actuation delay can be neglected and hence the closed-

Vehicle Model Parameters		(C-)ACC Parameters		Initial Conditions	
η_i	0.1	ν_i	0 (ACC), 1 (CACC)	$v_i(0)$	20 [m/sec]
$\omega_{g,i}$	10	$k_{p,i}$	0.25	$e_i(0)$	0 [m]
$\tau_{a,i}$	0	$k_{d,i}$	0.5	$u_i(0)$	0 [m/sec^2]
κ	-	$\omega_{c,i}$	0.5		

Table 3.1: Parameter set used in the simulations shown in Fig 3.2.

loop (C-)ACC vehicle dynamics of the individual vehicles are governed by

$$\begin{aligned} \dot{x}_i &= f_i(x_i, x_{i-1}, u_{i-1}) = A_{i,i}x_i + A_{i,i-1}x_{i-1} + B_{s,i}u_i + B_{c,i}u_{i-1}, \\ u_i &= K_{i,i}x_i + K_{i,i-1}x_{i-1}, \end{aligned} \tag{3.2}$$

where $x_i^T = [e_i \ v_i \ a_i \ u_{ff,i}] \in \mathbb{R}^{n_x}$ are the states of the i-th CACC equipped vehicle in the n-vehicle string for ($i \in \mathbb{N}_{[2,n]}$) with the longitudinal dynamics in (2.4). For the dynamics of the reference vehicle ($i = 0$) and the leader vehicle ($i = 1$), see (2.21) and (2.22), respectively, in Section 2.5. The actuation delay in longitudinal dynamics can also be incorporated by using (2.20) with (2.9), but is excluded for the sake of simplicity in the discussions in this chapter. Particular outputs of interest, whose propagation along the vehicle string will be inspected, are selected by choosing $\bar{z}_i$ accordingly in (3.1).

3.2 Time-Domain Illustration of String Stability

In this section, we present time-domain simulation results which are obtained by using the Network-Free CACC model in (3.1). These time-domain simulations illustrate the propagation of vehicle responses along the vehicle string and provide an intuitive understanding of the shockwave and interrelated string (in-)stability phenomenon. Based on these results, the effects of amplification of certain signals on realizing the set control objectives is discussed next. In Fig. 3.2, time-domain simulation results are shown, which are obtained by using the interconnected vehicle string model in (3.1) for a vehicle string formed by selecting $n = 12$, where individual vehicle outputs are chosen by selecting either $\bar{z}_i = e_i$, $\bar{z}_i = u_i$, or $\bar{z}_i = v_i, i \in \mathbb{N}_{[0,n]}$, accordingly in (3.1) with the parameter set given in Table 3.1. Note that the parameters for each vehicle in the string are taken the same, which corresponds to a homogeneous vehicle string. An exogenous input perturbation is then introduced by the reference vehicle in the string ($i = 0$) in the form of a step-wise change in the desired acceleration u_r, which is given as:

$$u_r(t) = \begin{cases} 1 \text{ m/sec}^2 & , 20 \leq t \leq 30, \\ 0 & , \text{ otherwise.} \end{cases}$$

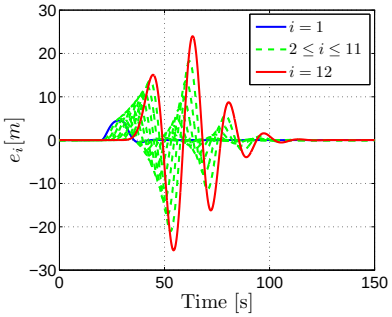

(a) Propagation of e_i in ACC, $h_{d,i} = 0.3, i \in \{1, \ldots, 12\}$.

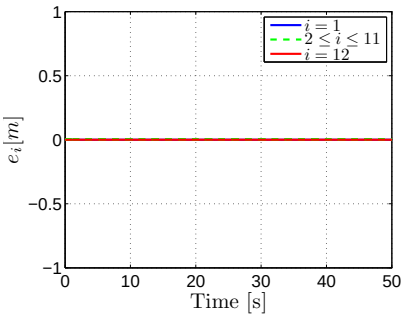

(b) Propagation of e_i in CACC, $h_{d,i} = 0.3, i \in \{1, \ldots, 12\}$.

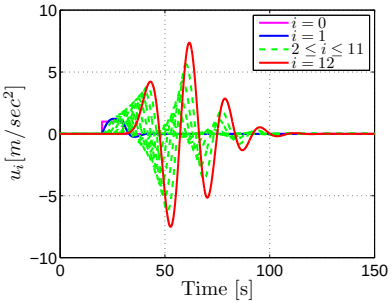

(c) Propagation of u_i in ACC, $h_{d,i} = 0.3, i \in \{1, \ldots, 12\}$.

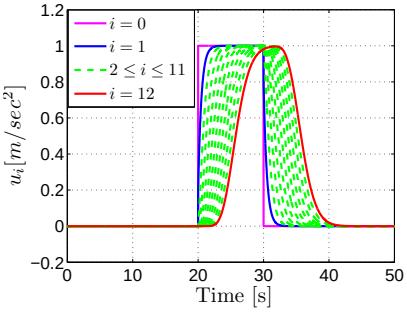

(d) Propagation of u_i in CACC setting, $h_{d,i} = 0.3, i \in \{1, \ldots, 12\}$.

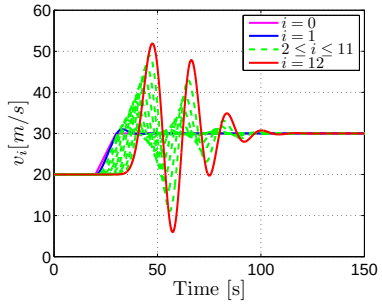

(e) Propagation of v_i in ACC setting, $h_{d,i} = 0.3, i \in \{1, \ldots, 12\}$.

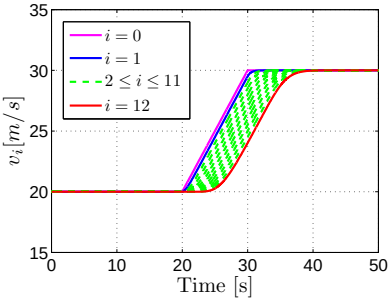

(f) Propagation of v_i in CACC setting, $h_{d,i} = 0.3, i \in \{1, \ldots, 12\}$.

Figure 3.2: Illustration of the propagation of the effect of the disturbance $u_r(= u_0)$ on e_i, u_i and v_i, $h_{d,i} = 0.3$ sec.

The responses e_i, u_i and v_i of the vehicles in the platoon to this exogenous perturbation as the vehicle index (i) increases are shown in Fig. 3.2, where a small headway-time value $h_d = 0.3$ sec. is selected in order to demonstrate the improved string stability property that can be achieved with the use of CACC (see Fig. 3.2.b.d.f) when compared to the use of ACC (see Fig. 3.2.a.c.e).

The simulation results show that the vehicles in the ACC-setting achieve the vehicle following objective (i.e. regulating e_i to 0 asymptotically) only when the platoon reaches a constant speed in steady state after the perturbation vanishes (i.e. $u_r = 0$), whereas in the CACC-setting, the vehicles are capable of realizing the convergence of e_i to 0 also in the presence of time-varying perturbations $u_r(t)$, hence improving the vehicle following performance. Fig. 3.2.a.c.e clearly illustrate the amplification of the responses along the vehicle string (indicating string instability) for the ACC-setting, while no such amplification occurs for the CACC-setting (indicating string stability). In practice, the amplification of e_i, u_i, and v_i for increasing i (as present in the ACC-setting) endangers safety, compromises vehicle dynamics limitations and passenger comfort, and adversely affects traffic throughput in the following ways:

- The amplification of the distance errors e_i mainly influences the inter-vehicle spacing which is of crucial importance especially from a safety perspective. To compensate for such a deviation from the desired inter-vehicle spacing, the constant r_i in (2.1) would have to be set much higher which contradicts with the objective of increasing the traffic throughput;

- The amplification of the control efforts u_i (i.e. desired acceleration) mainly affects reliable operation of the vehicle following controller. Amplified control efforts u_i may result in acceleration requests that exceed the limitations of vehicle dynamics and may also compromise passenger comfort;

- The amplification of velocity deviations in v_i can bring the traffic to a full stop kilometers away from the disturbance source and cause traffic instabilities resulting in so-called *ghost traffic jams*, therewith seriously compromising traffic throughput.

As illustrated in Fig. 3.2, the CACC controller presented in Section 2.3 allows smaller inter-vehicle distances without the amplification of distance errors e_i, velocity deviations v_i, and the control efforts u_i.

Although time-domain illustrations, as presented in this section, are useful for the intuitive understanding of the propagation of disturbances, and therewith of the related string (in)-stability phenomenon, for parametric analyses that can aid the design of CACC systems, we need analytical tools to quantify the amplifications leading to system-theoretic string stability conditions. Therefore, we will introduce such mathematical tools and system-theoretic conditions for such string stability analysis in the following sections.

3.3 Frequency-domain Based String Stability Conditions

For the evaluation of string stability, one considers the amplification of the distance error, the velocity, the acceleration or the control effort along the vehicle string [77, 49, 61]. One can investigate the propagation of particular outputs corresponding to vehicle i, either in response to the exogenous disturbance input u_r or with respect to its predecessor $(i-1)$. These two different perspectives on investigating response propagation along the vehicle string relate to the notions of *weak* and *strong* string stability. To study these distinct string stability notions, the so-called *weak* and *strong string stability transfer functions* will be introduced next.

Weak String Stability

The weak string stability requirement can be interpreted as a condition on the maximal amplification of the effect of a perturbation (in this case $u_r = u_0$) at the front of the string on the responses along the vehicle string. Such amplification can be quantified by the magnitude of the so-called *weak string stability* transfer function, defined as

$$\begin{aligned} S^w_{\Delta_{i,r}}(s) :&= \frac{\Delta_i(s)}{u_r(s)}, \quad i \in \mathbb{N}_{[1,n]}, s \in \mathbb{C}, \\ &= \frac{\Delta_i(s)}{\Delta_r(s)} \frac{\Delta_r(s)}{u_r(s)}. \end{aligned} \tag{3.3}$$

Herein, $\Delta_i(s) := \mathscr{L}(\delta_i)$ with δ_i as the signal of interest for the evaluation of string stability, $\Delta_r(s) := \mathscr{L}(\delta_0)$, and $\mathscr{L}$ denotes, as before, the Laplace operator. Assuming that

$$S^w_{\Delta_{r,r}} := \frac{\Delta_r(s)}{u_r(s)} \tag{3.4}$$

exists and has a bounded $\mathcal{H}_\infty$-norm

$$\gamma^r := \left\| S^w_{\Delta_{r,r}}(s) \right\|_{\mathcal{H}_\infty} = \sup_{\omega \in \mathbb{R}} \left| S^w_{\Delta_{r,r}}(j\omega) \right|, \tag{3.5}$$

the maximum amplification from u_r to δ_i can be represented by the $\mathcal{H}_\infty$-norm of the weak string stability transfer function in (3.3) as follows:

$$\left\| S^w_{\Delta_{i,r}}(s) \right\|_{\mathcal{H}_\infty} = \sup_{\omega \in \mathbb{R}} \left| S^w_{\Delta_{i,r}}(j\omega) \right|, \tag{3.6}$$

where for the linear system given in (3.1) the weak string stability transfer function can be expressed as

$$S^w_{\Delta_{i,r}}(s) = C_{z,i}(sI - A^{NF}_{\bar{x}_n})^{-1} B_r. \tag{3.7}$$

Vehicle Model Parameters		(C-)ACC Parameters	
η_i	0.1	ν_i	0 (ACC), 1 (CACC)
$\omega_{g,i}$	10	$\omega_{c,i}$	2
$\tau_{a,i}$	0	$k_{p,i}$	4
κ	–	$k_{d,i}$	2

Table 3.2: Parameter set used for the frequency-domain and dissipation-based string stability analyses.

In accordance with [42, 49], we now formulate the following condition for *weak string stability*:

$$\left\| S^w_{\Delta_{i,r}}(s) \right\|_{\mathcal{H}_\infty} \leq \gamma^r, \forall i \in \mathbb{N}_{[1,n]}, \tag{3.8}$$

where γ^r is given as in (3.5).

Remark 3.1. When the i-th vehicle control command u_i is selected as the particular output of interest, the weak string stability condition in (3.8) becomes

$$\left\| S^w_{\Delta_{i,r}}(s) \right\|_{\mathcal{H}_\infty} \leq 1, \forall i \in \mathbb{N}_{[1,n]}, \tag{3.9}$$

since in that case, by definition $\gamma^r = 1$. ◁

In Fig. 3.3(a), 3.3(b), Bode plots of $S^w_{\Delta_{2,r}}$ are shown which are obtained for $z_2 = u_2$ (i.e. $C_{z,2} = [0_{1\times 4}\ K_{2,1}\ K_{2,2}\ 0_{1\times 4}\ \dots\ 0_{1\times 4}]_{1\times n_x(n+1)}$ for $i = 2$ in (3.7)) in an n-vehicle string with the parameter-set given in Table 3.2. For

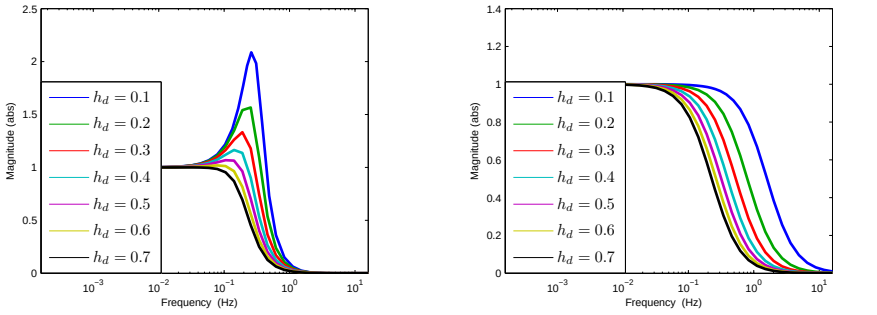

(a) $S^w_{\Delta_{2,r}}(j\omega) = |\frac{u_2(j\omega)}{u_r(j\omega)}|$ for an ACC string. (b) $S^w_{\Delta_{2,r}}(j\omega) = |\frac{u_2(j\omega)}{u_r(j\omega)}|$ for a CACC string.

Figure 3.3: Weak string stability analysis of the Network-Free (C-)ACC vehicle string for different headway-times (h_d).

illustrative purposes, we consider in this analysis a two-vehicle string (i.e. $n = 2$). Here, it can be seen that the response of the ACC string satisfies the condition (3.9) only for relatively large headway-time values (larger than 0.7 sec), whereas the NF(ideal)-CACC system is weakly string stable according to (3.8) for all headway-time values that were considered.

Strong String Stability

Another (in general more stringent) condition for string stability is obtained when the propagation of specific signals is inspected from vehicle $i-1$ to vehicle i and is described in terms of the *strong string stability* transfer function, which is defined as

$$\begin{aligned} S^s_{\Delta_{i,i-1}}(s) &:= \frac{\Delta_i(s)}{\Delta_{i-1}(s)}, \;\; i \in \mathbb{N}_{[1,n]}, s \in \mathbb{C}, \\ &= \frac{\Delta_i(s)}{u_r(s)} \left(\frac{\Delta_{i-1}(s)}{u_r(s)} \right)^{-1}, \\ &= S^w_{\Delta_{i,r}}(s)(S^w_{\Delta_{i-1,r}}(s))^{-1}. \end{aligned} \tag{3.10}$$

Remark 3.2. To guarantee existence of the strong string stability transfer function in (3.10), we require that the weak string stability function is functionally controllable [57] (i.e. $S^w_{\Delta_{i-1,r}}$ is of full rank), such that $(S^w_{\Delta_{i-1,r}})^{-1}$ indeed exists. $\lhd$

Based on this definition, we formulate the following condition for *strong string stability* as in [49]:

$$\left\| S^s_{\Delta_{i,i-1}}(s) \right\|_{\mathcal{H}_\infty} \leq 1, \;\; \forall i \in \mathbb{N}_{[1,n]}, \tag{3.11}$$

where

$$\left\| S^s_{\Delta_{i,i-1}}(s) \right\|_{\mathcal{H}_\infty} = \sup_{\omega \in \mathbb{R}} \left| S^s_{\Delta_{i,i-1}}(j\omega) \right|. \tag{3.12}$$

In Fig. 3.4(a), 3.4(b), Bode plots of the strong string stability function $S^s_{\Delta_{2,1}}$ are shown which are obtained from (3.10) by selecting $z_2 = u_2$ (i.e. $C_{z,2} = [0_{1\times 4}\ K_{2,1}\ K_{2,2}\ 0_{1\times 4} \ldots 0_{1\times 4}]_{1\times n_x(n+1)}$ for $i = 2$ in (3.7)) and $z_1 = u_1$ (i.e. $C_{z,1} = [K_{1,0}\ K_{1,1}\ 0_{1\times 4}\ 0_{1\times 4}\ \ldots\ 0_{1\times 4}]_{1\times n_x(n+1)}$ for $i = 1$ in (3.7)) in an n-vehicle string with the parameter set given in Table 3.2. Similar to the weak string stability analysis results presented in the previous section, for illustrative purposes, we consider a two-vehicle string (i.e. $n = 2$) in this analysis. The analysis shows that the response of the ACC string satisfies the strong string stability condition in (3.11) only for relatively large headway-time values (larger than 0.7 sec), whereas the NF(ideal)-CACC system is strongly string stable according to (3.11) for all headway-time values that were considered.

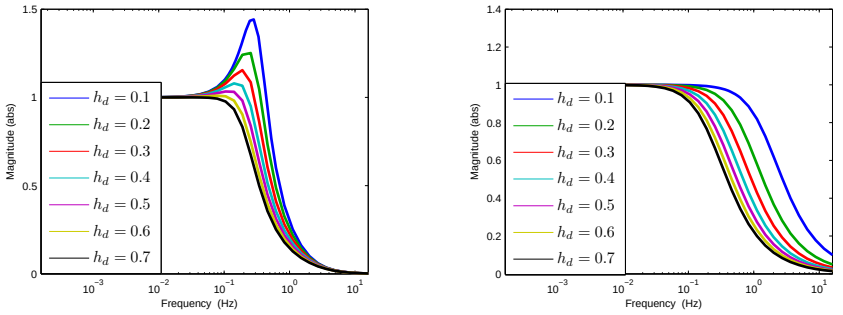

(a) $S^s_{\Delta_{2,1}}(j\omega) = |\frac{u_2(j\omega)}{u_1(j\omega)}|$ for an ACC string. (b) $S^s_{\Delta_{2,1}}(j\omega) = |\frac{u_2(j\omega)}{u_1(j\omega)}|$ for a CACC string.

Figure 3.4: Strong string stability analysis of the Network-Free (C-)ACC vehicle string for different headway-times (h_d).

The strong string stability condition presented in this section forms the basis of the network-aware string stability analysis method in Section 4.2, which will be experimentally validated in Chapter 5 with CACC-equipped prototype vehicles.

3.4 Dissipation Inequality-based String Stability Conditions

Next, the propagation of disturbances through the interconnected vehicle string is inspected by using a notion of *string stability* which is formulated in terms of an $\mathcal{L}_2$-gain requirement from disturbance inputs to controlled outputs. This allows to formulate the string stability conditions in the form of dissipation inequalities for which conditions in terms of Linear Matrix Inequalities (LMIs) can be formulated and numerical solutions can be obtained. When Linear Time-Invariant (LTI) systems are considered, these dissipation inequality-based conditions are identical to their $\mathcal{H}_\infty$-based counterparts presented in Section 3.3. However, in the networked CACC setting considered in Section 4.3, we will analyse string stability also for systems that are subject to time-varying network-induced effects. In this case frequency-domain conditions for string stability are not applicable while the dissipation inequality-based formulation of string stability can be used. In addition, in the latter case Lyapunov techniques for $\mathcal{L}_2$-gain analysis can be used for these type of time-varying systems [69, 15].

Weak String Stability

Similar to the frequency-domain based condition for the evaluation of weak string stability, one considers the amplification of the effect of a disturbance at the front of the string on the distance error, the velocity, the acceleration or the control effort along the vehicle string as vehicle index (i) increases [77, 49, 61]. In this work, the focus will be on the propagation of the control effort u_i along the string in the definition of dissipation inequality-based conditions for string stability.

Definition 3.1. *The control system given by (3.1) is said to be $\mathcal{L}_2$-stable with gain $\bar{\theta}_{n,i}$, if there is a $\mathscr{K}_\infty$-function[1] β such that for any exogenous input $u_r \in \mathcal{L}_2$, and any initial condition $\bar{x}_n(0)$, each corresponding solution to (3.1) satisfies*

$$\|\bar{z}_i\|_2 \leq \beta(|\bar{x}_n(0)|) + \bar{\theta}_{n,i} \|u_r\|_2 . \tag{3.13}$$

Furthermore, we say that the control system (of an $n-$vehicle string) in (3.1) is weakly string stable (WSS) if (3.13) is satisfied for $\bar{\theta}_{n,i} \leq 1$ for all $i \in \mathbb{N}_{[1,n]}$.

Remark 3.3. Note that for the linear system (3.1), the $\mathcal{L}_2$-gain of the system according to Definition 3.1 equals the $\mathcal{H}_\infty$-norm of the weak string stability transfer function in (3.6) (with $S^w_{\Delta_{i,r}}(s)$ as in (3.7)) [69]. ◁

This definition for weak string stability expresses that, since we focus on the propagation of the control effort u_i, $i \in \mathbb{N}_{[1,n]}$, as the particular output of interest, we require the $\mathcal{L}_2$-gain from u_r to output $\bar{z}_i = u_i = C_{z,i}\bar{x}_n$, $i \in \mathbb{N}_{[1,n]}$ to be less than or equal to one ($\bar{\theta}_{n,i} \leq 1$) for weak string stability. To guarantee WSS as defined above, it is sufficient to satisfy the following dissipation inequality-based condition [69].

Condition 3.1. *The control system (of an $n-$vehicle string) given by (3.1) is WSS if there exists a continuously differentiable, positive definite, and proper storage function $\bar{V} : \mathbb{R}^{(n+1)n_x} \to \mathbb{R}_{\geq 0}$ that satisfies the dissipation inequality*

$$\left\langle \nabla \bar{V}(\bar{x}_n), f(\bar{x}_n, u_r) \right\rangle \leq \bar{\theta}^2_{n,i} \|u_r\|^2 - \|C_{z,i}\bar{x}_n\|^2 \tag{3.14}$$

for all $\bar{x}_n \in \mathbb{R}^{(n+1)n_x}$ and all $u_r \in \mathbb{R}$ with $\bar{\theta}_{n,i} \leq 1, \forall i \in \mathbb{N}_{[1,n]}$.

Control commands of individual vehicles within the vehicle string can be selected by using $\bar{z}_i = u_i = C_{z,i}\bar{x}_n$ accordingly in (3.1). To verify the condition in (3.14), a quadratic storage function $\bar{V}(\bar{x}_n) = \bar{x}_n^T \bar{P} \bar{x}_n$ was chosen to compute the $\mathcal{L}_2$-gain from u_r to u_i (e.g. $C_{z,2} = [0_{1\times 4}\ K_{2,1}\ K_{2,2}\ 0_{1\times 4}\ \dots\ 0_{1\times 4}]_{1\times n_x(n+1)}$ for $i = 2$) and we minimize $\bar{\theta}_{n,i}$ subject to the LMIs

$$\begin{pmatrix} (A_{\bar{x}_n})^T \bar{P} + \bar{P} A_{\bar{x}_n} + C_{z,i}^T C_{z,i} & \bar{P} B_r \\ B_r^T \bar{P} & -\bar{\theta}^2_{n,i} I \end{pmatrix} \preceq 0, \ \bar{P} = \bar{P}^T \succ 0. \tag{3.15}$$

[1] A continuous function $\beta : [0, \infty) \to [0, \infty)$ is said to belong to class $\mathscr{K}_\infty$ if it is strictly increasing, $\beta(0) = 0$, and $\lim_{s\to\infty} \beta(s) = \infty$.

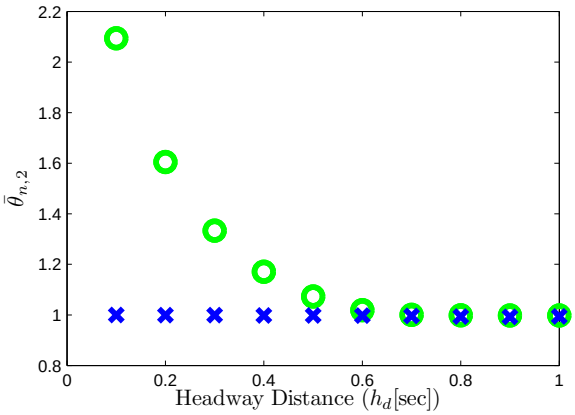

Figure 3.5: $\mathcal{L}_2$-gain ($\bar{\theta}_{n,2}$) from u_r to $u_{n,2}$ for ACC (o) and CACC (x).

This analysis has been performed for various headway-time values (h_d) which yield the results presented in Fig. 3.5 for the second vehicle ($i = 2$) in an n-vehicle string with the parameter set in Table 3.2. The analysis shows that the response of the ACC string satisfies the condition (3.14) with $\bar{\theta}_{n,i} = 1$ only for relatively large headway-time values (larger than 0.7 sec), whereas the NF(ideal)-CACC system is string stable according to (3.14) for all headway-time values that were considered. Also, the $\mathcal{L}_2$-gains for corresponding headway-time values equal the peak amplitude values of the corresponding Bode plots of the weak string stability transfer function in Fig. 3.3a-b. This is no surprise due to the well known relation between the $\mathcal{L}_2$-gain and the $\mathcal{H}_\infty$-norm for LTI systems, as we already mentioned before in Remark 3.3. This analysis forms the basis for the evaluation of the network-aware CACC modelling and string stability analysis pursued in Chapter 4 by providing the ideally achievable (no network) $\mathcal{L}_2$-gain in (3.14) and shows that $\bar{\theta}_{n,i}$ is lower bounded by $\bar{\theta}^*_{n,i} = 1$ which is also in accordance with the DC gain of the Bode plots in Fig. 3.3 and Fig 3.4. This lower bound of 1 on $\bar{\theta}_{n,i}$ is a direct consequence of the vehicle following objective (achieved by the proposed (C-)ACC controller). In Section 4.3, we will employ the dissipation-inequality based Condition 3.1 presented here, for the weak string stability analysis of interconnected vehicle strings that are subject to time-varying network-induced effects.

A dissipation inequality-based counterpart of the frequency-domain based strong string stability condition given in (3.11) is of interest for future research but is not considered in this thesis.

Propagation of $\mathcal{L}_2$-gains

Fig. 3.6 demonstrates the use of these dissipation-based tools for the inspection of the propagation of the $\mathcal{L}_2$-gain from u_r to u_i as vehicle index (i) increases (i.e. $\bar{\theta}_{n,i}$ in (3.14) as i is varied) for the case of a string of 5 vehicles ($n = 5$ in (4.1)). Three different scenarios are presented in Fig. 3.6.a-c., all with the same headway-time (i.e. $h_{d,i} = h_d = 0.1, \forall i \in \{1, \ldots, 5\}$). These scenarios are respectively an ACC-controlled string, a CACC-controlled string, and a mixed string where the third vehicle ($i = 3$) is equipped with ACC while the rest is equipped with CACC. In Fig. 3.6.d-f., the effect of varying the headway-time is visible. In Fig. 3.6.a,b,d,e it can be observed that the $\mathcal{L}_2$-gain propagation is idempotent (i.e. of the same power) throughout the string as the vehicle index increases when vehicles are equipped with identical (C-)ACC controllers. In the ACC setting, the $\mathcal{L}_2$-gain is amplified whereas in the CACC-string Fig. 3.6.b, the $\mathcal{L}_2$-gain remains the same backward in the string as $\bar{\theta}_{n,i} = 1$. In these figures, one can also observe that the $\mathcal{L}_2$-gain according to (3.15) is lower bounded by $\bar{\theta}^*_{n,i} = 1$. This lower bound of 1 on $\bar{\theta}_{n,i}$ is a direct consequence of the vehicle following objective (achieved by the proposed (C-)ACC controller).

3.5 Conclusions

Besides the vehicle following objective, the attenuation of the effect of disturbances on the vehicle responses along the vehicle string, captured by the notion of *string stability*, is of crucial importance in longitudinal automation of vehicle platoons. String stability is an essential requirement which relates to aspects such as safety, comfort, traffic flow stability, and traffic throughput. In this chapter, string stability analysis methods have been presented by using the interconnected vehicle string models developed in Chapter 2. Time-domain simulations are used to illustrate the occurrence of the shockwaves that indicate string instability. For the analysis of string stability, mathematical tools for quantifying the amplitude of the propagation of vehicle responses have been presented which make use of frequency-domain and dissipation inequality-based techniques. String stability analysis results have been presented for the ideally achievable (no network) (C-)ACC setting by using frequency-based and dissipation inequality-based methods for string stability analyses. These analyses form the basis for the evaluation of the network-aware CACC modelling and analysis framework which will be pursued in Chapter 4.

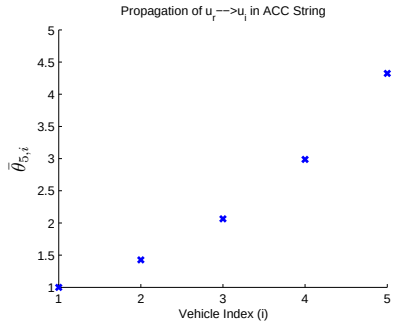

(a) $u_r \xrightarrow{\mathcal{L}_2} u_i$ in ACC string (h_d=0.1).

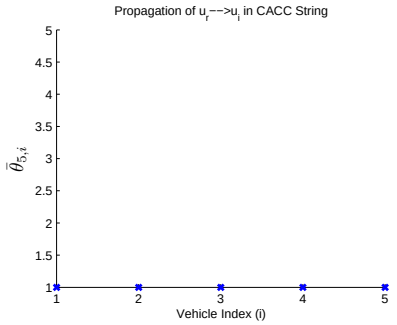

(b) $u_r \xrightarrow{\mathcal{L}_2} u_i$ in CACC string (h_d=0.1).

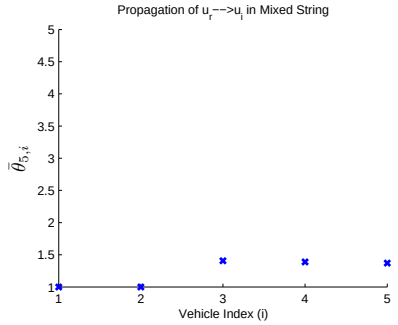

(c) $u_r \xrightarrow{\mathcal{L}_2} u_i$ in mixed (C-)ACC string (h_d=0.1).

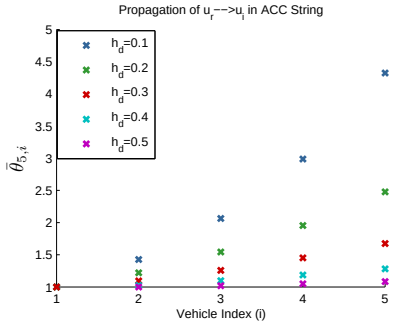

(d) $u_r \xrightarrow{\mathcal{L}_2} u_i$ in ACC string (varying h_d).

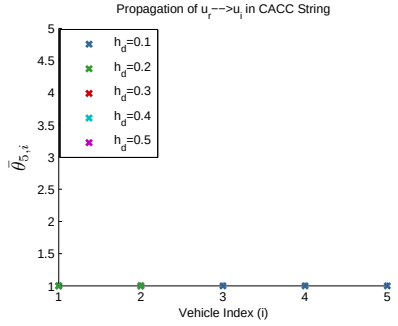

(e) $u_r \xrightarrow{\mathcal{L}_2} u_i$ in CACC string (varying h_d).

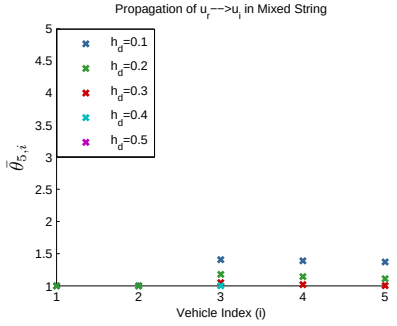

(f) $u_r \xrightarrow{\mathcal{L}_2} u_i$ in mixed (C-)ACC string (varying h_d).

Figure 3.6: Propagation of $\mathcal{L}_2$-gains (e.g. $u_r \to u_i$) as vehicle index (i) increases for three different string scenarios and different headway-times.

Chapter 4

Network-aware Cooperative Adaptive Cruise Control

4.1 Introduction

Cooperative Adaptive Cruise Control (CACC), is an extension of the currently available Adaptive Cruise Control (ACC) technology with the addition of information exchange between vehicles through wireless Vehicle-to-Vehicle (V2V) and Vehicle-to-Infrastructure (V2I) communication. CACC can significantly contribute to increasing the traffic flow on highways by utilizing information exchange between vehicles through wireless communication besides local sensor measurements. Wireless information exchange between vehicles provides means for overcoming sensory limitations of human or ACC operated vehicles. Significant improvements over existing ACC technology can be achieved already with relatively simple control algorithms and communication structures, but real-life implementation requires the consideration of the constraints imposed by the wireless communication. Given the fact that multiple nodes (vehicles) share the same medium with a limited bandwidth and capacity, wireless communication introduces network-induced imperfections such as transmission delays and packet losses. The impact of these imperfections on string stability requires a careful

analysis and tradeoffs between CACC performance and network specifications need to be made for achieving desired performance under these network-induced constraints.

In the scope of CACC, control over a wireless communication network is the enabling technology that makes CACC realizable; however, very few studies of CACC consider the imperfections that are introduced by the network [42, 70, 55, 54]. In [70], stability of a vehicle platooning control system which relies merely on wireless information exchange (i.e. without a local sensor such as radar) has been studied, whereas, in the control strategy we consider in this work, only the CACC input is transmitted via wireless communication as an addition to the underlying ACC controller which uses local sensor (e.g. radar) measurements. In [42], a continuous-time transfer function analysis of constant time delays was carried out which considers a time slotted token-passing type network similar to the discretisation-based approach presented in Section 4.2 which also considers constant time delays and fixed transmission intervals. However, different from [42], the discretisation-based approach adopted here also takes into account the sampling (and zero-order hold) of the information due to wireless communication. Moreover, the hybrid system-based Networked Control Systems (NCS) method in Section 4.3 also allows for analysis of effects of uncertain and time-varying sampling/transmission intervals and communication delays, which was not the case in [42]. The work presented in [55, 54, 53] are preliminary versions of the results presented in this thesis.

In this chapter, a network-aware modelling and analysis framework is built on the basis of the interconnected vehicle string model that was constructed in Chapter 2 and by using the string stability analysis tools presented in Chapter 3. In Chapter 2, the general control objective, the underlying longitudinal vehicle dynamics, and the control structure which together form the CACC vehicle model were introduced. Here, we will use the interconnected vehicle string model constructed in Section 2.5 in (2.23) which we repeat here for convenience

$$\begin{aligned} \dot{\bar{x}}_n &= \bar{A}_n \bar{x}_n + \bar{B}_{s,n} \bar{u}_n + \bar{B}_{c,n} \hat{\bar{u}}_n + B_r u_r, \\ \bar{z}_i &= C_{z,i} \bar{x}_n, \end{aligned} \tag{4.1}$$

where $\bar{x}_n = [x_0^T \; x_1^T \; x_2^T \; \cdots \; x_n^T]^T$ are the lumped states of the vehicles ($i \in \mathbb{N}_{[0,n]}$) in the vehicle string. For the network-aware string stability analyses in this chapter, we presume that the actuation delay can be neglected and hence the closed-loop (C-)ACC vehicle dynamics of the individual vehicle is governed by

$$\dot{x}_i = A_{i,i} x_i + A_{i,i-1} x_{i-1} + B_{s,i} u_i + B_{c,i} \hat{u}_{i-1}, \tag{4.2}$$

where $x_i^T = [e_i \; v_i \; a_i \; u_{ff,i}] \in \mathbb{R}^{n_x}$ are the states of the i-th CACC equipped vehicle in the n-vehicle string for ($i \in \mathbb{N}_{[2,n]}$) with the longitudinal dynamics in (2.4). For the dynamics of the reference vehicle ($i = 0$) and the leader vehicle ($i = 1$), see (2.21) and (2.22) in Section 2.5. The actuation delay in longitudinal

dynamics can also be incorporated by using (2.20) with (2.9) (as will be shown in Chapter 5), but is excluded for the sake of simplicity in the discussions in this chapter. Particular outputs of interest, whose propagation along the vehicle string will be inspected, are selected by choosing $\bar{z}_i$ accordingly in (4.1).

In this model, two types of data employed in the CACC controller are distinguished according to their way of being transferred as locally sensed $\bar{u}_n$ and wirelessly communicated $\hat{\bar{u}}_n$ information. This allows, on the one hand, to consider the local sensor measurements as internal dynamics of the interconnected system and, on the other hand, to focus on the effects of network-induced imperfections on the wirelessly communicated data. Based on this network-aware modelling approach, we extend the string stability analysis techniques presented in Chapter 3 to study the *string stability* properties of the string in which vehicles are interconnected by a vehicle following control law and a constant time headway spacing policy when wireless communication imperfections are present.

These analyses can be used to investigate tradeoffs between CACC performance (string stability) and network specifications (such as delays) which are essential in the multi-disciplinary design of CACC-based platooning systems. The main purpose of this chapter is to emphasize the necessity for considering CACC in a Networked Control Systems (NCS) framework by studying the effects of wireless communication on the performance of an existing CACC controller in terms of string stability. Moreover, we also show how these string stability analyses can provide the designer with guidelines for making the tradeoffs between control and network specifications.

In Section 4.2, we present the networked CACC model and derive a discrete-time interconnected system model following from a discretisation of the networked CACC model at the transmission instants (at which data is sent over the wireless network). In doing so, we propose a discretisation-based NCS modelling and analysis approach which incorporates the effects of the sampling and the zero-order-hold (of the data sent over wireless) in addition to constant wireless communication delays. We use the frequency-domain based string stability analysis presented in Section 3.3 to obtain maximum allowable time delays for different settings for the controller parameters (such as the time headway and the CACC parameters) and network parameters (such as the sampling interval). We demonstrate the results of such a discretisation-based string stability analysis by comparison to simulations with a networked CACC model of a vehicle string. This modelling and string stability analysis approach will be further extended in Chapter 5 where the validity of the presented framework is demonstrated in practice by experiments performed with CACC-equipped prototype vehicles.

In Section 4.3, we cast the networked, interconnected vehicle string model into the hybrid system framework of [29]. Based on the resulting model, we formulate the string stability analysis as an $\mathcal{L}_2$-stability requirement for hybrid system models, in the spirit of the string stability conditions in Section 3.4. Different from the analysis in Section 4.2, where a string stability analysis for

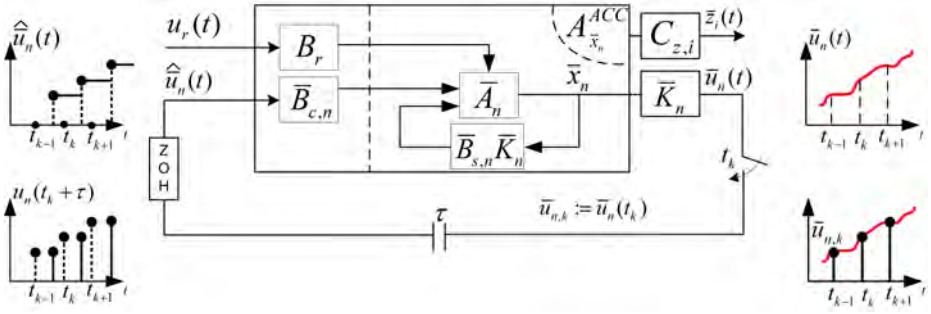

Figure 4.1: Schematic representation of the networked CACC model.

constant network-induced time delays is carried out for *fixed* transmission intervals, in Section 4.3, we allow for *uncertain and time-varying* transmission intervals and communication delays and obtain bounds on maximum allowable transmission intervals (MATI) and maximum allowable delays (MAD) for which string stability is still guaranteed. However, these analyses are limited to the small delay case (i.e. delays smaller than the sampling interval), whereas the analysis method in Section 4.2, also allows for large delays (larger than the sampling interval).

4.2 Networked CACC: Discretisation Approach

In this section, we extend the interconnected vehicle string model in (4.1) with network aspects such as sample-and-hold and delays induced by wireless communication and therewith derive a networked CACC vehicle string model which takes all these effects explicitly into account. The related networked CACC model schematics is shown in Fig. 4.1. The signal $\bar{u}_n$ is sent over the wireless network after being sampled at sampling instants $t_k = kT$, $k \in \mathbb{N}$ where T is the constant sampling interval. Note that the sampled data are sent over the wireless network to be used for the implementation of CACC and hence are typically subject to network-induced delays. These wireless communication delays are mainly due to the load on the wireless communication channel and the related contention delays (i.e. waiting time of nodes/vehicles contending for access to the network), and to a much lesser extent due to the physical transmission delay which is less than 10 msec [65, 86]. Therefore the delays are mainly affected by the number of vehicles that share the same network (i.e. reside in the same platoon). Given the fact that the number of vehicles in a platoon varies on a slow time-scale and, hence, has typically a much slower dynamics than the one of the vehicle string, we consider the delays as constant for string stability analysis.

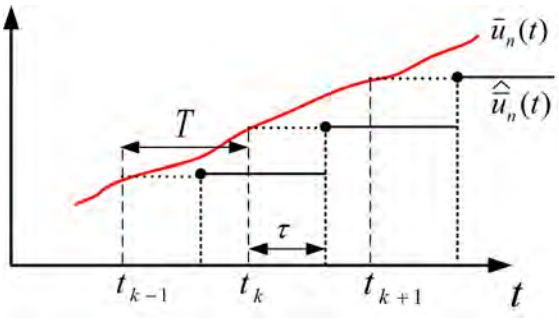

Figure 4.2: Comparison of the original and implemented signals.

When a large number of vehicles share the same network, this assumption may not hold due to the fact that packet dropouts become more significant [65]. A modelling and analysis approach for networked CACC model that can also take time-varying delays and transmission intervals into account will be presented in Section 4.3. Packet dropouts which may occur during transmission are not in the scope of the presented work.

Here, we consider constant, though uncertain and possibly large, network-induced delays τ that are modelled as

$$\tau = \tau^* + (l-1)T, \quad l \in \{1, 2, 3, \ldots\}, \quad \tau^* \in [0, T]. \tag{4.3}$$

By large delays we indicate delays that are larger than the sampling interval T (obtained in (4.3) for $l > 1$). The zero-order-hold (ZOH) device, see Fig. 4.1, transforming the delayed discrete-time control command $\bar{u}_{n,k} := \bar{u}_n(t_k)$ to the continuous-time control command $\hat{\bar{u}}_n(t)$ implemented at the vehicles, is assumed to respond instantaneously to newly arrived data (i.e. operates in an event-driven fashion). The difference between the originally sent signal $\bar{u}_n(t)$ and the implemented signal $\hat{\bar{u}}_n(t)$ is illustrated in Fig 4.2 for $l = 1$ (small delay case) in (4.3).

Now, by adopting the realistic assumption that a much higher sampling rate is employed for the locally sensed data used for the ACC functionality ($\bar{u}_n$ in (4.1)) than for the wirelessly communicated CACC commands ($\hat{\bar{u}}_n$ in (4.1)) we can model the ACC vehicle following controller as an inherently continuous-time dynamic coupling between vehicles. This allows to analyse in detail the effects of wireless communication inputs separately. The continuous-time networked CACC model for an n-vehicle string with delays as in (4.3) becomes

$$\begin{aligned} \dot{\bar{x}}_n &= A_{\bar{x}_n}^{ACC} \bar{x}_n + \bar{B}_{c,n} \hat{\bar{u}}_n(t) + B_r u_r, \\ \hat{\bar{u}}_n(t) &= \bar{u}_{n,k-l+1}, \quad t \in [t_k + \tau^*, t_{k+1} + \tau^*], \end{aligned} \tag{4.4}$$

where $\bar{u}_{n,k} := \bar{u}_n(t_k)$ and $A_{\bar{x}_n}^{ACC} = \bar{A}_n + \bar{B}_{s,n}\bar{K}_n$. This model takes the effects of sampling, zero-order-hold and delays due to communication over the wireless

network explicitly into account. In that sense, (4.4) represents a sampled-data model of the networked CACC platoon dynamics. Next, we will derive a *discrete-time* networked CACC model to be used for string stability analysis in Section 4.2.1. The discrete-time networked CACC model description is based on exact[1] discretisation of (4.4) at the sampling instants $t_k = kT$ by using $\bar{x}_{n,k} := \bar{x}_n(t_k)$, $\bar{u}_{r,k} := \bar{u}_r(t_k), k \in \mathbb{N}$:

$$\begin{aligned}\bar{x}_{n,k+1} = e^{A_{\bar{x}_n}^{ACC}T}\bar{x}_{n,k} + \int_0^{T-\tau^*} e^{A_{\bar{x}_n}^{ACC}s}ds\bar{B}_{c,n}\bar{u}_{n,k-l+1} \\ + \int_{T-\tau^*}^{T} e^{A_{\bar{x}_n}^{ACC}s}ds\bar{B}_{c,n}\bar{u}_{n,k-l} + \int_0^T e^{A_{\bar{x}_n}^{ACC}s}dsB_r u_{r,k}. \end{aligned} \tag{4.5}$$

Next, we formulate this discrete-time model in state-space form using the augmented state vector $\xi_k = [\bar{x}_{n,k}^T \ \bar{u}_{n,k-1}^T \ \bar{u}_{n,k-2}^T \ ... \ \bar{u}_{n,k-l}^T]^T$ as also employed in [11]. Then, the discrete-time networked CACC NCS model is given by

$$\xi_{k+1} = A_\xi(\tau, T)\xi_k + B_\xi(\tau, T)\bar{u}_{n,k} + \Gamma_r(T)u_{r,k}, \tag{4.6}$$

with

$$\begin{aligned} A_\xi(\tau,T) &= \begin{bmatrix} e^{A_{\bar{x}_n}^{ACC}T} & M_{l-1} & M_{l-2} & \cdots & M_0 \\ 0 & 0 & 0 & \cdots & 0 \\ 0 & I & 0 & \cdots & 0 \\ \vdots & & \ddots & \cdots & \\ 0 & \cdots & 0 & I & 0 \end{bmatrix}, \\ B_\xi(\tau,T) &= \begin{bmatrix} M_l^T & I & 0 & \cdots & 0 \end{bmatrix}^T, \\ \Gamma_r(T) &= \int_0^T e^{A_{\bar{x}_n}^{ACC}s}dsB_r, \\ M_j(\tau,T) &= \begin{cases} \int_{T-t_{j+1}}^{T-t_j} e^{A_{\bar{x}_n}^{ACC}s}ds\bar{B}_{c,n} & \text{if } 0 \le j \le 1, \\ 0 & \text{if } 1 < j \le l, \end{cases} \end{aligned}$$

where $t_0 := 0$, $t_1 = \tau^*$ and $t_2 := T$. The CACC inputs $\bar{u}_{n,k} = [u_{1,k} \ ... \ u_{n,k}]^T$ are sent over the wireless network and will be represented as a full state-feedback control law for the discrete-time model (4.6) by using the augmented state vector ξ_k as follows:

$$\bar{u}_{n,k} = \begin{bmatrix} \bar{K}_n & 0_{n\times ln} \end{bmatrix} \xi_k =: K_\xi \xi_k. \tag{4.7}$$

Next, we substitute (4.7) into (4.6) to obtain the closed-loop networked CACC model:

$$\xi_{k+1} = \overline{A_\xi}(\tau, T)\xi_k + \Gamma_r(T)u_{r,k} \tag{4.8}$$

[1]This discretisation is exact for a piecewise constant sampled approximation of the input signal u_r at the sampling frequency $\frac{1}{T}$. Such an approximation of the input signal $u_r(t)$ is considered to be sufficiently accurate given the fact that this signal is typically low-frequent in practice compared to the sampling frequency $\frac{1}{T}$, see also Section 5.2.

with $\overline{A}_\xi(\tau,T) = A_\xi(\tau,T) + B_\xi(\tau,T)K_\xi$, and the output equation

$$z_{i,k} = C_{\Delta_i}\xi_k = \left[\, C_{z,i} \;\; 0 \;\; \ldots \;\; 0 \,\right] \xi_k. \tag{4.9}$$

We will use this model in the next section to perform a string stability analysis of the networked CACC vehicle string dynamics.

4.2.1 Model-based String Stability Analysis

String stability of the discrete-time networked CACC model in (4.8) is analysed by using a discrete-time frequency-domain approach. Similar to the continuous-time frequency-domain string stability condition given in Section 3.3, string stability is analysed based on the magnitude of the discrete-time strong string stability transfer function ($S^s_{\Delta_{i,i-1}}(z)$), where z is the $\mathcal{Z}$-transform variable and $\Delta_i(z) = \mathcal{Z}\{\delta_i(k)\}$ for a discrete-time signal $\delta_i(k)$. Specifically, the condition for string stability is then given as

$$|S^s_{\Delta_{i,i-1}}(e^{j\omega})| = \left| \frac{\Delta_i(e^{j\omega})}{\Delta_{i-1}(e^{j\omega})} \right| \leq 1, \forall \omega \in [0,\pi)\,, i \in \mathbb{N}_{[1,n]}, \tag{4.10}$$

where $\delta_i \in \{q_i, v_i, a_i\}$ is the signal whose propagation along the string is of interest. To compute $S^s_{\Delta_{i,i-1}}(z)$ we note that

$$\begin{aligned} \frac{\Delta_i(z)}{\Delta_{i-1}(z)} &= \frac{\Delta_i(z)}{u_r(z)} \left(\frac{\Delta_{i-1}(z)}{u_r(z)} \right)^{-1}, \\ &= \Psi_{\Delta_{i,r}}(z)(\Psi_{\Delta_{i-1,r}}(z))^{-1}, \end{aligned} \tag{4.11}$$

where the discrete-time transfer functions $\Psi_{\Delta_{i,r}}(z)$ are extracted from (4.8), (4.9) by using

$$\Psi_{\Delta_i,r}(z) = C_{\Delta_i}(zI - \overline{A}_\xi(\tau,T))^{-1}\Gamma_r(T), \;\; i \in \mathbb{N}_{[1,n]}, \tag{4.12}$$

where C_{Δ_i} in (4.9) is such that $\delta_i(k) = C_{\Delta_i}\xi_k$. Here, we assume the existence of the inverse $(\Psi_{\Delta_{i-1,r}}(z))^{-1}$ in (4.11), see also Remark 3.2.

Discrete-time transfer functions are extracted by using (4.12) with $\delta_i = v_i$ in order to inspect the velocity response of the vehicle string to a disturbance input $u_{r,k}$. Using these transfer functions and condition (4.10), we will analyse string stability for a range of time headways, delays and sampling intervals.

Here, we demonstrate the string stability analysis approach of the interconnected vehicle string for which the schematic representation and the control structure block diagram are shown in Fig. 4.3. The discrete-time networked CACC model was obtained for a range of delay levels ($0 \leq \tau \leq 200$ msec.) in (4.3)). We analysed string stability for delays larger than the sampling interval and therewith illustrate the applicability of the presented string stability analysis approach for the large delay case.

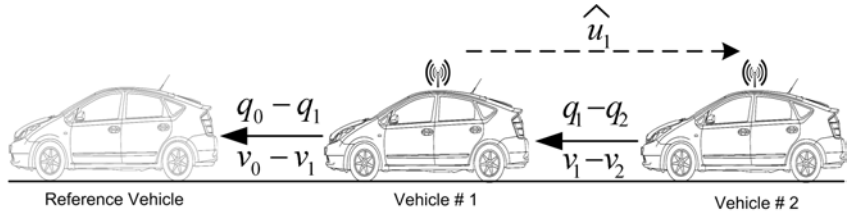

(a) Schematic representation of CACC vehicle string.

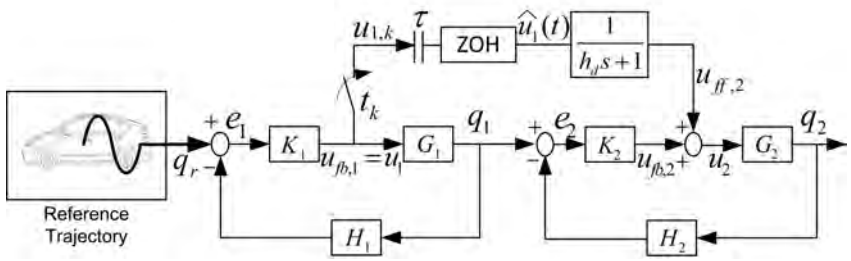

(b) Control structure block diagram.

Figure 4.3: 2-vehicle string (a) Schematic representation, (b) Control structure block diagram.

In Fig. 4.4, the maximum allowable constant time delay (τ) levels are shown for string stable operation of the networked CACC vehicle string of identical vehicles with $\eta = 0.3$. The results are obtained for different bandwidths (ω_c) of the underlying vehicle following controllers denoted by $K_1(s) = K_2(s) = \omega_c(\omega_c + s)$ in Fig. 3.(b) for which the control law was given in Section 2.3 in (2.10). The maximum allowable time delay values for which the string stability condition (4.10) is satisfied, is depicted with a color code for different sampling intervals (T), and different headway times (h_d). From Fig. 4.4, we conclude that in order to achieve string stability for smaller time headways, the communication network needs to be able to guarantee smaller bounds on the delays. The analyses also show that a high sampling frequency may help to achieve string stability with relatively small inter-vehicle distances (h_d) while tolerating larger delays. However, from a practical point of view, increasing the sampling frequency at which the wireless network operates, may have counteracting effects. Namely, a larger sampling frequency may limit the number of vehicles that can operate reliably via the same network, hence also limiting the number of vehicles in a string , and may lead to larger network-induced delays due to increased chances of packet collisions. Another observation is related to the selection of the vehicle following controller bandwidths ω_c. A high bandwidth of the ACC-controller results in improved robustness to communication delays, however this

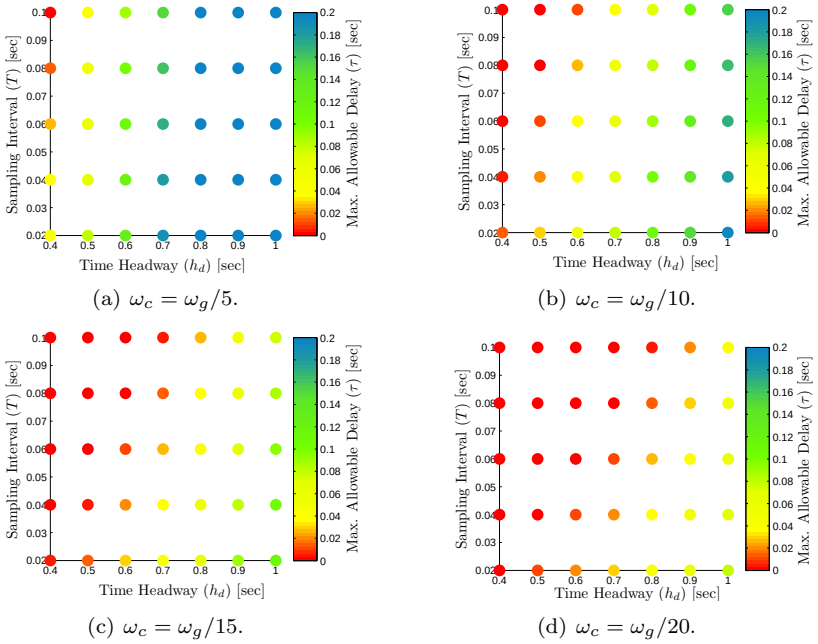

(a) $\omega_c = \omega_g/5$. (b) $\omega_c = \omega_g/10$.

(c) $\omega_c = \omega_g/15$. (d) $\omega_c = \omega_g/20$.

Figure 4.4: Maximum allowable delay (τ) levels for given vehicle following controllers ($K_1(s) = K_2(s) = \omega_c(\omega_c + s)$) with different ACC-controller bandwidths (ω_c).

choice impairs passenger comfort and also risks exceeding vehicle dynamics limitations. Therefore, reliable operation of a networked CACC system involves making multi-disciplinary design tradeoffs between the specifications for the vehicle following controller, network performance and string stability performance criteria. The presented modelling and analysis framework can be used as a design tool for the designer in making these tradeoffs. In the next section, we present simulation results validating this approach towards string stability analysis.

4.2.2 Simulation Results

For validation of the results, presented in the previous section, simulations were performed using the sampled-data NCS model in (4.4) with $n = 2$. Numerical values for the frequency-domain analysis results given in Fig. 4.4.(b) are given in Table 4.1 (for $\eta = 0.3$, $\omega_c = \omega_g/10$). Two representative (T, h_d) pairs marked with gray are selected for comparison with simulation results. In Fig. 4.5, velocity plots corresponding to the representative (T, h_d) pairs marked in Table 4.1

T \ h_d	0.4	0.5	0.6	0.7	0.8	0.9	1.0
0.02	15	30	55	80	110	150	195
0.04	5	20	45	70	100	140	180
0.06	0	10	35	60	90	130	170
0.08	0	0	25	50	80	120	165
0.10	0	0	10	40	70	110	155

Table 4.1: Numerical values of the maximum allowable (constant) time delay levels (τ [msec]) depicted in Fig. 4.4.(b). for different headway time h_d [sec] and sampling interval T [sec] values.

are given. In Fig. 4.5.(a),(c), string stability is evaluated by inspecting amplification of the response to a velocity disturbance. Hence, the peak of the velocity response for the preceding vehicle (v_1) constitutes the string stability boundary which is marked with the horizontal line in Fig. 4.5. CACC under ideal conditions (without network effects) is also included for comparison. Simulation results in Fig. 4.5 show that the velocity response of the follower vehicle (v_2) becomes larger than its predecessor (v_1) when the strong string stability boundary on the time delays given in Fig. 4.4 are exceeded. The simulation results support the model-based analysis results and demonstrate how string stability performance can be affected by the network. In Fig. 4.5.(b),(d), corresponding frequency-response functions are shown. Here it can also be seen that even the case without delay (i.e. $\tau = 0$) differs slightly from the ideal CACC due to the effect of sampling. These results demonstrate the applicability and accuracy of the presented discretisation-based string stability analysis methods.

4.2.3 Conclusions

In this section, the effect of sampling frequency, zero-order-hold and constant network delays on string stability was inspected by using the networked CACC model. In particular, string stability was studied by using discrete-time frequency response plots. Herewith, the maximum allowable delays were obtained for various network, vehicle following controller, and inter-vehicle spacing parameters. We demonstrated the validity of the results by performing simulations with the sampled-data NCS model of a 2-vehicle string. This network-aware CACC modelling and string stability analysis approach will be further validated in Chapter 5 with experimental results performed on prototype vehicles. There are many other imperfections and constraints that play a role in CACC-based vehicle platooning, such as variable sampling/transmission intervals, variable transmission delays, and communication constraints. In the next section, we

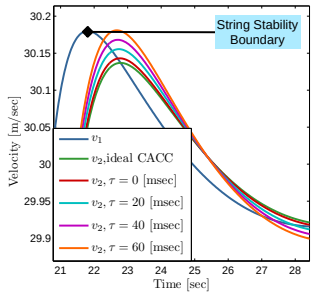

(a) $T = 0.02, h_d = 0.6$.

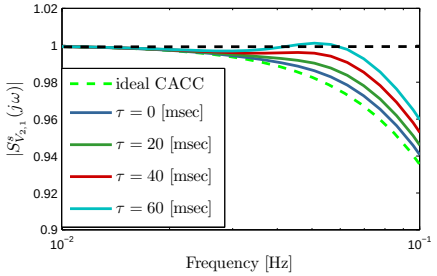

(b) $T = 0.02, h_d = 0.6$.

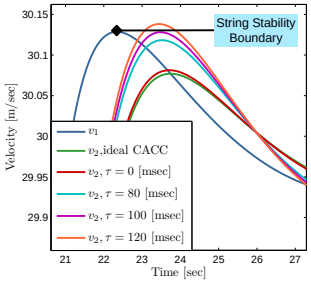

(c) $T = 0.02, h_d = 0.8$.

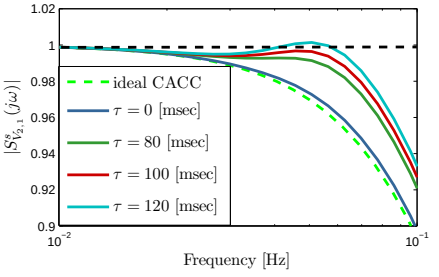

(d) $T = 0.02, h_d = 0.8$.

Figure 4.5: Simulation results and corresponding bode plots for representative (T, h_d) pairs in Fig. 4.4.(b) and Table 4.1.

will present a hybrid system-based NCS modelling and analysis framework in order to incorporate these type of NCS imperfections in the CACC platooning model and subsequent string stability analysis.

4.3 Networked CACC: Hybrid System Approach

In the previous section, the effect of sampling frequency, zero-order-hold and network delays on string stability was inspected by using a discretisation approach where the wireless communication delays and transmission intervals were assumed to be constant. This assumption on network operation may not be valid especially when the effect of packet dropouts becomes more significant. Therefore, we will use a hybrid system-based NCS modelling and analysis approach which takes time-varying nature of transmission intervals and delays explicitly into account. For this purpose, we cast the interconnected vehicle string model in (4.1) into the hybrid system framework of [29] and formulate the string stability analysis by using the dissipation-based conditions introduced in Section

3.4 as an $\mathcal{L}_2$-stability requirement for the resulting hybrid system models. Different from the analysis in Section 4.2, where a discretisation-based analysis of string stability has been pursued in the frequency-domain for the case of constant time delays and fixed sampling/transmission intervals, here, we allow for uncertain and time-varying sampling/transmission intervals and communication delays. The analysis pursued in this section will provide bounds on maximum allowable transmission intervals (MATI) and maximum allowable delays (MAD) while string stability is still guaranteed.

In the CACC model given in (4.1), the interconnected vehicle string was formulated such that the control inputs ($\bar{u}_n$ and $\hat{\bar{u}}_n$) are kept separate according to their way of being acquired by the host vehicle (i.e. through direct measurement or through wireless communication, respectively). Also, the model permits to express the CACC control commands that are actually feedforward signals as state feedback control laws. Now, by adopting the realistic assumption[2] that a much higher sampling rate is employed for the locally sensed data that is used for the ACC functionality, we can consider the ACC vehicle following controller as inherently continuous-time dynamic coupling between vehicles. This results in a model formulation which allows us to inspect the effects of wireless communication inputs separately. Continuous-time plant and controller equations for the NCS setup depicted in Fig. 4.6 are obtained by substituting (2.24) into (2.23) and are given as

$$\begin{aligned} \dot{\bar{x}}_n &= A_{\bar{x}_n}^{ACC}\bar{x}_n + \bar{B}_{c,n}\hat{\bar{u}}_n + B_r u_r, \\ y &= \bar{u}_n = \bar{K}_n\bar{x}_n, \\ \hat{\bar{u}}_n &= \hat{y}, \end{aligned} \tag{4.13}$$

where $A_{\bar{x}_n}^{ACC} = \bar{A}_n + \bar{B}_{s,n}\bar{K}_n$, $y \in \mathbb{R}^{n_y}$ is the output of the plant, and $u_r \in \mathbb{R}^{n_r}$ is the exogenous input. At each transmission instant $t_k, k \in \mathbb{N}$, CACC control commands are generated by using the sampled measurements which are subsequently sent over the network. They arrive at the controller after a transmission delay of τ_k. Therefore, the controller updates occur at $t_k + \tau_k$ and the control input is implemented through a zero-order-hold (ZOH). The difference between the implemented piecewise continuous control command ($\hat{\bar{u}}_n$) and the actual CACC control command ($\bar{u}_n$) is captured by the error introduced by the network and is defined as

$$e_u := \hat{\bar{u}}_n - \bar{u}_n. \tag{4.14}$$

In between the control command updates, the network operates in a zero-order-hold (ZOH) fashion and, therefore, between the times $t_k + \tau_k$ and $t_{k+1} + \tau_{k+1}$

$$\dot{\hat{\bar{u}}}_n = 0. \tag{4.15}$$

[2]For typical values of the sampling and wireless communication frequencies in an actual implementation of the CACC system, see Chapter 5.

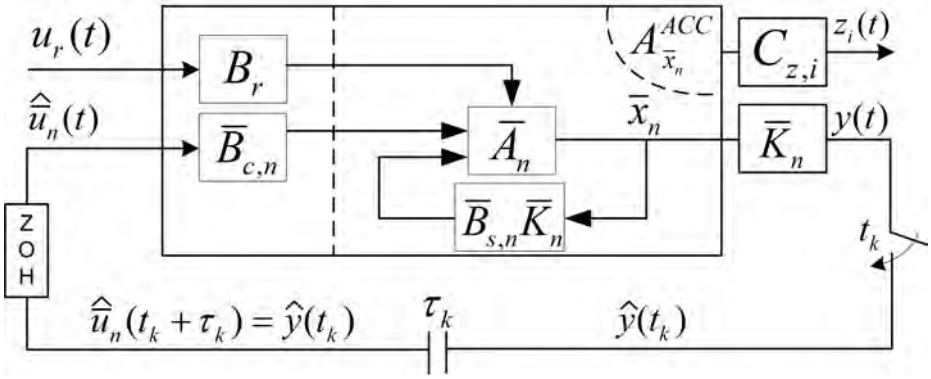

Figure 4.6: NCS model.

Now, the NCS model dynamics in between the control command updates can be written in terms of the plant and the error states by using (4.14) and (4.15) in (4.13) as follows:

$$\dot{\bar{x}}_n = f(\bar{x}_n, e_u, u_r) := A_{11}\bar{x}_n + A_{12}e_u + A_{13}u_r \tag{4.16a}$$
$$\dot{e}_u = g(\bar{x}_n, e_u, u_r) := A_{21}\bar{x}_n + A_{22}e_u + A_{23}u_r \tag{4.16b}$$

with

$$\begin{aligned} A_{11} &= A^{ACC}_{\bar{x}_n} + \bar{B}_{c,n}\bar{K}_n, & A_{12} &= \bar{B}_{c,n}, \\ A_{13} &= B_r, & A_{21} &= -\bar{K}_n(A^{ACC}_{\bar{x}_n} + \bar{B}_{c,n}\bar{K}_n), \\ A_{22} &= -\bar{K}_n\bar{B}_{c,n}, & A_{23} &= -\bar{K}_nB_r. \end{aligned} \tag{4.17}$$

At update instants $t_k + \tau_k$, the error is reset according to

$$\begin{aligned} e_u((t_k+\tau_k)^+) &= \hat{\bar{u}}_n((t_k+\tau_k)^+) - \bar{u}_n((t_k+\tau_k)), \\ &= \bar{u}_n(t_k) + h(k, e_u(t_k)) - \bar{u}_n(t_k+\tau_k), \\ &= h(k, e_u(t_k)) - e_u(t_k) + e_u(t_k+\tau_k), \end{aligned} \tag{4.18}$$

where $h(k, e_u(t_k))$ is related to the protocol that is employed and determines which node (vehicle) obtains access to the network at each transmission instant, see [51, 29] for more details. Two commonly adopted protocols are the Try-Once-Discard (TOD) and the Round Robin (RR) protocol. In this work, we consider static RR-type protocols in which the order of the nodes (vehicles) accessing the network is fixed. The reason to consider these protocols is due to their suitability for decentralized implementations when compared to the TOD protocol. Note that the sampled-data (SD) protocol forms a special case by taking $h(k, e_u) = 0$ for all $k \in \mathbb{N}$ and all $e_u \in \mathbb{R}$.

4.3.1 Hybrid System Model Formulation

The networked CACC model will now, in the spirit of [29], be cast into the hybrid system framework as developed in [25] for the upcoming string stability analysis. For this purpose, we introduce the auxiliary variables $s \in \mathbb{R}^n$, $\kappa \in \mathbb{N}$, $\tau \in \mathbb{R}_{\geq 0}$ and $\ell \in \{0, 1\}$ to reformulate the model in terms of so-called flow equations and reset equations of the form

$$\mathcal{H}^{NCS} := \begin{cases} \dot{\xi} & = F(\xi), \quad \xi \in C, \\ \xi^+ & = G(\xi), \quad \xi \in D, \end{cases} \tag{4.19}$$

where $\xi = [\bar{x}_n^T, e^T, s^T, \kappa, \tau, \ell]^T$ denotes the states of the hybrid system $\mathcal{H}^{NCS}$; C and D are subsets of $\mathbb{R}^{n_\xi}$; $F : C \to \mathbb{R}^\xi$ and $G : D \to \mathbb{R}^\xi$ are the flow and jump mappings, respectively; and ξ^+ denotes the value of the state after a reset. The variable s is a dummy variable used to store the error value (e_u) according to (4.18) at the last transmission instant t_k to be used at the next control command update instant $t_k + \tau_k$, κ is the transmission counter, τ is a timer variable that keeps track of how much time elapsed since the last transmission event, and ℓ is a boolean logic operator that determines whether the next event in the hybrid system will be a transmission ($\ell = 0$) or an update reset ($\ell = 1$). The hybrid system $\mathcal{H}_{NCS}$ is now given by the flow equations

$$\begin{aligned} \dot{\bar{x}}_n &= f(\bar{x}_n, e_u, u_r), \\ \dot{e}_u &= g(\bar{x}_n, e_u, u_r), \\ \dot{s} &= 0, \quad \dot{\tau} = 1, \\ \dot{\kappa} &= 0, \quad \dot{\ell} = 0, \end{aligned} \tag{4.20}$$

when $(\ell = 0 \wedge \tau \in [0, \tau_{mati}])$ or $(\ell = 1 \wedge \tau \in [0, \tau_{mad}])$ where $\tau_{mad} \leq \tau_{mati}$ is the maximum allowable delay (MAD), and $\tau_{mati} \geq t_{k+1} - t_k, k \in \mathbb{N}$, is the maximum allowable transmission interval (MATI). We also note that $\tau_k \leq \min(\tau_{mad}, t_{k+1} - t_k), k \in \mathbb{N}$. This condition implies that an update will occur before the next transmission instant. In other words, as opposed to the discrete-time framework presented in Section 4.2, the analysis in this section is limited to so-called small delays. Transmission ($\ell = 0$) and update ($\ell = 1$) reset equations can be derived based on (4.18) and lead to, respectively,

$$\begin{aligned} (\bar{x}_n^+, e_u^+, s^+, \tau^+, \kappa^+, \ell^+) &= (\bar{x}_n, e_u, h(k, e_u) - e_u, 0, \kappa + 1, 1), \\ (\bar{x}_n^+, e_u^+, s^+, \tau^+, \kappa^+, \ell^+) &= (\bar{x}_n, s + e_u, -s - e_u, \tau, \kappa, 0). \end{aligned} \tag{4.21}$$

For more details on this NCS hybrid system formulation, see [29].

4.3.2 Problem Formulation and Analysis Approach

The networked CACC model in (4.13) allows to inspect the influence of the exogenous input u_r on a particular controlled output variable

$$\bar{z}_i = C_{z,i}(\bar{x}_n) \tag{4.22}$$

in terms of an induced $\mathcal{L}_2$-gain. The hybrid model $\mathcal{H}_{NCS}$ (described by the flow (4.20) and reset equations (4.21)) expanded with the output (4.22) is denoted by $\mathcal{H}^z_{NCS}$.

Definition 4.1 ([29]). *The hybrid system $\mathcal{H}^z_{NCS}$ is said to be $\mathcal{L}_2$-stable with gain θ, if there is a $\mathscr{K}_\infty$-function[3] S such that for any $0 < \delta \leq \tau_{mati}$, any exogenous input $u_r \in \mathcal{L}_2$, and any initial condition $\xi(0)$, each corresponding solution to $\mathcal{H}^z_{NCS}$ satisfies*

$$\|\bar{z}_i\|_2 \leq S(|\xi(0)|) + \theta \|u_r\|_2 , \tag{4.23}$$

where $\xi = [\bar{x}_n^T, e_u^T, s^T, \kappa, \tau, \ell]^T$ denotes the states of the hybrid system (4.20), (4.21).

Problem 4.1. *Given the ideal closed-loop system in (4.13) with $\hat{\bar{u}}_n = \bar{u}_n$ which is designed without the consideration of the network effects, determine the value of τ_{mati} and τ_{mad} so that the networked CACC model $\mathcal{H}^z_{NCS}$ is still guaranteed to have an $\mathcal{L}_2$-gain less than or equal to θ in (4.23).*

As mentioned before, in this work, we consider the propagation of the control effort, (i.e. $u_i, i \in \mathbb{N}_{[2,n]}$) as the particular output of interest. In accordance with the weak string stability condition presented in Section 3.4, we require the $\mathcal{L}_2$-gain from u_r to u_i to be less than or equal to one (i.e. θ in (4.23) should satisfy $\theta \leq 1$) for string stability. Control commands of individual vehicles can be selected by using the output equation $\bar{z}_i = C_{z,i}\bar{x}_n$ accordingly in (4.22).

4.3.3 $\mathcal{L}_2$-Stability Analysis of the Hybrid System

An $\mathcal{L}_2$-gain analysis of a hybrid system, in this case supporting the formulation of conditions for string stability, requires conditions on the flow (4.20) and jumps (4.21) of (some) system states during reset occurrences.

Conditions on Resets

We assume that there exists a Lyapunov function $W : \mathbb{N} \times \mathbb{R}^{n_e} \to \mathbb{R}_{\geq 0}$ which satisfies

$$\underline{\alpha}_W |e_u| \leq W(\kappa, e_u) \leq \overline{\alpha}_W |e_u|, \ \forall \kappa, \tag{4.24a}$$

$$W(\kappa + 1, h(\kappa, e_u)) \leq \lambda W(\kappa, e_u), \tag{4.24b}$$

[3] A continuous function $S : [0, \infty) \to [0, \infty)$ is said to belong to class $\mathscr{K}_\infty$ if it is strictly increasing, $S(0) = 0$, and $\lim_{s\to\infty} S(s) = \infty$.

for constants $0 < \underline{\alpha}_W \leq \overline{\alpha}_W$ and $0 < \lambda < 1$. Additionally, it is assumed that

$$W(\kappa + 1, e_u) \leq \lambda_W W(\kappa, e_u), \tag{4.25}$$

for some constant $\lambda_W \geq 1$ for almost all $e_u \in \mathbb{R}^{n_e}$ and all $\kappa \in \mathbb{N}$. Moreover, it is assumed that

$$\left| \frac{\partial W}{\partial e_u}(\kappa, e_u) \right| \leq M_1, \ \forall \kappa, \forall e_u, \tag{4.26}$$

for some constant $M_1 > 0$.

The evolution of the states at update instants is determined by $h(k, e_u(t_k))$ in (4.18) and is related to the communication protocol which orchestrates the access of different nodes in the system to the network. For exact definitions of the protocols, see [51]. For the static Round Robin (RR) protocol which we consider in this work, the Lyapunov functions and corresponding constants in (4.24), (4.25) and (4.26) are obtained using the following lemma.

Lemma 4.1 ([29])**.** *Let ι denote the number of nodes in the network. For the Round Robin (RR) protocol there is a $W_{RR} : \mathbb{N} \times \mathbb{R}^{n_e} \to \mathbb{R}_{\geq 0}$ that is locally Lipschitz in its second argument and satisfies* (4.24)*,* (4.25) *and* (4.26) *with $\lambda_{RR} = \sqrt{\frac{\iota - 1}{\iota}}$, $\underline{\alpha}_{W,RR} = 1$, $\overline{\alpha}_{W,RR} = \sqrt{\iota}$, $\lambda_{W,RR} = \sqrt{\iota}$ and $M_{1,RR} = \sqrt{\iota}$.*

Remark 4.1. For the Sampled-Data (SD) protocol considered in this work these constants are obtained by using Lemma 4.1 with ($\iota = 1$) and are given as:

$$\begin{aligned} \lambda_{SD} &= 0, \\ \underline{\alpha}_{W,SD} = \overline{\alpha}_{W,SD} = \lambda_{W,SD} &= M_{1,SD} = 1, \end{aligned} \tag{4.27}$$

and (4.24b) is satisfied for the SD protocol for any $\lambda \in (0, 1)$. ◁

Conditions on Flow

The following growth condition on the flow of the NCS model (4.16) is used:

$$|g(\bar{x}_n, e_u, u_r)| \leq m_{\bar{x}_n}(\bar{x}_n, u_r) + M_{e_u}|e_u|, \tag{4.28}$$

where $m_{\bar{x}_n} : \mathbb{R}^{n_x} \times \mathbb{R}^{n_r} \to \mathbb{R}_{\geq 0}$ and $M_{e_u} \geq 0$ is a constant, and, additionally, it is assumed that a storage function $V : \mathbb{R}^{n_x} \to \mathbb{R}_{\geq 0}$ exists which satisfies the condition

$$\begin{aligned} \langle \nabla V(\bar{x}_n), f(\bar{x}_n, e_u, u_r) \rangle \leq &-m^2_{\bar{x}_n}(\bar{x}_n, u_r) + \gamma^2 W^2(\kappa, e_u) \\ &+ \mu(\theta^2 |u_r|^2 - |\bar{z}_i|^2), \end{aligned} \tag{4.29}$$

where $f(\bar{x}_n, e_u, u_r)$ is as in (4.16a), with $\mu > 0, \gamma > 0$ as constants, and the bounds

$$\underline{\alpha}_V(|\bar{x}_n|) \leq V(\bar{x}_n) \leq \overline{\alpha}_V(|\bar{x}_n|), \tag{4.30}$$

for some $\mathscr{K}_\infty$-functions $\underline{\alpha}_V$ and $\overline{\alpha}_V$. Essentially the condition above is a (slightly extended version of) dissipativity-based formulation for the system

$$\dot{\bar{x}}_n = f(\bar{x}_n, e_u, u_r)$$

to have an $\mathcal{L}_2$-gain smaller than or equal to θ between the exogenous input u_r and the output $\bar{z}_i$ as in (4.22).

Consider now the differential equations

$$\dot{\phi}_0 = -2L_0\phi_0 - \gamma_0(\phi_0^2 + 1), \tag{4.31a}$$

$$\dot{\phi}_1 = -2L_1\phi_1 - \gamma_0(\phi_1^2 + \frac{\gamma_1^2}{\gamma_0^2}), \tag{4.31b}$$

where $L_\ell \geq 0$ and $\gamma_\ell > 0$, $\ell = 0, 1$, are the real constants given as

$$L_0 = \frac{M_1 M_e}{\underline{\alpha}_W};\ L_1 = \frac{M_1 M_e \lambda_W}{\lambda \underline{\alpha}_W};\ \gamma_0 = M_1\gamma;\ \gamma_1 = \frac{M_1\gamma\lambda_W}{\lambda}. \tag{4.32}$$

Based on the above conditions we can now employ the following theorem guaranteeing upper bounds on $\mathcal{L}_2$-gain of $\mathcal{H}^z_{NCS}$.

Theorem 4.2 ([29])**.** *Consider the system $\mathcal{H}^z_{NCS}$ that satisfies the aforementioned conditions. Suppose $\tau_{mati} \geq \tau_{mad} \geq 0$ satisfy*

$$\phi_0(\tau) \geq \lambda^2\phi_1(0) \text{ for all } 0 \leq \tau \leq \tau_{mati} \tag{4.33a}$$

$$\phi_1(\tau) \geq \phi_0(\tau) \text{ for all } 0 \leq \tau \leq \tau_{mad} \tag{4.33b}$$

for solutions ϕ_0 and ϕ_1 of (4.31) corresponding to certain chosen initial conditions $\phi_\ell(0) > 0$, $\ell = 0, 1$, with $\phi_1(0) \geq \phi_0(0) \geq \lambda^2\phi_1(0) \geq 0$, $\phi_0(\tau_{mati}) > 0$ and λ as in (4.24b). Then the system $\mathcal{H}^z_{NCS}$ is $\mathcal{L}_2$-stable with gain θ.

By using a numerical search algorithm, quantitative numbers for τ_{mati} and τ_{mad} can be obtained with the help of the above theorem by constructing the solutions to (4.31) for various initial conditions. Computing the τ value of the intersection of ϕ_0 and the constant line $\lambda^2\phi_1(0)$ provides τ_{mati} according to (4.33a), while the intersection of ϕ_0 and ϕ_1 gives a value for τ_{mad} due to (4.33b). Different values of the initial conditions $\phi_0(0)$ and $\phi_1(0)$ lead to different solutions of the differential equations in (4.31), and thus, to different storage functions in (4.30). In this way, tradeoff curves between τ_{mati} and τ_{mad} can be obtained that indicate when $\mathcal{L}_2$-stability of the NCS is still guaranteed with gain θ.

4.3.4 String Stability Analysis

In Chapter 3, dissipation inequality-based string stability analysis methods have been introduced and the propagation of disturbances through the interconnected vehicle string was inspected by using the notion of so-called *string stability* which

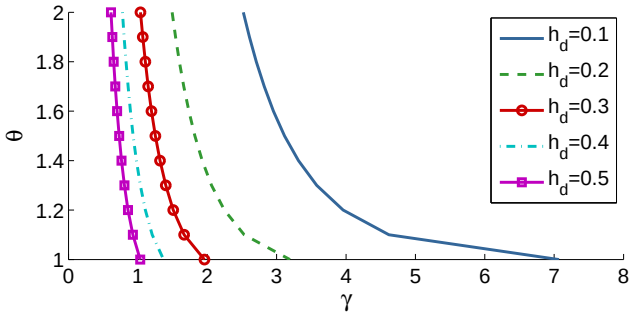

Figure 4.7: Tradeoff curves for θ and γ with different headway-times (h_d).

is extended here in order to account for the wireless communication imperfections. Next, we will further pursue dissipation inequality-based string stability analysis for the hybrid system setting for which Linear Matrix Inequalities (LMIs) can be formulated and numerical solutions can be obtained. Here, we demonstrate the $\mathcal{L}_2$-stability analysis framework on the string stability evaluation for two alternative use-scenarios with different network structures and provide quantitative results that can aid the designer with guidelines for making tradeoffs between control and network specifications.

MATI-MAD Analysis for Sampled-Data Setting

In the CACC setting considered here, we assume that all vehicle data is sampled and transmitted synchronously in the network (i.e. the protocol function $h = 0$ in (4.18)). This scenario might be implemented using GPS-based clock-synchronisation. The data exchange between two vehicles where the preceding vehicle broadcasts its data to its predecessor can be thought of as such a network. This guarantees that condition (4.24b) is satisfied for any $\lambda \in [0, 1)$, and λ remains as a free parameter in this case. Additional network parameter values are obtained by using Lemma 4.1 for a single node ($\iota = 1$). The flow conditions in (4.29) are checked for the system H^z_{NCS} for the controlled output $\bar{z}_i = \bar{u}_i = C_{z,i}\bar{x}_n$ by using a quadratic storage function $V(\bar{x}_n) = \bar{x}_n^T P \bar{x}_n$, and taking $m(\bar{x}_n, u_r) = |A_{21}\bar{x}_n + A_{23}u_r|$, and $W(\kappa, e_u) = |e_u|$. For the CACC vehicle string in (4.16), this leads to the following LMIs:

$$\begin{pmatrix} \Omega_i & PA_{12} & A_{21}^T A_{23} + PA_{13} \\ A_{12}^T P & -\gamma^2 I & 0 \\ A_{13}^T P + A_{23}^T A_{21} & 0 & A_{23}^T A_{23} - \mu\theta^2 I \end{pmatrix} \preceq 0,$$
$$P = P^T \succ 0, \tag{4.34}$$

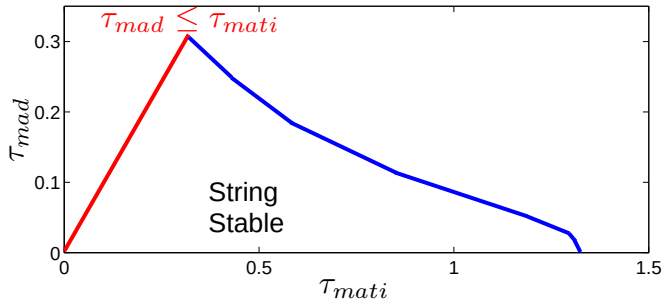

Figure 4.8: String stable solution region for a fixed headway-time ($h_d = 0.5$).

where $\Omega_i = A_{11}^T P + P A_{11} + A_{21}^T A_{21} + \mu C_{z,i}^T C_{z,i}$. These LMIs are solved for $n = 2$ to obtain tradeoff curves between the $\mathcal{L}_2$-gain θ and γ in (4.29) with the controlled output $\bar{z}_2 = u_2 = C_{z,2}\bar{x}_n$ for different headway-time constants (h_d) as presented in Fig. 4.7.

Now, by selecting the string stable pairs $(\theta, \gamma) = (1, \gamma^*)$ derived from the results in Fig. 4.7, we can obtain the constants given in (4.32) that are used to solve the differential equations (4.31). Finally, from Theorem 4.2, quantitative numbers for τ_{mati} and τ_{mad} are obtained by constructing solutions to (4.31) for different initial conditions and $0 < \lambda < 1$ which result in the confined region as shown in Fig. 4.8, where $\mathcal{H}_{NCS}^z$ is $\mathcal{L}_2$-stable with gain $\theta^* = 1$ for a representative headway time ($h_d = 0.5$).

Delay-free MATI Analysis of RR Network

Next, we demonstrate the analysis framework for a CACCC vehicle string equipped with an RR-type protocol. This allows the string stability analysis of vehicle strings with asynchronous data exchange, and permits flexibility in communication topology. To this end, Lemma 4.1 is used in a similar manner to compute network-related parameters for a vehicle string with n vehicles. Note that, the number ι of nodes in Lemma 4.1 equals $n - 1$ since the last vehicle does not transmit. MATI results shown in Fig. 4.9 are obtained by solving LMI conditions in (4.34) with $\theta = 1$, indicating an $\mathcal{L}_2$-gain from u_r to u_i, $i \in \mathbb{N}_{[2,n]}$, by using Theorem 4.2. This, in turn, implies $\mathcal{L}_2$ weak string stability. These quantitative results can guide the designer in making tradeoffs between the number of cars (n) allowed in the network, the network specifications (related to τ_{mati}) and CACCC performance (in terms of the headway time h_d), while string stability is guaranteed.

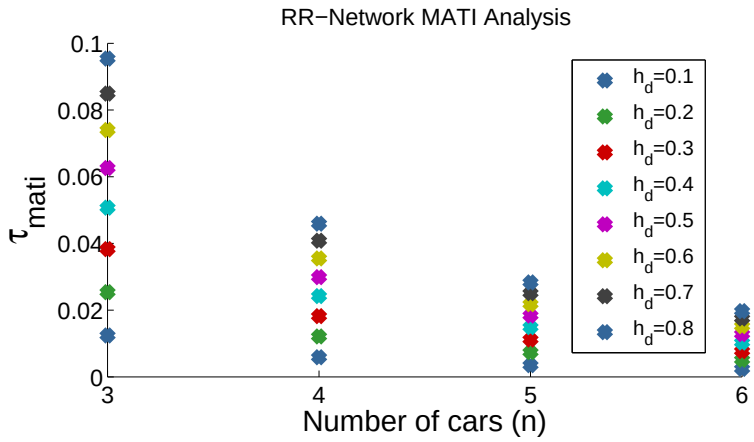

Figure 4.9: MATI vs. vehicle string size for different headway-time values (h_d) guaranteeing string stability, i.e. $\mathcal{L}_2$-gain $\theta = 1$.

4.4 Discussion and Conclusions

In this chapter, we presented a novel modelling and analysis approach for string stability of interconnected vehicle strings in the face of communication effects induced by the wireless network used to communicate between the vehicles. For this purpose, two different NCS modelling and analysis approaches have been adopted. First, in Section 4.2, the effect of sampling frequency, zero-order-hold and constant network delays was inspected by modelling the networked CACC vehicle platoon dynamics as a discrete-time NCS model. String stability was studied by using discrete-time frequency-domain criteria. Herewith, the maximum allowable delay was obtained for various network, vehicle following controller, and inter-vehicle spacing parameters. We demonstrated the validity of the results by performing simulations with the sampled-data NCS model. This network-aware CACC modelling and string stability analysis approach will be validated in Chapter 5 with experimental results performed on prototype vehicles.

Next, we have cast the networked vehicle string model into a hybrid system modelling framework. This modelling approach permits the to formulate string stability analysis as an $\mathcal{L}_2$-stability requirement for hybrid system models. $\mathcal{L}_2$-stability results for Networked Control Systems based on hybrid system models are subsequently used to perform string stability analyses of the Cooperative Adaptive Cruise Controller (CACC) which was presented in Chapter 2.3. These analyses provide bounds on tolerable transmission intervals and delays in face of scheduling constraints requiring network protocols. The main contribution of this approach is the flexibility introduced by allowing for time-varying sampling

intervals/delays which bears potential for representing abstractions of realistic network implementations. We demonstrated the strength of this general framework by two possible use-scenarios based on the synchronous sampled-data (SD) network setting and the Round Robin (RR)-type network.

The analyses presented in this chapter provide quantitative results that can be used as guidelines to assist the designer for making multi-disciplinary design tradeoffs between control and network specifications.

Chapter 5

Experimental Validation

In this chapter, the validity of the network-aware modelling and string stability analysis framework, that was developed in Chapter 4, is demonstrated in practice by experiments performed with prototype vehicles equipped with Cooperative Adaptive Cruise Control (CACC) [53]. In particular, the main goal of these experiments is to test string stability properties for a range of time headways and communication delays in order to validate the model-based analyses that are obtained by using the Networked Control Systems (NCS) discretisation approach in Section 4.2.

In Section 5.1, we extend the networked CACC vehicle string model such that the actuation delay present in the prototype vehicles is taken into account in the longitudinal vehicle dynamics model. Subsequently, we obtain string stable operation conditions for the prototype vehicles by using the network-aware modelling and discretisation-based string stability analysis method presented in Section 4.2 which incorporates the effects of the sampling and the zero-order-hold (ZOH) in addition to constant wireless communication delays. Herewith, we obtain maximum allowable constant time delays for a range of headway times and sampling intervals for which the boundary of string stability will be revealed and, therewith, find appropriate settings for which experiments will be carried

out. In Section 5.2, the CACC-related components instrumented in the test vehicles and the implementation of the CACC system are explained in detail. We use two of these CACC-equipped vehicles in the experiments where the leader vehicle is programmed to track a predefined velocity trajectory. This velocity trajectory is designed in Section 5.3 such that the interconnected vehicle string is excited in a frequency range of interest for experimentally assessing string stability properties. In Section 5.4, experiments carried out for representative operating conditions are discussed and the assessment of string stability properties based on these test data is demonstrated. The experimental results are then compared with the model-based results. For the validation of the model-based string stability analyses presented in Section 4.2, experiments have been carried out at representative operating points with different time headway values where the (constant) wireless communication delay was regulated at different levels in order to support the experimental analysis of string stability for different delay magnitudes. These experimental results show how string stability is compromised by wireless communication delays and demonstrate the reliability and practical validity of the network-aware modelling and string stability analysis method presented in Chapter 4 in practice.

5.1 Model-based Results

In Section 4.2, a network-aware modelling framework was presented for the analysis of string stability properties of the interconnected vehicle string constructed in Section 2.5 in (2.26) for which the continuous-time model is given as follows:

$$\begin{aligned} \dot{\bar{x}}_n &= A_{\bar{x}_n}^{ACC}\bar{x}_n + \bar{B}_{c,n}\hat{\bar{u}}_n + B_r u_r, \\ \bar{z}_i &= C_{z,i}\bar{x}_n, \end{aligned} \tag{5.1}$$

where $A_{\bar{x}_n}^{ACC} := \bar{A}_n + \bar{B}_{s,n}\bar{K}_n$ ($\bar{A}_n, \bar{B}_{s,n}, \bar{B}_{c,n}$ are as given in (2.23)), $\bar{z}_i$ is the particular output of interest whose propagation throughout the string is of interest, and $\bar{x}_n = [\tilde{x}_0^T\ \tilde{x}_1^T\ \tilde{x}_2^T\ \cdots\ \tilde{x}_n^T]^T$ is the lumped state involving the states $\tilde{x}_i$ of the individual vehicles in the vehicle string. The dynamics of each of these individual, CACC-equipped, vehicles are governed by the following closed-loop (C-)ACC vehicle model constructed in Section 2.4:

$$\dot{\tilde{x}}_i = \tilde{A}_{i,i}\tilde{x}_i + \tilde{A}_{i,i-1}\tilde{x}_{i-1} + \tilde{B}_{s,i}u_i + \tilde{B}_{c,i}\hat{u}_{i-1}. \tag{5.2}$$

Here the longitudinal vehicle dynamics model with actuator delay is used as in (2.20) with the augmented state vector $\tilde{x}_i^T = [x_i^T\ \tilde{p}_i^T]$ where $x_i^T = [e_i\ v_i\ a_i\ u_{ff,i}] \in \mathbb{R}^{n_x}$, are the states of the i-th CACC equipped vehicle and $\tilde{p}_i = [p_{i,1}\ p_{i,2} \dots p_{i,\kappa}]^T \in \mathbb{R}^{\kappa}$ are the states of the state-space representation of the κ-th order Padé approximation of the actuator delay as in (2.9). The model is extended with the actuator delay here as such actuation delay is essential in

Vehicle Model Parameters		(C-)ACC Parameters	
η_i	0.1	ν_i	1 (CACC)
$\omega_{g,i}$	10	$\omega_{c,i}$	0.5
$\tau_{a,i}$	0.2	$k_{p,i}$	0.25
κ	4	$k_{d,i}$	0.5

Table 5.1: Parameter set used in the model-based analysis in Fig 5.1.

the CACC-equipped prototype vehicles that are used in the experiments. In (5.2), u_i represents the control command (of the i-th vehicle) and $\hat{u}_{i-1}$ are the control commands (of the $(i-1)$-th vehicle) as received by the i-th vehicle over the wireless network, which are, therefore, subject to wireless communication imperfections.

The effect of sample-and-hold and network delays that occur due to wireless communication and sampled-data implementation of the CACC controller over a wireless link are incorporated in the CACC control action by using the following relation between the continuous-time and discrete-time control commands:

$$\hat{\bar{u}}_n(t) = \bar{u}_{n,k-l+1}, \quad t \in [t_k + \tau^*, t_{k+1} + \tau^*], \tag{5.3}$$

where $\bar{u}_{n,k} := \bar{u}_n(t_k)$, $t_k = kT$, $k \in \mathbb{N}$, T is the constant sampling interval, and

$$\tau = \tau^* + (l-1)T, \quad l \in \{1, 2, 3, \ldots\}, \quad \tau^* \in [0, T]. \tag{5.4}$$

Herein, τ and T are the constant, though uncertain, network-induced delays and the sampling interval, respectively, whose effects on string stability are inspected. Based on this network-aware modelling approach, we analysed frequency-domain conditions given in (4.10) for (strong) string stability to obtain string stable operating conditions for a range of time headways h_d and communication delays τ of the interconnected vehicle string in (5.1) by using the vehicle dynamics and (C-)ACC controller parameters given in Table[1] 5.1 ($\eta = 0.1$ and $\tau_a = 0.2$ in (2.8)) which were identified for the prototype vehicles in [61]. String stability of the discrete-time CACC NCS model in (4.8) is then analysed by using the discrete-time frequency response based methods presented in Section 4.2.1 which are based on the magnitude of the discrete-time string stability transfer function ($S^s_{\Delta_{i,i-1}}(z)$) by using (4.11). Discrete-time transfer functions are extracted by using (4.12) with $\delta_i = v_i$ in order to inspect the velocity response of the vehicle string to a disturbance input u_r. Using these transfer functions and condition (4.10), we analysed string stability for a range of time headways, delays and sampling intervals. Fig. 5.1 shows the results of such analysis by depicting the

[1] Hereafter, the subindex (i) in the vehicle parameters will be omitted in the notation since the prototype vehicles are identical.

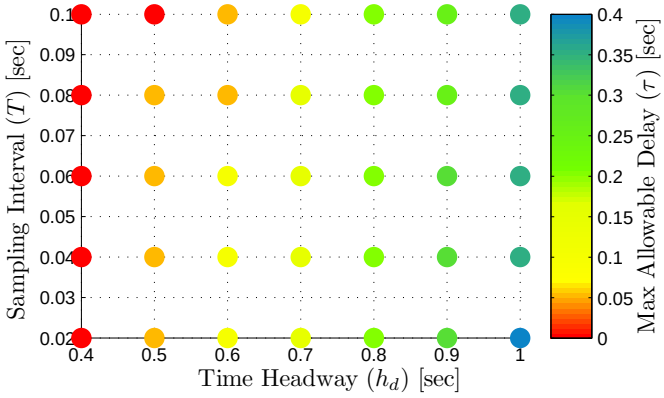

Figure 5.1: Maximum allowable (constant) time delays (τ) for different sampling interval (T) and headway-time (h_d).

maximum allowable (constant) time delay τ guaranteeing string stable operation of the CACC vehicle string for different headway-time values h_d and sampling intervals T. Here, the vehicle parameters in (2.8) are taken as $\eta = 0.1$ with the actuator delay $\tau_a = 0.2$ sec. for which a fourth-order Padé approximant was used ($\kappa = 4$ in (2.9)). The order of the Padé approximation is chosen such that frequency response functions resulting from this approximation represent the real dynamics of the system up to the frequencies of interest which are relevant for string stability analysis. The bandwidth of the underlying ACC controller is taken as $\omega_c = \omega_g/20$ ($\omega_g := \frac{1}{\eta}$) in (2.11) based on speed of response and passenger comfort [61].

From Fig. 5.1, we conclude that in order to achieve string stability for smaller time headways, the communication network needs to be able to guarantee smaller bounds on the delays. The analyses also show that a high sampling frequency may help to achieve string stability with relatively low inter-vehicle distances (h_d) while tolerating larger delays. However, from Fig. 5.1 one can conclude that this effect is rather small. Moreover, from a practical and communication point of view, increasing the sampling frequency limits the number of vehicles that can operate reliably over the same network. Therefore, reliable operation of a CACC system involves making multi-disciplinary design tradeoffs between the specification for the vehicle following controller, network performance and string stability performance criteria. The presented analyses can be used as a design tool for the designer in making these tradeoffs. In Section 5.4, we present experimental results performed with CACC-equipped prototype vehicles for validating this approach towards string stability analysis. Experimental results will be presented for selected operating conditions based on the model-based results presented in this section.

Figure 5.2: Prototype vehicles instrumented with CACC.

5.2 Vehicle Instrumentation

To validate the model-based analysis results and to demonstrate the technical feasibility of employing CACC implemented over a delay-inducing communication network, the CACC control system presented in Section 2.3 has been implemented in two similarly adapted vehicles in cooperation with the Dutch Organization for Applied Scientific Research (TNO) [61, 53]. The Toyota Prius III Executive of the type shown in Fig. 5.2 was selected because of its modular setup and ex-factory ACC functionality. Fig. 5.3 shows a schematic representation of the components related to the experimental setup [61]. In this figure, the CACC-related components are categorized into original vehicle components, CACC-specific components, and the vehicle gateway. These three groups of components are subsequently explained next. By making use of original vehicle systems, only a limited number of components needed to be added. A long-range radar is used to measure the relative position and speed of multiple objects among which the preceding vehicle measurements are extracted and used for realizing the vehicle following functionality. The Power Management Control (PMC) determines the setpoints for the electric motor, the hydraulic brakes, and the engine. Finally, the Human-Machine Interface (HMI) consists of levers through which the (C-)ACC settings (such as desired headway time, cruising speed etc.) can be configured by the driver and a display that provides information on the operation of the system.

Some CACC-specific components had to be implemented in the vehicle in order to run the CACC system. The main component is a real-time computer

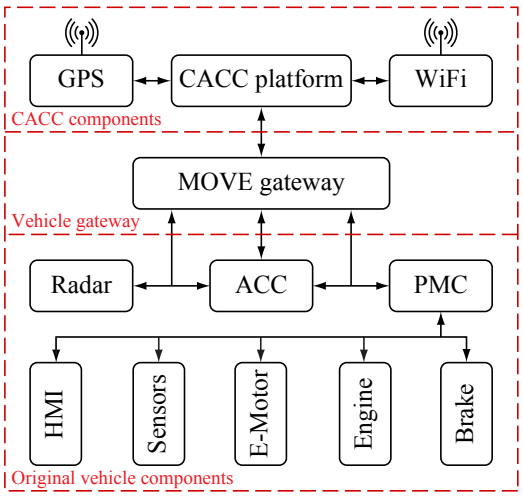

Figure 5.3: Schematic representation of the test vehicle instrumentation.

platform that executes the CACC control functionality. The wireless communication device, operating according to the IEEE 802.11p standard in ad-hoc mode, allows for communication of the vehicle motion and controller information between the CACC-equipped vehicles with an update rate of 25 Hz (corresponding to a sampling interval $T = 40$ msec.). A GPS receiver, with an update rate of 2 Hz, has been installed to allow for synchronisation of measurement data using its time stamp. Note, however, that for the particular experiments presented in this chapter, a much higher clock update rate is required than that might be necessary for normal CACC operation in order to accurately regulate the communication delays at different (constant) levels. Therefore, measurement time-stamps of test vehicles have been more accurately synchronised based on their CPU clocks with an update rate of 100 Hz.

Finally, the MOVE gateway (developed by TNO) is the interface between the original vehicle systems and the real-time CACC platform. It runs at 100 Hz, converting the acceleration setpoints u_i from the CACC platform, into vehicle actuator setpoints, such that the requested acceleration is accurately realized. The gateway also processes the vehicle sensor data and presents these to the CACC platform. Furthermore, the gateway is connected to the vehicle HMI (digital display and levers). As a result, the CACC can be operated like the ex-factory ACC system. To guarantee safe and reliable operation, the gateway also contains several safety features. The gateway employs multiple I/O for the communication with the vehicle systems; a single CAN bus is used for communication with the CACC platform. Further details on the test vehicles can be found in [61].

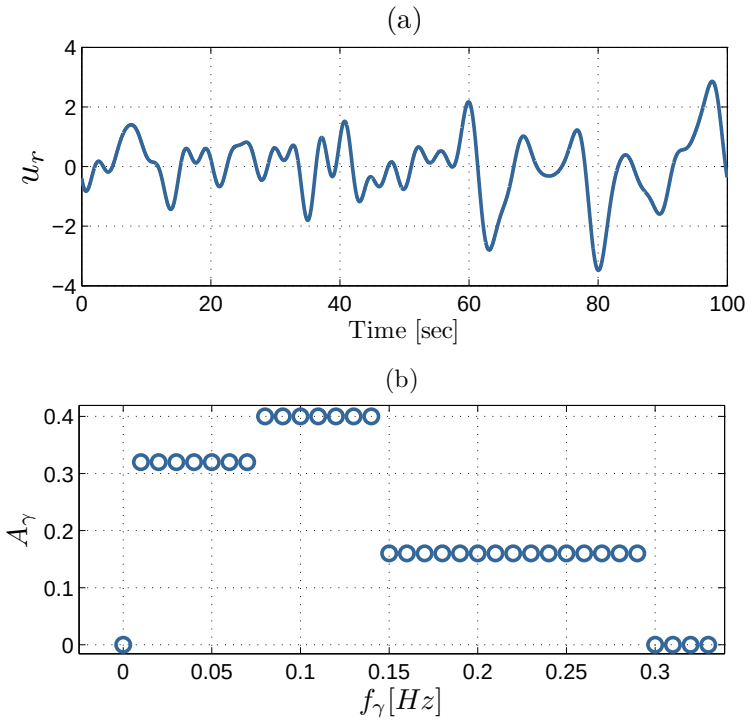

Figure 5.4: Multi-sine velocity excitation signal for the leader vehicle: a) time-domain; b) frequency-domain.

5.3 Experiment Design

For the sake of repeatability of the experiments, the leader vehicle is programmed to track a predefined velocity trajectory which has been designed as a random phase multisine excitation input [59, 18]. The time-domain velocity excitation signal depicted in Fig. 5.4.a is obtained by using a multisine transformation which allows to synthesize test signals with predefined spectral properties as shown in Fig. 5.4.b. For an accurate estimation of the string stability frequency response function (FRF) $S^s_{V_{2,1}}$ in (4.10) from the experimental data, the designed excitation signal needs to excite the frequency range of interest for the assessment of string stability. Here, the frequency bin for amplitudes A_γ is weighted at user-selected equidistant frequencies (f_γ) that are chosen on the discrete grid γf_0 such that better estimation can be achieved within a specific frequency range that is relevant for string stability (in this case the frequency range [0,0.3] Hz) with a sufficiently high spectral resolution (in this case $f_0 = 0.01\ Hz$). Moreover, the excitation signal is designed such that it guarantees a sufficiently high frequency

domain resolution while vehicle-related limitations such as maximum acceleration are also respected. The corresponding N-sample multisine time-series with period $T_0 = 1/f_0$ which is sampled at a sampling frequency $f_s = 1/T_s$ can be obtained by performing an inverse discrete fast Fourier transform (DFFT) of the predefined spectrum and is given by

$$u_r(kT_s) = \sum_{\gamma=1}^{F} A_\gamma cos(2\pi f_\gamma k T_s + \phi_\gamma), k = \{0, 1, \ldots, N-1\}, \tag{5.5}$$

where $N = f_s T_0$, ϕ_γ represents the random phase shifts and $f_\gamma = \gamma f_0, \gamma \in \{1, 2, \ldots, F\}$. The ultimate velocity excitation signal used in the experiments is constructed by repeating the above excitation signal multiple times after an initial platoon formation phase during which cars come to steady platoon operation to avoid transient behaviour.

5.4 Experimental String Stability Analysis

A sample data set from the experiments is shown in Fig. 5.5.a. This experiment was carried out with a headway time $h_d = 1.0$ sec. The local vehicle following controller (ACC) operates at a higher frequency (100 Hz) than the CACC controller which relies on the wireless transmission frequency (of 25 Hz). CACC updates are broadcast by the leader vehicle to the follower at fixed transmission intervals ($T = 40$ msec. corresponding to a wireless communication frequency of 25 Hz). In the experiments, the communication delay is artificially regulated by the receiver to certain values for assessing string stability properties experimentally for a range of constant delay levels. Fig. 5.5.c. shows an example of the actually realized communication delay over time, which is indeed approximately constant and almost equal to the 'desired' delay (in this case $\tau = 750$ msec). A 10 msec. offset exists due to the fact that the on-board computer, regulating the delays, operates at 100 Hz. Consecutive spikes around 280 sec. are due to packet dropouts. Two consecutive periods of the steady-state response (see Fig. 5.5.b.) are selected to compute the maximum likelihood (ML) [59] estimate of the string stability frequency response function (in this case $\widehat{S^s}_{V_{2,1}}$) in (4.10) and (4.11) as follows:

$$\begin{aligned} \widehat{S^s}_{V_{2,1}}(z_\gamma) &= \frac{|\hat{V}_2(z_\gamma)|}{|\hat{V}_1(z_\gamma)|}, \\ &= \frac{M^{-1}\sum_{m=1}^{M}|V_2^{[m]}(z_\gamma)|}{M^{-1}\sum_{m=1}^{M}|V_1^{[m]}(z_\gamma)|} \end{aligned} \tag{5.6}$$

with $z_\gamma = e^{-j2\pi f_\gamma T_s}$, where $V_i^{[m]}(z_\gamma)$ is the frequency spectrum of the time-series velocity data of the i-th vehicle ($v_i^{[m]}$), and M is the number of periods of the multisine used in the estimation as depicted in Fig. 5.5.b. for $M = 2$.

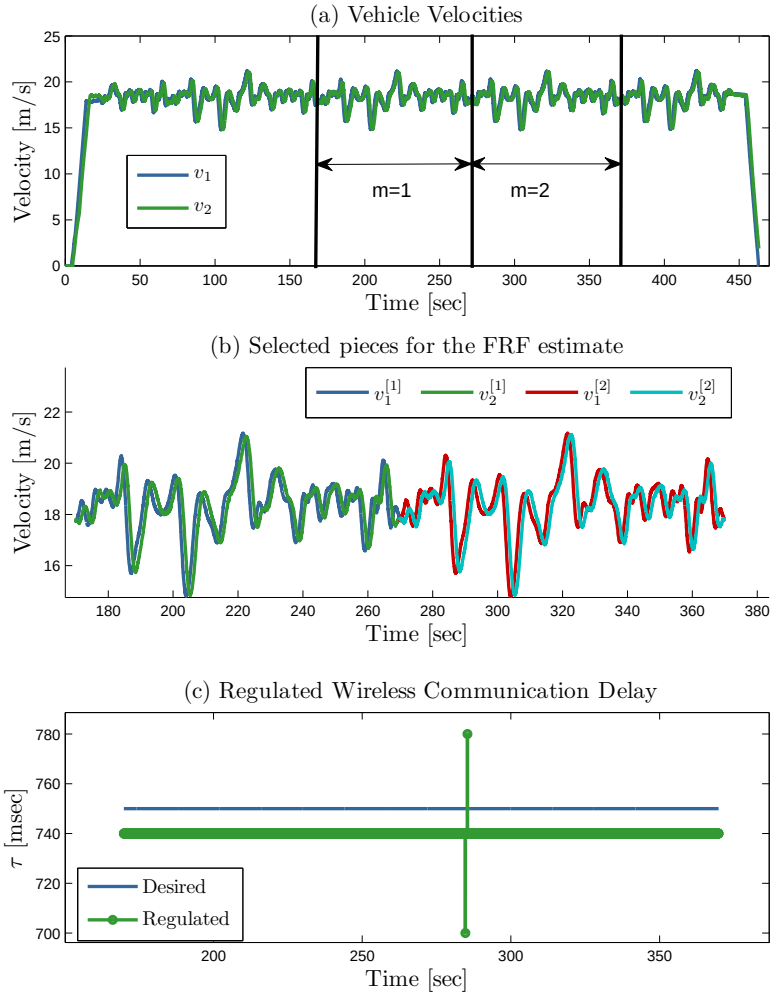

Figure 5.5: Sample data set from an experiment with $h_d = 1.0$ sec. and $\tau = 750$ msec.

In Fig. 5.6, the gain and phase of the estimated string stability frequency response function are shown which were obtained by averaging two periods of the multisine from the sample experimental data in Fig. 5.5.b. In this way, the effects of road conditions and transient dynamics on the frequency response

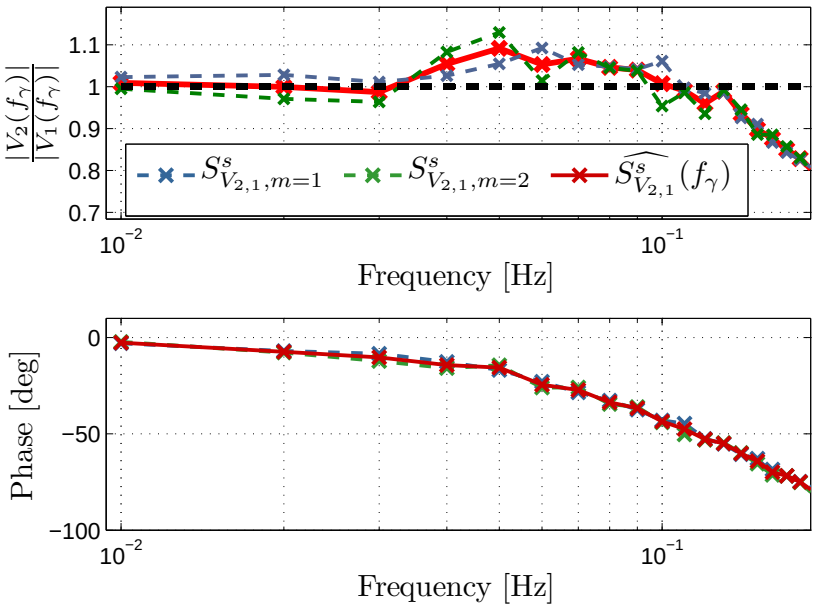

Figure 5.6: Estimated frequency response plot with $h_d = 1.0$ sec. and $\tau = 750$ msec.

function (FRF) estimation is reduced.

For the validation of the CACC model-based string stability analysis results presented in Fig. 5.1, experiments were carried out at a wider range of representative operating points with different time headway values h_d where the wireless communication delay τ was regulated at different levels in order to support the experimental analysis of string stability for different delay magnitudes.

In Fig. 5.7, model-based string stability frequency response functions as in (4.11) are shown which were obtained by using the networked CACC model in (4.8) and are compared with the estimated FRF from experimental data for $h_d = 0.8$ sec. where the wireless communication delay was regulated at $\tau = 450$ msec. This result shows how string stability is compromised by wireless communication delays that exceed maximum allowable delay values given in Fig. 5.1. Moreover, this figure also shows that there is a good match of the experimentally obtained data with the model-based data.

Fig. 5.8 further demonstrates how the model-based results presented in Fig. 5.1 can be used to obtain string stability boundaries on maximum allowable delays (where the analyses were done for a smaller time headway of $h_d = 0.6$ sec.). These figures show that the discrete-time approach is very accurate in predicting

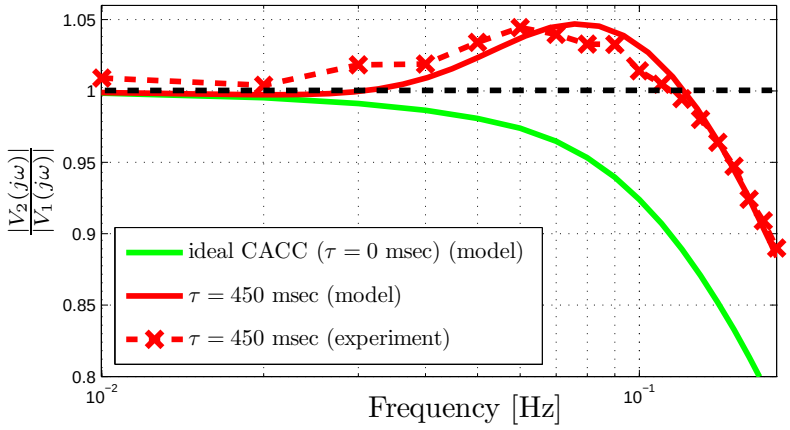

Figure 5.7: Estimated FRF with $h_d = 0.8$ sec.

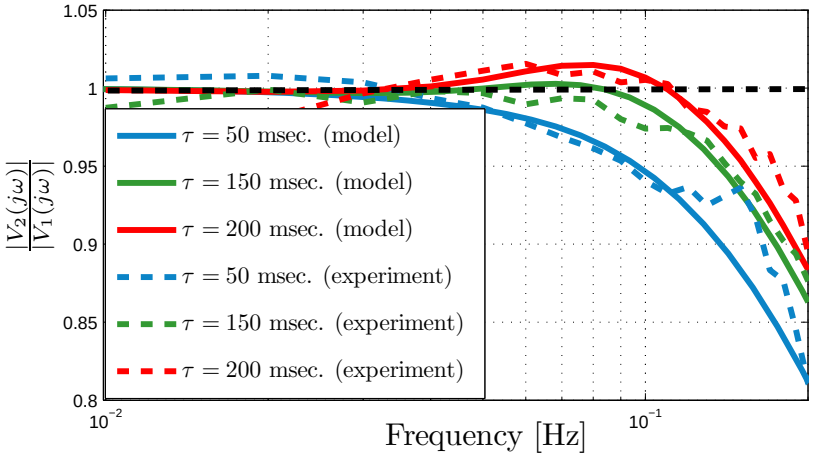

Figure 5.8: Estimated FRF with $h_d = 0.6$ sec.

the string stability properties of the sampled-data interconnected vehicle string model. The FRF estimates based on real experiment data in Fig. 5.7 and Fig. 5.8 show how string stability is compromised by wireless communication delays and demonstrate the reliability and practical validity of the analysis method presented in Section 4.2.

5.5 Conclusions

In this chapter, we showed how the network-aware modelling and string stability analysis framework developed in Section 4.2 can be used as a multi-disciplinary design tool to investigate tradeoffs between wireless network specifications and headway policies in terms of their influence on string stability. We demonstrated the validity of the model-based analysis results by real experiments with Cooperative Adaptive Cruise Controller (CACC)-equipped vehicles. Experiments were carried out for varying time headways and communication delays in order to validate the model-based analyses. Experimental results show how string stability is compromised by wireless communication delays and these results also demonstrate the reliability and practical validity of the analysis method presented in Section 4.2 which incorporates the effects of the sampling and the zero-order-hold in addition to constant wireless communication delays.

Chapter 6

Cooperative Driving with a Heavy-Duty Truck in Mixed Traffic: Experimental Results[1]

This chapter describes the implementation and testing of a Cooperative Adaptive Cruise Control (CACC) strategy on a heavy-duty truck. The adopted control strategy utilizes additional information exchange through wireless communication to improve vehicle following behaviour achieved by the underlying Adaptive Cruise Controller (ACC). The control method is evaluated in a mixed traffic condition. It is shown that the truck can perform smooth predecessor following in most of the test scenarios even for small inter-vehicle distances. Furthermore, the results demonstrate how string stability is affected by wireless communication imperfections and ac-(de)celeration limitations of the heavy-duty truck in a heterogeneous platoon.

[1] This chapter is based on [52].

6.1 Introduction

The desire towards meeting the ever-increasing transportation demands through efficient and eco-friendly means of transportation has led to research in Intelligent Transportation Systems (ITS) technologies. Cooperation between vehicles can play an important role in achieving the set goals.

An extended adaptive cruise control system that is using information exchange through wireless communication in addition to the locally available sensor measurements (e.g. a radar or a lidar) to keep a desired distance, is called Cooperative Adaptive Cruise Control (CACC). CACC equipped vehicles are able to drive safely at reduced inter-vehicle distances without amplification of disturbances (i.e. string instability) that have an adverse effect on traffic flow stability. The attenuation of disturbances, which results in string stable traffic flow, together with reduced inter-vehicle distances increases the traffic throughput. Additionally, these two effects (improved string stability and smaller inter-vehicle distances) result in a reduction of the fuel consumption. The main criteria to evaluate longitudinal control algorithms is the minimum achievable inter-vehicle distance while satisfying string stability [78, 49].

String stability experiments with two identical CACC equipped passenger cars were presented in [49, 61, 53] and in Chapter 5 of this thesis. These experiments show that string stable behaviour can be achieved in practice by choosing a sufficiently large headway time. Platooning experiments with automated heavy-duty trucks were performed by California PATH [43]. The problem addressed in these experiments is string instability caused by the large actuation delays of the truck, and that the use of a constant distance spacing policy can also lead to string instability. This is due to the fact that string stable behaviour cannot be achieved by using only sensed preceding vehicle information in combination with a constant distance headway policy [80, 77, 68].

Especially heavy-duty trucks can benefit from CACC. This particular benefit of CACC for trucks stems from the fact that the aerodynamic drag of a truck is high due to the flat frontal surface. Therefore, close distance driving will result in a significant fuel reduction. An experiment with two European heavy-duty trucks with an inter-vehicle distance of 10 m shows that the fuel reductions for the following truck and the leading truck respectively are as much as 20% and 6%, respectively [8]. In [10], the inter-vehicle distance between two American heavy-duty trucks is varied between 3 - 10 m resulting in a fuel reduction of $10-12\%$ for the following truck and a fuel reduction of $5-10\%$ for the leading truck. Both experiments were performed at a velocity of 80 km/h.

In addition to the high drag coefficient, a heavy-duty truck also has a high total weight. As a consequence, a lot of energy is lost when the vehicle is braking. Therefore, an unstable traffic flow will increase the fuel consumption, because

the vehicle has to ac-(de)celerate more than required. For the above reasons, the CACC technology is especially beneficial for the transport sector where fuel costs can be as high as 1/3 of the total operational costs [4]. Also the limited acceleration performance of heavy-duty trucks has a large effect on the traffic throughput, because heavy-duty trucks cannot recover as fast from a braking action that occurs in an unstable traffic flow. Research proves that if 10 % of the vehicles are equipped with ACC, the fuel consumption would be reduced about 7 % [9].

The contributions of this chapter are (string stable) heterogeneous vehicle following experiments with a CACC-equipped heavy-duty truck performed during the Grand Cooperative Driving Challenge (GCDC). The GCDC is an event in which multiple teams tested their CACC vehicle and benchmarked it to the CACC vehicles of other competitors [62]. The Automotive Technology Team (ATeam[2]) of Eindhoven University of Technology participated with a heavy-duty truck. In these experiments, a constant headway time spacing policy was used in which the headway time parameter was varied. The experiments were performed in mixed traffic scenarios that mimic realistic traffic situations. The experiments performed by California PATH were done using two trucks with different inertias, where the following truck has half the mass of the leading vehicle. Analysis shows that a lighter following truck makes string stable behaviour possible [49, 71]. The experiments presented in this chapter were performed with a heavy-duty truck following a much lighter passenger vehicle. This demonstrates the effect of the limited performance of a heavy-duty truck on string stability. Also the effect of temporary wireless communication failures, which often occur, on the platoon performance is discussed.

This chapter describes the CACC control methodology and presents the results of the performance of the ATeam heavy-duty truck during the GCDC and it is organized as follows. The vehicle following control algorithm that was used to satisfy the control objective is described in Section 6.2, which consists of a low-level vehicle controller and a high-level platoon controller. The low-level vehicle controller and the high-level platoon controller are explained in Section 6.3 and 6.4, respectively. The hardware setup and information of the GCDC are given in Section 6.6. Section 6.7 presents the experimental results obtained during the GCDC. Finally, conclusions and recommendations are given in Section 6.8.

[2]The ATeam (Automotive Technology Team) is an initiative of the Eindhoven University of Technology to promote and demonstrate the possibilities of cooperative driving and is named after the newly established Automotive Technology M.Sc. programme. The team cooperates with TMC Mechatronics B.V. and DAF trucks N.V. The team consists of students, PhD students and employees of the university, DAF trucks and TMC. In 2013, the ATeam is renewed as ATeam 2.0 with an ambition to realize fully autonomous driving.

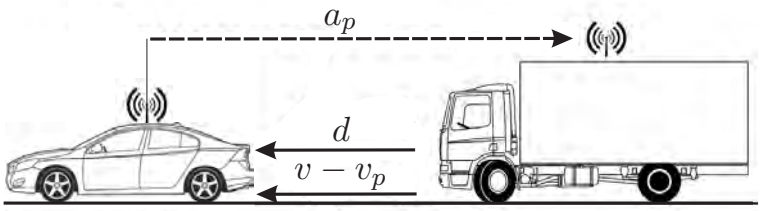

Figure 6.1: Illustration of a truck following a passenger vehicle.

6.2 Vehicle Following Objective

The ACC algorithm uses the inter-vehicle distance d and the relative velocity to the preceding vehicle $v - v_p$ that is obtained by using a radar or a lidar (v_p represents the velocity of the preceding vehicle and v is the velocity of the follower vehicle, see Fig. 6.1). Additionally, as is illustrated in Fig. 6.1, the CACC approach employed in this chapter uses the acceleration of the preceding vehicle a_p which is acquired by wireless communication. The main reason for using wireless communication is the fact that the preceding vehicle acceleration cannot be measured accurately by remote sensing.

A constant headway time policy is used to determine the desired inter-vehicle distance d_r, which is related to the vehicle velocity v and is given as

$$d_r = h_d v + r. \tag{6.1}$$

Here h_d is the headway time (s) and r the safety distance (m) at standstill. Then the distance error e (m) is defined as

$$e = d - d_r, \tag{6.2}$$

where d is the actual distance (m). The (vehicle following) control objective is to regulate the distance error e and its derivative $\dot{e}$ to zero. Additionally, the controller should ensure string stability. These control objectives are realized

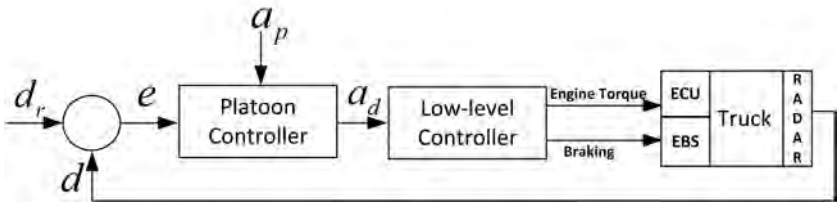

Figure 6.2: Layered control structure.

by a layered control structure as shown in Fig. 6.2. A high-level controller, namely the platoon controller which will be explained in Section 6.4, computes the desired acceleration of the truck based on the employed C-ACC strategy in order to regulate the error e to zero. The low-level controller realizes the desired acceleration by sending control commands to the Electronic Control Unit (ECU) and/or the Electronic Braking System (EBS).

6.3 Low-level Controller

Distance control of a heavy-duty truck is more involved than controlling the distance of passenger vehicles. This is due to [6]:

- the low power-to-weight ratio;
- the actuation delays and lags in the ECU and EBS;
- the disturbances during gear shifting, (and by wind and by road inclination);
- the braking system that often consists of service brakes, engine brake and a transmission retarder.

To overcome these challenges nonlinear controllers are used in [43, 44] to control the inter-vehicle distance of heavy-duty trucks. Here, we employ a layered control structure to deal with this, see Fig. 6.2. The easiest way to deal with the complexity of the control problem is to divide the longitudinal vehicle control system into high- and low-level controllers. The high-level controller determines the desired acceleration of the vehicle on the basis of the position and velocity relative to the other vehicles in the string. The low-level controller determines the input commands to the engine and the braking system to realize the desired acceleration (note that in previous chapters we only focussed on the high-level controllers). The latter is vehicle specific and relies on known or identified vehicle parameters and the engine map. In fact, the low-level controller takes care that the high-level controller is not vehicle specific. In this way, the same high-level controller can be used for different types of vehicles. The low-level controller is tuned by using measurements on a chassis dynamometer. The dynamometer enables accurate measurements of the characteristics of the power train. Therefore, a relatively simple control algorithm already achieves sufficient vehicle following performance. Since the used heavy-duty truck is already equipped with a controller that automatically brakes on the basis of a given desired acceleration, only a controller for the power train is designed.

This low-level controller is composed of three parts as illustrated in Fig. 6.3. Firstly, the required wheel force F_w is derived to overcome friction forces and fulfil the desired acceleration a_d. Secondly, the engine torque T_e is calculated to generate the requested wheel force. Finally, the corresponding engine torque

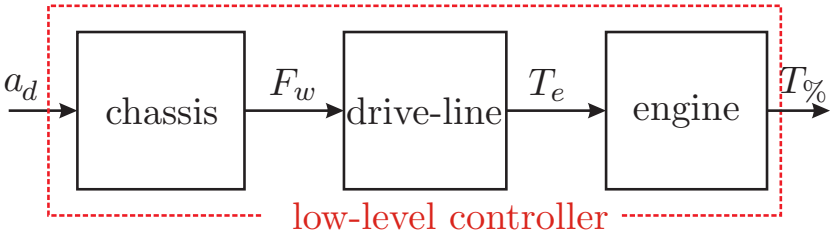

Figure 6.3: Block scheme of the low-level control algorithm.

command ($T_\%$) is obtained as the percentage of the maximum available torque at the current engine speed.

The requested engine torque T_e (Nm) can be determined by using

$$F_w = Ma_d + F_f, \tag{6.3}$$
$$T_e = F_w[r_f r_g r_w \eta_d(n_g)]^{-1}, \tag{6.4}$$

where M is the mass of the truck, F_w the required wheel force (N), and $\eta_d(n_g)$ represent the losses in the gearbox and the drive-line. The losses are dependent on the selected gear n_g. Furthermore, r_f, r_g and r_w are, respectively, the final drive ratio, current gear ratio and wheel radius. The total friction force F_f (N) is a summation of the aerodynamic friction, rolling resistance and static friction

$$F_f = C_a v^2 + C_r v + C_s, \tag{6.5}$$

where C_a, C_r and C_s are the aerodynamic, roll and static friction coefficients.

The input to the engine can be determined by using an inverse engine map

$$T_\% = E_{MAP}(\omega_e, T_e), \tag{6.6}$$

where the torque request ($T_\%$) to the engine is expressed as percentage of the maximum available torque at the current engine speed. The input variables of the map are the engine speed ω_e and the required engine torque T_e. The engine map is obtained by using measurements on a chassis dynamometer. The dynamometer can handle a limited amount of torque and, therefore, only a part of the engine map can be measured (up to 40% of the maximum torque). The complete map is obtained by extrapolation.

Feedback in the low-level controller is not required because the parameters are determined by measurements on the vehicle itself and it is observed that the desired acceleration sufficiently matches the actual acceleration of the vehicle. Any mismatch is compensated by feedback of the platoon controller. Note that estimation techniques are available that can adapt the weight and drag coefficients on the run [6], but these are not employed in the scope of this work.

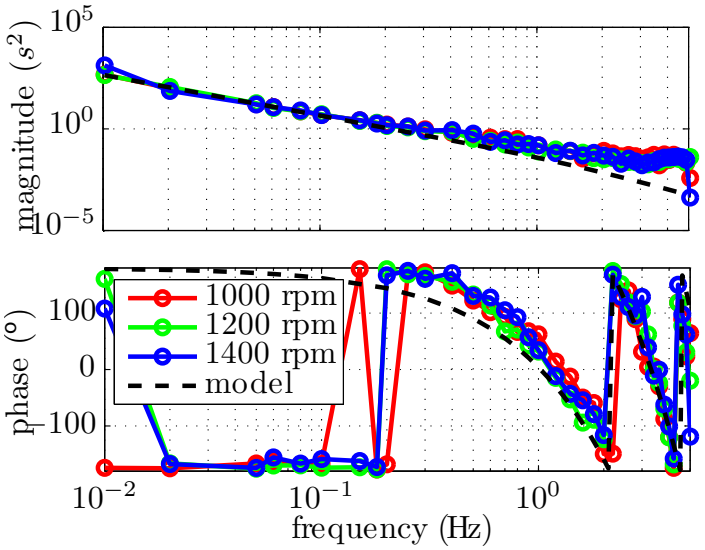

Figure 6.4: FRF plot of low-level system, $P_d(j\omega)$, at different engine speeds (rpm).

The dynamics of the low-level system (vehicle including low-level control) are determined by measuring the frequency response function (FRF) of the transfer function $\frac{V(s)}{A_d(s)}$ on the dynamometer, where $V(s)$ and $A_d(s)$ are the Laplace transforms of the velocity v and the desired acceleration a_d, respectively. Let us now recall that CACC aims to control the inter-vehicle distance. Therefore, the measured FRF is integrated once resulting in the transfer function $P_d(s) = \frac{V(s)}{A_d(s)}\frac{1}{s}$. Fig. 6.4 shows this frequency response function $P_d(j\omega)$ for engine speeds of 1000, 1200 and 1400 rpm. The figure shows that the FRFs are almost identical for different engine speeds. The magnitude has an almost perfect slope of -2. The phase starts at the corresponding -180° angle, but decreases due to a constant delay in the system. A third-order low-level vehicle model with actuator delay as in [49] is fitted (dotted black line) on top of the FRF results leading to

$$P_d(s) = \frac{1}{s^2(\tau s + 1)} e^{-\theta s}, \tag{6.7}$$

where an actuation delay $\theta = 0.4$ and a lag $\tau = 0.1$ are used. It was observed that the actuation delay (θ) had a significantly stronger effect on the dynamical behaviour of the truck than the lag (τ).

6.4 Platoon Controller

For regulating the distance error given in (6.2), the platoon controller in [49] uses feedforward and feedback expressed in the Laplace-domain as

$$\begin{aligned} A_d(s) &= U_{fb}(s) + U_{ff}(s) \\ &= C_{fb}(s)E(s) + C_{ff}(s)A_p(s). \end{aligned} \tag{6.8}$$

As before, uppercase letters are used to indicate the Laplace transform of the corresponding lower case variable, e.g. $E(s) = \mathcal{L}\{e(t)\}$. In (6.8), the feedback controller C_{fb} and the feedforward filter C_{ff} use, respectively, the distance error and the preceding vehicle acceleration as input. The feedback part of the CACC controller consists of a PD controller and an additional low-pass filter based on the spacing policy. In the Laplace domain it is given as

$$U_{fb}(s) = C_{fb}(s)E(s) = \frac{K_p + K_d s}{1 + h_d s}E(s). \tag{6.9}$$

Parameters K_p and K_d are the proportional and differential gain, respectively. For the truck $K_p = 0.3$ and $K_d = 0.7$ are used. The cut-off frequency of the low-pass filter is equal to the headway time h_d [37].

The feedforward part of the CACC controller is given as

$$\begin{aligned} U_{ff}(s) = C_{ff}(s)A_p(s) &= [H(s)P_d(s)s^2]^{-1}A_p(s) \\ &= \frac{\tau s + 1}{h_d s + 1}A_p(s). \end{aligned} \tag{6.10}$$

In (6.10), the preceding vehicle acceleration is compensated for the low-level vehicle dynamics of (6.7) and the headway policy of (6.1), where $H(s) = 1 + h_d s$.

The bandwidth of the open-loop low-level vehicle model (6.7) with the feedback controller (6.9), i.e. $C_{fb}P_d$, is approximately 0.1 Hz. For comparison, the bandwidth of the passenger vehicle in [49] is 0.6 Hz. The low bandwidth of the truck is a significant performance limiting factor for the operation of the truck in a heterogeneous platoon.

6.5 String Stability Analysis

String stability can be determined by using the string stability transfer function $\frac{V(s)}{V_p(s)}$ which is expressed as [49]

$$SS(s) = \frac{(C_{ff}(s)s^2 + C_{fb}(s))P_d(s)}{1 + H(s)C_{fb}(s)P_d(s)}. \tag{6.11}$$

A condition for strong string stability as in Section 3.3 can now be formulated as

$$|SS(j\omega)| \leq 1, \forall \omega \in \mathbb{R}. \tag{6.12}$$

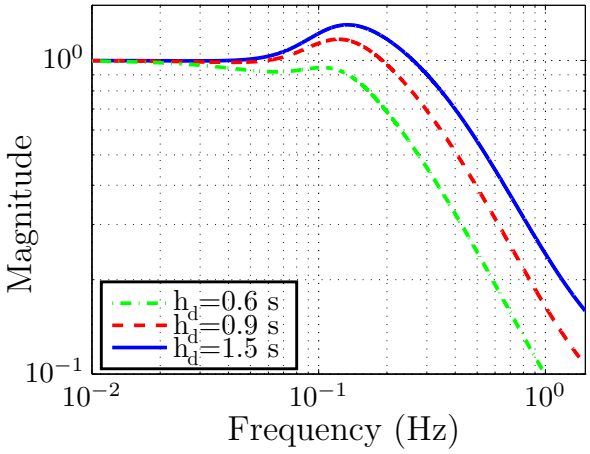

Figure 6.5: Magnitude of the string stability transfer function $|SS(j\omega)|$ for different headway times.

In (6.11), it is assumed that there is no communication delay. The magnitude of the string stability transfer function in (6.11) is given in Fig. 6.5 for different headway times. Although the CACC platoon controller design (6.8)-(6.10) is such that string stable operation is achieved irrespective of the headway distance in the ideal situation of no actuator delay, i.e. $\theta = 0$, when actuator delay is considered, the magnitude of $|SS(j\omega)|$ lies partly above 1 for headway times of 0.6 s and 0.9 s, which indicates string instability. The CACC truck is string stable for a headway time of 1.5 s. Therefore, the minimum headway time guaranteeing string stability is mainly influenced by the actuation delay (θ) in the vehicle model (6.7).

6.6 Experiments

The experiments are performed using a DAF XF104 460. This truck has a maximum power of 340 kW, a maximum torque of 2300 Nm and weighs about 12 tons. The hardware used to implement CACC is built around a real-time (RT) system that is using the MATLAB xPC TARGET environment that is running at 100 Hz. The radar unit, the Electronic Braking System (EBS) and the Electronic Control Unit (ECU) are connected to the Real-Time (RT) system by a Controller Area Network (CAN) bus connection as shown in Fig 6.6. A torque command sent by the low-level controller of Section 6.3 is sent to the ECU. A negative desired acceleration (< -0.8 m/s^2) is directly sent to the EBS. A built-in controller in the EBS realizes the desired deceleration (a_{br}). The GPS, which is used to acquire accurate timing, position and heading information is

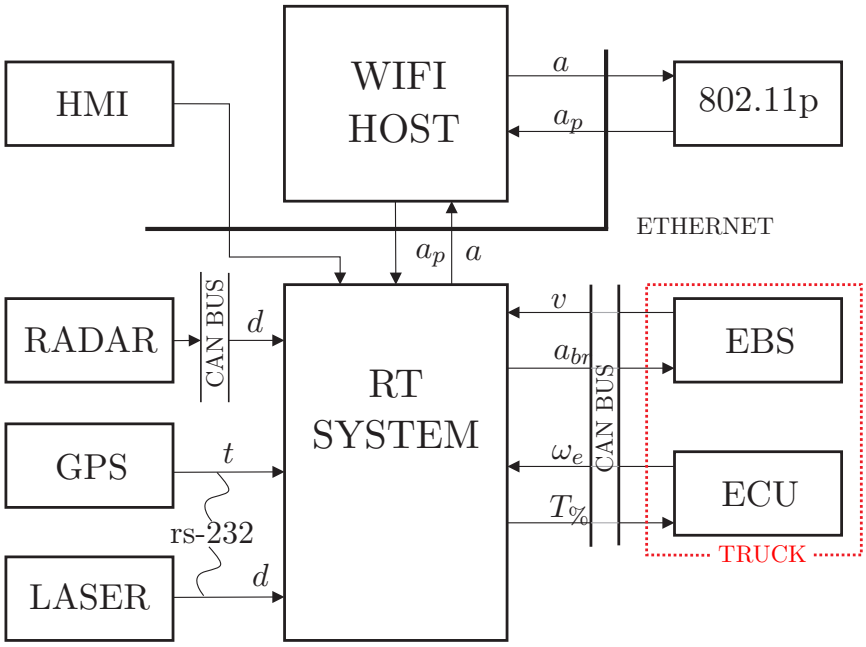

Figure 6.6: Scheme of real-time control system.

connected to the RT system with a serial port connection (RS-232). The radar unit, which is used as main distance measuring device, is connected by a separate CAN. At standstill, when the radar unit is not able to detect any objects, a laser distance measuring device is used. This laser unit is connected by RS-232. GPS is not used to determine the distances between vehicles because the related position errors are too large. Furthermore, the RT system is controlled using a xPC (RT) host and steering wheel switches. The WIFI host, RT host and wireless hardware are connected using the same LAN network.

The data that is wirelessly routed via a WIFI host. This WIFI host processes all WIFI related tasks. This relieves the real-time system. The packets are transmitted over the air by the IEEE 802.11p protocol [1]. This protocol is broadcast based and is specially designed for automotive applications. The data packets are encoded/decoded using the ASN.1 notation and sent at a 10 Hz update rate according to the GCDC specifications [2]. The main data the packets contain are acceleration, heading information, position, velocity and, time stamp information. However, the CACC algorithm that is used here only requires the acceleration of the preceding vehicle; the additional data can be used in case another control strategy is used. Moreover, it can be used to determine which data is coming from the preceding vehicle or whether or not the data is reliable.

Figure 6.7: ATeam truck (most forward truck) during the GCDC.

The experimental data was collected during the Grand Cooperative Driving Challenge (GCDC) [2, 62]. The goal of the GCDC is to accelerate the deployment of cooperative driving technology. The GCDC has taken place on the A270 highway between Helmond and Eindhoven in the Netherlands in May 2011. The Automotive Technology Team (ATeam) of the Eindhoven University of Technology participated in the GCDC with a heavy-duty truck. Apart from one other heavy-duty truck, the other competitors used passengers vehicles.

The challenging aspects of the GCDC are [60]:

- Firstly, a strategy for deployment of cooperative driving technology needs to be introduced;
- Secondly, robust and fail-safe control systems need to be designed;
- Thirdly, communication between vehicles and between vehicle and infrastructure has to be standardized;
- Finally, wireless communication in real-time environments has to be demonstrated.

Note that each team has only one vehicle at its disposal. This turns the challenge into a true cooperative task.

The challenge consists of three scenarios where the cooperative vehicles are tested on different aspects: Automatically pulling away if a traffic light turns green, smoothly joining a slower moving platoon in front and smooth vehicle

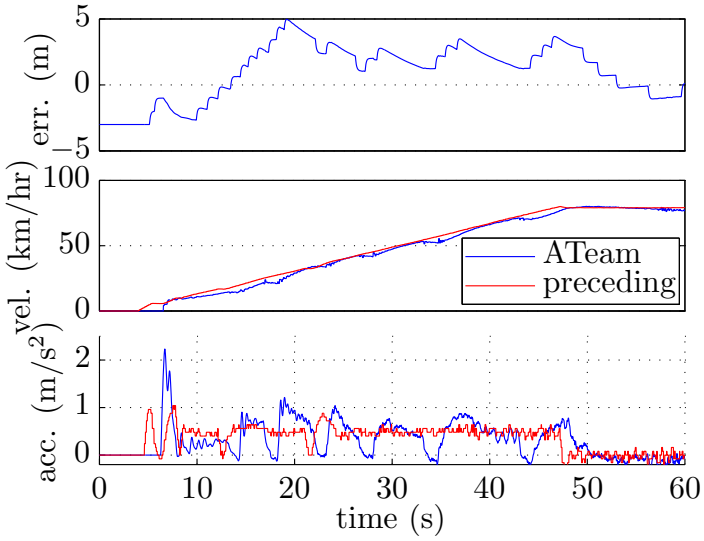

Figure 6.8: Following behaviour from standstill to 90 km/h.

following during close distance driving. In this chapter, the focus is on smooth close distance following behaviour only. Fig. 6.7 shows a heat during the GCDC.

6.7 Experimental Results

During the GCDC event, the vehicle following capabilities of the truck were tested. The results presented here involve following a passenger vehicle of other competitors. Figures 6.8, 6.9, 6.10, and 6.11 show the distance error, the velocity and the acceleration of the ATeam truck and the directly preceding vehicle. In the analysis of the presented results, it should be noted that the sequencing of the vehicles in the platoon was different at each run and, it can be seen that the performance of the truck depends heavily on the behaviour of the predecessor.

Fig. 6.8 shows the vehicle following behaviour of the truck from standstill to maximum speed. Here it can be seen that the truck is able to follow the preceding vehicle with a maximum error of about 5 m. The preceding vehicle has, except for two gear changes, an almost constant acceleration of 0.5 m/s^2. The acceleration profile of the truck shows that the truck shifted gear six times. The gear changes of the truck take more time than the gear changes of the preceding vehicle. As a result of this, the truck has to accelerate much faster afterwards than the preceding vehicle to keep the error small. After a gear change, the acceleration of the truck may therefore exceed the acceleration of the preceding

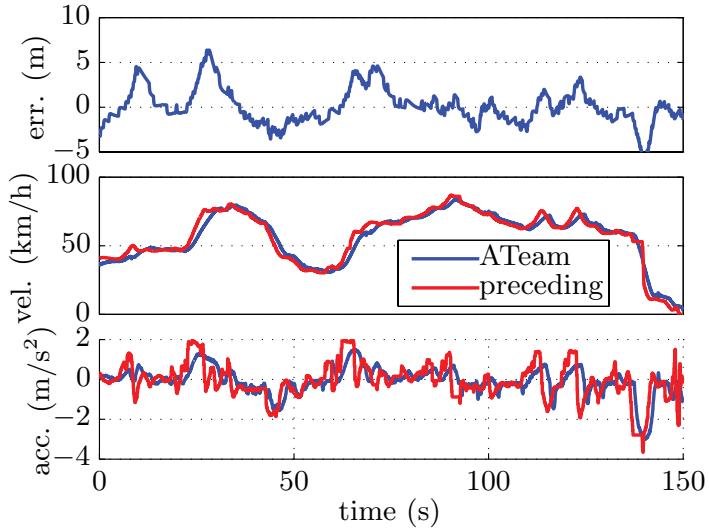

Figure 6.9: Following behaviour of the ATeam truck using a headway-time (h_d) of 1.5 s.

vehicle as is shown in Fig. 6.8. Here it can be seen that the preceding vehicle has an almost linear increase of the velocity, the velocity increase of the truck is more aggressive. This introduces unavoidable shockwaves in the traffic flow. Figures 6.9, 6.10 and 6.11 show the vehicle following capabilities of the ATeam truck for different headway times of 1.5, 0.9 and 0.6 s respectively. Fig. 6.9 shows that a headway time of 1.5 s results in a smooth and string stable following behaviour (as expected from the model-based string stabilty analysis in Section 6.5). This is evident from the truck acceleration that does not exceed the acceleration of the preceding vehicle. It should be noted that determination of string stability on the basis of experimental data is not straightforward. This is because the level of amplification of the acceleration does not determine string stability as is described in Section 6.5 [61].

At about 140 s in Fig. 6.9 it is visible that the wireless communication fails and the system is not receiving acceleration updates. A larger negative error occurs, because the feedback controller is unable to keep the error small at large decelerations ($a_p \approx -3$ m/s^2). Large negative errors must be avoided because these are safety critical. The positive distance error, which is not safety critical, increases occasionally to 6 m.

Fig. 6.10 shows the performance of the truck for a headway time of 0.9 s. Although, the analytic string stability analysis in Section 6.5 concludes string instability, the figure shows smooth vehicle following behaviour. This is related

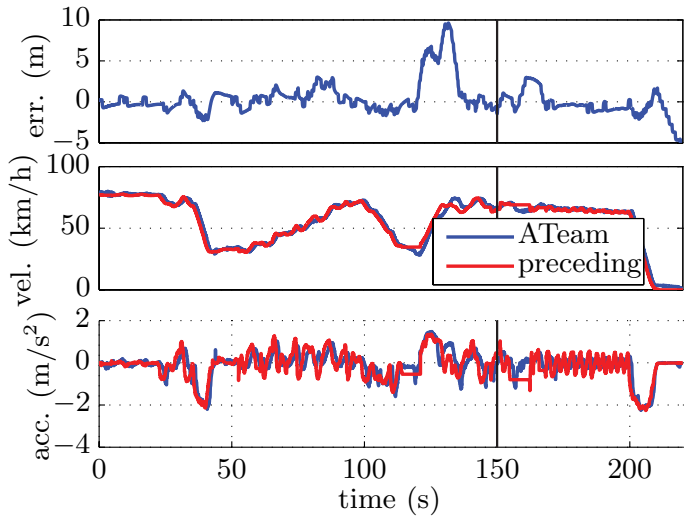

Figure 6.10: Following behaviour of the ATeam truck using a headway-time (h_d) of 0.9 s.

to the fact that frequencies where string instability can occur are not triggered by the excitation signal. The acceleration of the truck only exceeds the preceding vehicle acceleration a couple of times (at around 120 s and 160 s). These exceeding accelerations are caused by failures of the wireless communication. On such occasions, the feedback controller is not able to reduce the resulting distance error smoothly.

The performance of the truck using a headway time of 0.6 s is shown in Fig. 6.11. Still, the truck is able to attenuate the disturbances introduced by the preceding vehicle. The number of times the acceleration of the truck exceeds the acceleration of the preceding vehicle is still limited. If the acceleration of the truck exceeds that of the preceding vehicle, it is the result of a large error caused by the acceleration limits of the truck.

From the experiments, it can be concluded that platooning with a truck is indeed more challenging than with only passenger cars. The difficulty of heavy-duty truck control is mainly due to the limited acceleration capability and the gear changes of the truck. A solution is to increase the headway since this results in smoother following behaviour. However increasing the headway time is not desirable, because it reduces the benefits of CACC. Another cause of a large distance error is the failure of the wireless communication. This is not specifically related to heavy-duty truck control, but it occurs more frequently than for a platoon with only passenger vehicles because of the dimensions of the

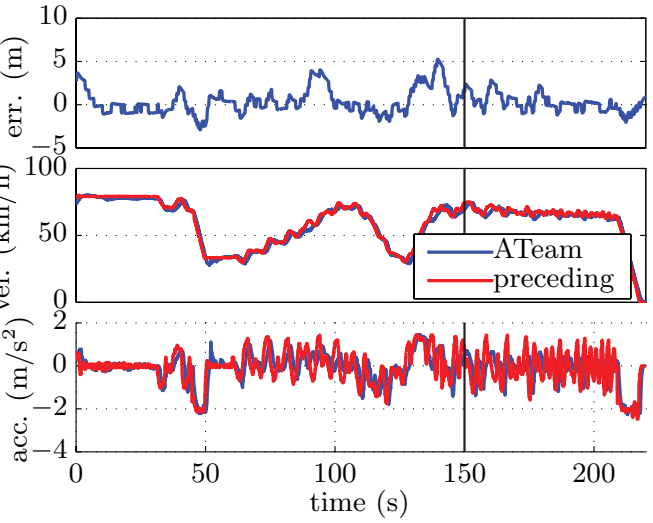

Figure 6.11: Following behaviour of the ATeam truck using a headway-time (h_d) of 0.6 s.

truck and its negative effects on signal reception quality. Another less visible cause is that the EBS of this truck only accepts brake requests smaller than -0.7 m/s^2. This results in aggressive braking while smooth braking would be sufficient.

6.8 Conclusions and Recommendations

This chapter reports on the implementation and experimental testing of a CACC algorithm on a heavy-duty truck operating in a heterogeneous platoon. The experiments show that the performance of this control strategy is satisfactory under normal operating conditions. The ATeam truck smoothly follows the preceding vehicle most of the time even in scenarios with headway time values that were smaller than the admissible string stable headway values revealed by model-based analysis. This might be due to the fact that operating frequencies where string instability can occur are not triggered by the excitation signal.

The experiments show that in case wireless communication fails and the system only relies on feedback control, the controller is not able to keep the distance error small which confirms the benefit of CACC over mere ACC. Sensor fusion and data estimation techniques could be used to overcome wireless communication failures, but were not considered in the scope of this work. A large distance error also occurs when the truck cannot keep up due to gear changes and ac-

celeration limits. The CACC algorithm reacts too aggressively to these large distance errors resulting in non-smooth following behaviour, which seems to be string unstable.

To solve this, a more involved feedback controller needs to be adopted that can cope with large distance errors. A specific solution could be to temporarily increase the headway time if the distance error is increasing. Another recommendation is to study the string stability performance of other CACC algorithms that use data of vehicles other than the directly preceding vehicle. These controllers can be used if the communication with the preceding vehicle fails in order to ensure safe fallback strategies.

Chapter 7

Conclusions and Recommendations

In this thesis, we considered a vehicle platooning system which regulates inter-vehicle distances in a vehicle string. The development of vehicular platooning systems is motivated by their potential benefits in making more efficient use of the existing ground transportation infrastructure by achieving reduced inter-vehicle distances at highway speeds and, therewith, increasing traffic throughput while maintaining traffic flow stability. All together, these aspects contribute to reduced travel times, improved ride quality and fuel economy. For vehicular platooning systems, the so-called *string stability* property, which relates to the attenuation of the effects of disturbances as they propagate throughout the vehicle string, is of major importance. Indeed, in the absence of string stability, the amplification of disturbances poses risks on safe and reliable operation of the individual vehicle following controllers and compromises traffic flow stability, ride quality, fuel economy and traffic throughput.

A Cooperative Adaptive Cruise Control (CACC) system, which is an extension of the currently available Adaptive Cruise Control (ACC) technology, can improve the performance of existing vehicle follower systems by utilizing information exchange between vehicles through wireless communication besides local sensor measurements. A CACC-equipped vehicle is able to overcome sensory limitations of human- or ACC-operated vehicles and can, therefore, react much faster to the behaviour of neighbouring vehicles. Proof-of-concept demonstrations with platoons of CACC vehicles have recently confirmed the practical feasibility of such cooperative automated longitudinal control systems. Significant improvements over existing ACC technology can be achieved already with relatively simple control algorithms and communication structures. However, wireless communication introduces network-induced imperfections due to limited

bandwidth of the wireless network, and the fact that multiple nodes are sharing the same medium. These imperfections can adversely effect the string stability properties of CACC-systems and the implementation of CACC for real traffic conditions requires consideration of the constraints imposed by the wireless communication needed to implement CACC. The impact of these network-induced imperfections on string stability requires careful modelling and analysis. Moreover, tradeoffs between CACC performance and network specifications need to be made for achieving desired performance under these network-induced constraints.

The main purpose of this thesis has been to emphasize the necessity for considering CACC in a Networked Control Systems (NCS) framework by studying the effects of wireless communication on the performance of (existing) CACC controllers in terms of string stability. Therefore, we approached the design of a CACC system from a Networked Control System (NCS) perspective and employed NCS modelling and analysis methods for the analysis of string stability properties of vehicular platoons. Moreover, we also show how these string stability analyses can provide the designer with guidelines for making the tradeoffs between control and network specifications.

This thesis provided the following main contributions:

i) Development of an interconnected vehicle string model, where two types of data employed in the CACC controller are distinguished according to the way they are being transferred, i.e. either locally sensed or wirelessly communicated information, see Chapter 2. This allows us to analyse in detail the effects of wireless communication deficiencies in the inputs separately;

ii) Tools for quantifying the propagation of vehicle responses have been presented which provide system-theoretic conditions for parametric analyses of string stability properties of CACC systems, see Chapter 3;

iii) We cast the interconnected vehicular system dynamics into a Networked Control System (NCS) model that incorporates the network-induced effects due to the wireless communication, see Chapters 2 and 4;

iv) Based on this network-aware modelling approach, we have developed techniques to study the so-called *string stability* property of the vehicle platoon in the presence of effects induced by the wireless network. The analyses provide quantitative results that can be used as guidelines to assist the designer for making multi-disciplinary design tradeoffs between control and network specifications, see Chapter 4;

v) Finally, we demonstrated the validity of the model-based analysis results by real experiments with Cooperative Adaptive Cruise Controller (CACC)-equipped passenger vehicles, see Chapter 5. Experiments were carried out for varying inter-vehicle distances and communication delays in order to

validate the model-based analyses. Experimental results show how string stability is compromised by wireless communication delays and demonstrate the reliability and practical validity of the network-aware modelling and string stability analysis method. Furthermore, in Chapter 6, experiments have been carried out with a heavy-duty truck which show improved string stable behaviour of the truck within a heterogeneous vehicle string in a multi-vendor setting and address the effects of wireless communication losses and vehicle dynamics limitations on string stability properties of heavy-duty vehicles.

7.1 Main Conclusions

In this thesis, we have shown via time-domain simulations and system theoretic analyses how Cooperative Adaptive Cruise Control (CACC) system can improve the performance of vehicle follower systems by utilizing information exchange between vehicles through wireless communication in addition to local sensor measurements. Besides the vehicle following objective, the attenuation of the effect of disturbances on the vehicle responses along the vehicle string, captured by the notion of *string stability*, is of crucial importance in longitudinal automation of vehicle platoons and relates to aspects such as safety, comfort, traffic flow stability, and traffic throughput.

Model-based analyses and experimental results presented in this thesis show how string stability can be compromised by the network-induced effects on shared information between vehicles. The analyses provided bounds on tolerable transmission intervals and delays in face of scheduling constraints requiring network protocols. To achieve string stability for reduced inter-vehicle distances, the communication network needs to be able to guarantee smaller bounds on the delays. The analyses also show that a high sampling frequency may help to achieve string stability with relatively low inter-vehicle distances while tolerating larger delays. However, from a practical point of view, increasing the sampling frequency at which the wireless network operates may have counteracting effects. Namely, a larger sampling frequency may limit the number of vehicles that can operate reliably via the same network, hence also limiting the number of vehicles in a string, and may lead to larger network-induced delays due to increased chances of packet collisions. Therefore, reliable operation of a networked CACC system involves making multi-disciplinary design tradeoffs between the specifications for the vehicle following controller, network performance and string stability performance criteria. The presented modelling and analysis framework can be used as a design tool for the designer in making these tradeoffs.

7.2 Recommendations

As an extension of the presented work in this thesis, several directions for future research can be highlighted.

In the interconnected vehicle string model in Chapter 2, we considered a PD-type vehicle following controller where the additional CACC input has been implemented in a feedforward fashion and uses only the information received (wirelessly) from the directly preceding vehicle. However, the modelling approach would also allow for different control strategies and communication with more than one vehicle. Communication with more than one vehicle can further improve the vehicle following performance and the string stability properties by providing the ability to respond to arising situations further ahead in the vehicle platoon. Besides, information transmitted from multiple sources would improve robustness to wireless communication imperfections by allowing to compensate for losses and delays. A more general CACC synthesis approach in an NCS framework that allows co-design of controller and information flow structures and which also incorporates the network effects during the design process (e.g. a priori guarantee string stability in the presence of certain network deficiencies) can reveal these potential benefits to its fullest.

In Chapter 4, we demonstrated the strength of the modelling and analysis framework by two possible use-scenarios based on the synchronous sampled-data (SD) network setting and the Round Robin (RR)-type network although we believe that other scenarios for the communication protocol should also be analysed. The framework presented in this thesis is set up in a general manner such that different communication structures and network topologies can be envisioned as well. Moreover, incorporating other network-induced imperfections (such as packet dropouts) and constraints, apparent in a CACC controlled vehicle string, in the proposed modelling and analysis framework, would also be of interest.

Furthermore, the potential benefits of cooperative driving can be further exploited by also taking control of the lateral dynamics of the vehicles via automated steering. This would allow to extend the operation of platooning systems to multiple-lanes and allow the implementation of automated vehicles in a broader range of traffic scenarios in order to eliminate undesired disturbances that might be introduced in scenarios such as highway merging, platoon joining, and splitting. This would require the consideration of propagation of disturbances in two dimensions, which is captured by the notion of *mesh stability*.

The potential of these Intelligent Transportation Systems (ITS) technologies can be exploited to their full extent when all participating vehicles are equipped. However, the deployment of these technologies and their acceptance by society will naturally only develop over time, where in the intermediate phase, automated and manually driven vehicles will share the same traffic infrastructure. For this matter, research considering the feasibility of these technologies in a

partially equipped traffic is important for roll-out of this technology in practice.

Finally, extensive experimental studies should be conducted in the light of the aforementioned conclusions and research directions in order to test the practical feasibility of CACC systems in real traffic conditions (on a larger scale) before such systems can be deployed. Especially, the effects of increased network traffic and its effects on system performance when a large number of vehicles share the same network (which would be the case in real traffic) require a careful consideration.

Bibliography

[1] IEEE 1609 - Family of standards for Wireless Access in Vehicular Environments (WAVE), 2009.

[2] Rules & technology document (available online: http://www.gcdc.net), Februari 2011. Grand Cooperative Driving Challenge organised by TNO.

[3] A. Alam. *Fuel-Efficient Distributed Control for Heavy Duty Vehicle Platooning*. PhD thesis, KTH, Sweden, 2011.

[4] A.A. Alam, A. Gattami, and K.H. Johansson. An experimental study on the fuel reduction potential of heavy duty vehicle platooning. In *Intelligent Transportation Systems (ITSC), 2010 13th International IEEE Conference on*, pages 306 –311, Madeira Island, Portugal, Sept. 2010.

[5] M.J. Allen, J. Ryan, C.E. Hanson, and J.F. Parle. *String stability of a linear formation flight control system*. National Aeronautics and Space Administration, Dryden Flight Research Center, 2002.

[6] H. Bae, J. Ryu, and J. Gerdes. Road grade and vehicle parameter estimation for longitudinal control using GPS. Technical report, Stanford University, CA,USA, 2001.

[7] A. Bemporad, M. Heemels, and M. Johansson. *Networked control systems*, volume 406 of *Lecture notes in control and information sciences*. Springer, 2010.

[8] C. Bonnet and H. Fritz. Fuel reduction in a platoon: Experimental results with two electronically coupled trucks at close spacing. *SAE paper 2000 - 01 - 3056*, 2000.

[9] A. Bose and P. Ioannou. Analysis of traffic flow with mixed manual and intelligent cruise control vehicles: Theory and experiments. Technical report, California PATH Research Report, CA,USA, 2001.

[10] F. Browand, J. McArthur, and C. Radovich. Fuel saving achieved in the field test of two tandem trucks. Technical report, California PATH Research Report, CA,USA, July 2004.

[11] M.B.G. Cloosterman, N. van de Wouw, W.P.M.H. Heemels, and H. Nijmeijer. Stability of networked control systems with uncertain time-varying delays. *Automatic Control, IEEE Transactions on*, 54(7):1575–1580, 2009.

[12] R. D'Andrea and G.E. Dullerud. Distributed control design for spatially interconnected systems. *Automatic Control, IEEE Transactions on*, 48(9):1478–1495, 2003.

[13] M.C.F. Donkers. *Networked and event-triggered control systems*. PhD thesis, Eindhoven University of Technology, Netherlands, 2011.

[14] M.C.F. Donkers, W.P.M.H. Heemels, N. van de Wouw, and L. Hetel. Stability analysis of networked control systems using a switched linear systems approach. *Automatic Control, IEEE Transactions on*, 56(9):2101–2115, 2011.

[15] C. Ebenbauer, T. Raff, and F. Allgöwer. Dissipation inequalities in systems theory: An introduction and recent results. In *R. Jeltsch and G. Wanner (ed.), Invited Lectures of the International Congress on Industrial and Applied Mathematics 2007*, pages 23–42, Zurich, Switzerland, July 2009.

[16] J.A. Fax and R.M. Murray. Information flow and cooperative control of vehicle formations. *Automatic Control, IEEE Transactions on*, 49(9):1465–1476, 2004.

[17] R.E. Fenton. Automated highway system technology. In *Vehicular Technology Conference, 1980. 30th IEEE*, volume 30, pages 457–460, Dearborn, MI, USA, 1980.

[18] J. Figwer. Multisine transformationproperties and applications. *Nonlinear Dynamics*, 35(4):331–346, 2004.

[19] J.M. Fowler and R. D'Andrea. Distributed control of close formation flight. In *Decision and Control, 2002, Proceedings of the 41st IEEE Conference on*, volume 3, pages 2972–2977 vol.3, Las Vegas, NV, USA, 2002.

[20] H. Fujioka. Stability analysis for a class of networked/embedded control systems: A discrete-time approach. In *American Control Conference, 2008*, pages 4997–5002, Seattle, WA, USA, 2008.

[21] H. Fujioka. A discrete-time approach to stability analysis of systems with aperiodic sample-and-hold devices. *Automatic Control, IEEE Transactions on*, 54(10):2440–2445, 2009.

[22] H.N. Gao, T. Chen, and J. Lam. A new delay system approach to network-based control. *Automatica*, 44(1):39–52, 2008.

[23] Matías García-Rivera and Antonio Barreiro. Analysis of networked control systems with drops and variable delays. *Automatica*, 43(12):2054–2059, 2007.

[24] O. Gehring and H. Fritz. Practical results of a longitudinal control concept for truck platooning with vehicle to vehicle communication. In *Intelligent Transportation System, 1997. ITSC '97., IEEE Conference on*, pages 117–122, Boston, MA, USA, 1997.

[25] R. Goebel, R.G. Sanfelice, and A.R. Teel. Hybrid dynamical systems. *Control Systems, IEEE*, 29(2):28–93, 2009.

[26] G.H. Golub and C.F. Van Loan. *Matrix computations*, volume 3. The Johns Hopkins University Press, Baltimore, USA, 2012.

[27] L. Güvenç, I.M.C. Uygan, K. Kahraman, R. Karaahmetoğlu, I. Altay, M. Sentürk, M.T. Emirler, A.E.H. Karci, B.A. Güvenç, E. Altug, M.C. Turan, O.S. Tas, E. Bozkurt, U. Özgüner, K. Redmill, A. Kurt, and B. Efendioglu. Cooperative adaptive cruise control implementation of team mekar at the grand cooperative driving challenge. *Intelligent Transportation Systems, IEEE Transactions on*, 13(3):1062–1074, 2012.

[28] J.K. Hedrick, M. Tomizuka, and P. Varaiya. Control issues in automated highway systems. *Control Systems, IEEE*, 14(6):21–32, 1994.

[29] W.P.M.H. Heemels, A.R. Teel, N. van de Wouw, and D. Nešić. Networked control systems with communication constraints: Tradeoffs between transmission intervals, delays and performance. *Automatic Control, IEEE Transactions on*, 55(8):1781–1796, 2010.

[30] W.P.M.H. Heemels and N. van de Wouw. Stability and stabilization of networked control systems. In *Networked Control Systems*, Lecture notes in control and information sciences, pages 203–253. Springer, 2010.

[31] W.P.M.H. Heemels, N. van de Wouw, R. H. Gielen, M. C. F. Donkers, L. Hetel, S. Olaru, M. Lazar, J. Daafouz, and S. Niculescu. Comparison of overapproximation methods for stability analysis of networked control systems. In *Proceedings of the 13th ACM international conference on Hybrid systems: computation and control*, Stockholm, Sweden, April 2010.

[32] J.P. Hespanha, P. Naghshtabrizi, and Yonggang Xu. A survey of recent results in networked control systems. *Proceedings of the IEEE*, 95(1):138–162, 2007.

[33] L. Hetel, J. Daafouz, and C. Iung. Stabilization of arbitrary switched linear systems with unknown time-varying delays. *Automatic Control, IEEE Transactions on*, 51(10):1668–1674, 2006.

[34] S. Huang and W. Ren. Design of vehicle following control systems with actuator delays. *International Journal of Systems Science*, 28(2):145–151, 1997.

[35] P.A. Ioannou and C.C. Chien. Autonomous intelligent cruise control. *Vehicular Technology, IEEE Transactions on*, 42(4):657–672, 1993.

[36] M.E. Khatir and E.J. Davidson. Bounded stability and eventual string stability of a large platoon of vehicles using non-identical controllers. In *Decision and Control, 2004. CDC. 43rd IEEE Conference on*, volume 1, pages 1111–1116 Vol.1, Nassau, Bahamas, 2004.

[37] S. Klinge. *Stability Issues in Distributed Systems of Vehicle Platoons*. PhD thesis, Otto von Guericke Universitt Magdeburg, Germany, 2008.

[38] C. Langbort, R.S. Chandra, and R. D'Andrea. Distributed control design for systems interconnected over an arbitrary graph. *Automatic Control, IEEE Transactions on*, 49(9):1502–1519, 2004.

[39] C. Langbort and R. D'Andrea. Distributed control of spatially reversible interconnected systems with boundary conditions. *SIAM journal on control and optimization*, 44(1):1–28, 2005.

[40] W. Lawrenz. *CAN system engineering: from theory to practical applications*, volume 1. Springer, 1997.

[41] W.S. Levine and M. Athans. On the optimal error regulation of a string of moving vehicles. *Automatic Control, IEEE Transactions on*, 11(3):355–361, 1966.

[42] X. Liu, A. Goldsmith, S.S. Mahal, and J.K. Hedrick. Effects of communication delay on string stability in vehicle platoons. In *Proceedings of the IEEE Intelligent Transportation Systems Conference*, pages 625–630, Oakland,CA,USA, 2001.

[43] X. Lu and J. Hedrick. Longitudinal control design and experiments for heavy-duty trucks. In *Proceedings of the 2003 American Control Conference*, pages 36–41, Denver, CO, USA, 2003.

[44] X. Lu, S. Shladover, and J. Hedrick. Heavy-duty truck control: Short inter-vehicle distance following. In *Proceedings of the 2004 American Control Conference*, Boston, MA, USA, 2004.

[45] J. Martensson, A. Alam, S. Behere, M.A.A. Khan, J. Kjellberg, Kuo-Yun Liang, H. Pettersson, and D. Sundman. The development of a cooperative heavy-duty vehicle for the GCDC 2011: Team Scoop. *Intelligent Transportation Systems, IEEE Transactions on*, 13(3):1033–1049, 2012.

[46] S.M. Melzer and B. Kuo. A closed-form solution for the optimal error regulation of a string of moving vehicles. *Automatic Control, IEEE Transactions on*, 16(1):50–52, 1971.

[47] R.M. Murray. Recent research in cooperative control of multivehicle systems. *Journal of dynamic systems, measurement, and control*, 129(5):571–583, 2007.

[48] P. Naghshtabrizi, J.P. Hespanha, and A.R. Teel. Exponential stability of impulsive systems with application to uncertain sampled-data systems. *Systems & Control Letters*, 57(5):378–385, 2008.

[49] G. Naus, R. Vugts, J. Ploeg, M. Molengraft, and M. Steinbuch. String-stable cacc design and experimental validation: A frequency-domain approach. *Vehicular Technology, IEEE Transactions on*, 59:4268–4279, 2010.

[50] D. Nešić and A.R. Teel. Input-to-state stability of networked control systems. *Automatica*, 40(12):2121–2128, 2004.

[51] D. Nešić and A.R. Teel. Input-output stability properties of networked control systems. *Automatic Control, IEEE Transactions on*, 49(10):1650–1667, 2004.

[52] M.R.I. Nieuwenhuijze, T. van Keulen, S. Öncü, B. Bonsen, and H. Nijmeijer. Cooperative driving with a heavy-duty truck in mixed traffic: Experimental results. *Intelligent Transportation Systems, IEEE Transactions on*, 13(3):1026–1032, 2012.

[53] S. Öncü, J. Ploeg, N. van de Wouw, and H. Nijmeijer. Cooperative adaptive cruise control: Network-aware modelling and analysis. *IEEE Transactions on Intelligent Transportation Systems*, submitted.

[54] S. Öncü, N. van de Wouw, W.P.M.H. Heemels, and H. Nijmeijer. String stability of interconnected vehicles under communication constraints. In *Decision and Control (CDC), 2012 IEEE 51st Annual Conference on*, pages 2459–2464, Hawaii, USA, 2012.

[55] S. Öncü, N. van de Wouw, and H. Nijmeijer. Cooperative adaptive cruise control: Tradeoffs between control and network specifications. In *Intelligent Transportation Systems (ITSC), 2011 14th International IEEE Conference on*, pages 2051–2056, Washington,USA, 2011. IEEE.

[56] A. Pant, P. Seiler, and K. Hedrick. Mesh stability of look-ahead interconnected systems. *Automatic Control, IEEE Transactions on*, 47(2):403–407, 2002.

[57] R. V. Patel and N. Munro. *Multivariable system theory and design*, volume 4. Oxford, Pergamon Press International Series on Systems and Control, 1982.

[58] S. Patterson, B. Bamieh, A. El Abbadi, and M. Jovanovic. On the feasibility of large-scale automated highways. In *Proceedings of the 5th Annual International Conference on Mobile and Ubiquitous Systems: Computing, Networking, and Services*, page 3. ICST (Institute for Computer Sciences, Social-Informatics and Telecommunications Engineering), 2008.

[59] R. Pintelon and J. Schoukens. *System identification: a frequency domain approach*. Wiley-IEEE Press, 2004.

[60] J. Ploeg, J. de Jongh, B. Netten, and R. van Katwijk. Challenging aspects of time-critical cooperative driving, 2010.

[61] J. Ploeg, B.T.M. Scheepers, E. van Nunen, N. van de Wouw, and H. Nijmeijer. Design and experimental evaluation of cooperative adaptive cruise control. In *Intelligent Transportation Systems (ITSC), 2011 14th International IEEE Conference on*, pages 260–265, Washington, USA, 2011.

[62] J. Ploeg, S. Shladover, H. Nijmeijer, and N. van de Wouw. Introduction to the special issue on the 2011 grand cooperative driving challenge. *Intelligent Transportation Systems, IEEE Transactions on*, 13(3):989–993, 2012.

[63] M.B.G. Posthumus-Cloosterman. *Control over communication networks: modeling, analysis, and synthesis*. PhD thesis, Eindhoven University of Technology, Netherlands, 2008.

[64] R. Rajamani and S.E. Shladover. An experimental comparative study of autonomous and co-operative vehicle-follower control systems. *Transportation Research Part C: Emerging Technologies*, 9(1):15–31, 2001.

[65] R. Reinders, M. van Eenennaam, G. Karagiannis, and G. Heijenk. Contention window analysis for beaconing in vanets. In *Wireless Communications and Mobile Computing Conference (IWCMC), 2011 7th International*, pages 1481–1487, Istanbul, Turkey, 2011.

[66] Y. Sai Krishna, S. Darbha, and K. R. Rajagopal. Information flow and its relation to the stability of the motion of vehicles in a rigid formation. In *American Control Conference, 2005. Proceedings of the 2005*, pages 1853–1858 vol. 3, Portland, OR, USA, 2005.

[67] A. Sala. Computer control under time-varying sampling period: An LMI gridding approach. *Automatica*, 41(12):2077–2082, 2005.

[68] K. Santhanakrishnan and R. Rajamani. On spacing policies for highway vehicle automation. *Intelligent Transportation Systems, IEEE Transactions on*, 4(4):198 – 204, dec. 2003.

[69] A. van der Schaft. *L2-Gain and Passivity in Nonlinear Control*. Springer-Verlag New York, Inc., 1999.

[70] P. Seiler and R. Sengupta. Analysis of communication losses in vehicle control problems. In *American Control Conference, 2001. Proceedings of the 2001*, volume 2, pages 1491–1496, Arlington, VA, USA, 2001. IEEE.

[71] E. Shaw and J. Hedrick. String stability analysis for heterogeneous vehicle strings. New York, USA, July 2007.

[72] S.E. Shladover. Longitudinal control of automated guideway transit vehicles within platoons. *Journal of Dynamic Systems, Measurement and Control, vol. 100 no. 4*, 1978.

[73] S.E. Shladover, C.A. Desoer, J.K. Hedrick, M. Tomizuka, J. Walrand, Wei-Bin Zhang, D.H. McMahon, Huei Peng, S. Sheikholeslam, and N. McKeown. Automated vehicle control developments in the PATH program. *Vehicular Technology, IEEE Transactions on*, 40(1):114–130, 1991.

[74] S. Stankovic, D. Stipanovic, and D. Siljak. Decentralized dynamic output feedback for robust stabilization of a class of nonlinear interconnected systems. *Automatica*, 43:861–867, May 2007.

[75] S.S. Stankovic, S.M. Mladenovic, and D.D. Siljak. Headway control of a platoon of vehicles: inclusion principle and lq optimization. In *Decision and Control, 1998. Proceedings of the 37th IEEE Conference on*, volume 3, pages 3204–3205 vol.3, Tampa, FL, USA, 1998.

[76] S.S. Stankovic, M.J. Stanojevic, and D.D. Siljak. Decentralized overlapping control of a platoon of vehicles. *Control Systems Technology, IEEE Transactions on*, 8(5):816–832, 2000.

[77] D. Swaroop and J. Hedrick. Constant spacing strategies for platooning in automated highway systems. *Transactions of the ASME*, 121:462–470, 1996.

[78] D. Swaroop and J. Hedrick. String stability of interconnected systems. *IEEE Transactions on Automatic Control*, 41:349–357, 1996.

[79] D. Swaroop and J.K. Hedrick. Constant spacing strategies for platooning in automated highway systems. *Journal of dynamic systems, measurement, and control*, 121(3):462–470, 1999.

[80] D. Swaroop, J.K. Hedrick, C. Chienm, and P. Ioannou. A comparison of spacing and headway control laws of automatically controlled vehicles. *Vehicle System Dynamics*, 23:597–625, 1994.

[81] B. Van Arem, C.J.G. van Driel, and R. Visser. The impact of cooperative adaptive cruise control on traffic-flow characteristics. *Intelligent Transportation Systems, IEEE Transactions on*, 7(4):429–436, 2006.

[82] N. van de Wouw, P. Naghshtabrizi, M.B.G. Cloosterman, and J.P. Hespanha. Tracking control for sampled-data systems with uncertain time-varying sampling intervals and delays. *International Journal of Robust and Nonlinear Control*, 20(4):387–411, 2010.

[83] N. van de Wouw, D. Nešić, and W.P.M.H. Heemels. A discrete-time framework for stability analysis of nonlinear networked control systems. *Automatica*, 48(6):1144–1153, 2012.

[84] N. van de Wouw, D. Nešić, and W.P.M.H. Heemels. Stability analysis for nonlinear networked control systems: Discrete-time approach. In *Proc. IEEE Conf. on Decision and Control*, pages 7557–7563, Atlanta, GA, USA, 2010.

[85] E. van Nunen, M.R.J.A.E. Kwakkernaat, J. Ploeg, and B.D. Netten. Cooperative competition for future mobility. *Intelligent Transportation Systems, IEEE Transactions on*, 13(3):1018–1025, 2012.

[86] A. Vinel, Y. Koucheryavy, S. Andreev, and D. Staehle. Estimation of a successful beacon reception probability in vehicular ad-hoc networks. In *Proceedings of the 2009 International Conference on Wireless Communications and Mobile Computing: Connecting the World Wirelessly*, IWCMC '09, pages 416–420, New York, NY, USA, 2009. ACM.

[87] T.C. Yang. Networked control system: A brief survey. *IEE Proceedings-Control Theory and Applications*, 153(4):403–412, 2006.

[88] Liqian Zhang, Yang Shi, Tongwen Chen, and Biao Huang. A new method for stabilization of networked control systems with random delays. *Automatic Control, IEEE Transactions on*, 50(8):1177–1181, 2005.

[89] Wei Zhang, M.S. Branicky, and S.M. Phillips. Stability of networked control systems. *Control Systems, IEEE*, 21(1):84–99, 2001.

Summary

String Stability of Interconnected Vehicles: Network-aware Modelling, Analysis and Experiments

The ever increasing demand for mobility in today's life imposes additional burden on the existing ground transportation infrastructure for which a feasible solution in the near future lies in a more efficient use of currently available means of transportation. In today's traffic, limited human perception of traffic conditions and human reaction characteristics constrain the lower limits of achievable safe inter-vehicle distances. Besides, erroneous human driving characteristics may cause traffic flow instabilities which result in so-called shockwaves. In dense traffic conditions, a single driver overreacting to a momentary disturbance (e.g. a slight deceleration of the predecessor) can trigger a chain of reactions in the rest of the follower vehicles. The amplification of such a disturbance can bring the traffic to a full stop kilometers away from the disturbance source and cause traffic jams for no apparent reason.

Intelligent Transportation Systems (ITS) technologies can significantly contribute to improved traffic flow stability, throughput, and safety. Cooperative Adaptive Cruise Control (CACC), being one of the promising ITS technologies, extends the currently available Adaptive Cruise Control (ACC) with the addition of information exchange between vehicles through Vehicle-to-Vehicle (V2V) wireless communication. The general objective of a CACC system is to pack the driving vehicles together as tightly as possible in order to increase traffic flow while preventing amplification of disturbances throughout the string of vehicles, the latter of which is known as string instability.

Wireless information exchange between vehicles provides means of overcoming sensory limitations of human or ACC operated vehicles. Significant improvements over existing ACC technology can be achieved already with rela-

tively simple control algorithms and communication structures, but real-life implementation requires consideration of the constraints imposed by the wireless communication. In the scope of CACC, control over a wireless communication network is the enabling technology that makes CACC realizable; however, very few studies of CACC consider the imperfections that are introduced by the network. Given the fact that multiple nodes (vehicles) share the same medium with a limited bandwidth and capacity, wireless communication introduces network-induced imperfections such as transmission delays and packet losses. The impact of these imperfections on string stability requires a careful analysis and tradeoffs between CACC performance and network specifications need to be made for achieving desired performance under these network-induced constraints.

In this thesis, the design of a CACC system is approached from a Networked Control System (NCS) perspective and a novel NCS modelling framework for interconnected vehicle strings is presented. The interconnected vehicle string model arises from the dynamical coupling of a cascade of CACC vehicles, each of which is controlled to maintain a desired distance to its predecessor. In this model, two types of data employed in the CACC controller are distinguished according to the way they are being transferred, i.e. either locally sensed or wirelessly communicated information. This approach allows to cast the interconnected system dynamics with wireless communication constraints into a NCS model that incorporates the effects of sample-and-hold, transmission frequency, and network delays.

This modelling framework is extended with analysis tools for string stability in the presence of network effects. These analyses can provide the designer with guidelines for making multidisciplinary tradeoffs between control and network specifications and support the design of CACC systems that are robust to uncertainties introduced by wireless communication. The framework is set up in a general manner such that the inclusion of scheduling constraints induced by the wireless communication between vehicles can be incorporated as well. Using these analysis tools, the dependency of string stability on network-induced effects is studied. The analyses provide bounds on the maximum allowable transmission intervals (MATI) and maximum allowable delays (MAD) while string stability is still guaranteed.

Moreover, the validity of the presented analysis framework is demonstrated via experiments performed with CACC-equipped prototype passenger vehicles in a homogeneous string. Experimental results show that the developed NCS modelling framework captures the dependency of string stability on network-induced effects and confirm the string stable operation conditions obtained by model-based analyses. Furthermore, the CACC algorithm was implemented on a heavy-duty truck and tested during the Grand Cooperative Driving Challenge (GCDC) in a multi-vendor setting where participating teams tested their CACC-equipped vehicle and benchmarked it to the CACC vehicles of other competitors. These tests show improved string stable behaviour of the truck within

a heterogeneous vehicle string and the effects of wireless communication losses and vehicle limitations on string stability can also be addressed.

Acknowledgements

This dissertation is the result of a long and challenging journey, upon which many people have contributed and provided their support. I wouldn't have been able to carry out this challenging task without the support of the people to whom I would like to express my sincere gratitudes.

First, I would like to express my thanks to my supervisors Henk Nijmeijer, Maurice Heemels, and Nathan van de Wouw for their guidance, support, and trust during the research that has led to this dissertation. Being guided by such distinguished scientists has been a privilege for me. Dear Henk, thanks for being my advisor and giving me the opportunity to work in your group. I am grateful for your trust and valuable advice throughout this research. Dear Maurice, thank you for all your contributions, pleasant discussions, and also for sharing your enthusiasm and creativity with me. Dear Nathan, your scientific conciseness and high level of standards have raised the quality of this thesis far beyond the limits that I could have achieved by myself. I have always admired your sharpness and attention to detail. I consider myself fortunate for having the chance to work directly with you and getting your support at every stage of producing this dissertation. Also, many thanks for your determination and supportive attitude which have made it possible for me to continue this research during the more challenging times.

I would also like to thank Levent Güvenç, Carlos Canudas-de-Wit, Bart de Schutter, and Paul van den Bosch for being part of my Ph.D. committee and for giving their valuable comments on the draft version of this dissertation. Special thanks to Levent Güvenç, for being my inspiration to pursue a Ph.D. study and expanding my horizons.

I would also like to thank HTAS and the Connect and Drive project partners for the funding and the collaboration during this research. I would like to express special thanks to the TNO Integrated Vehicle Safety Group for developing and making the prototype vehicles available for the experimental results which are presented in this dissertation. Especially, I would like to thank Jeroen Ploeg,

for his inspiring and pleasant collaboration in this project. Jeroen, besides your in-depth technical knowledge and experience, your positive attitude and sense of humour made even some tough and frustrating times (that are also inherently part of a Ph.D. study) more enjoyable and easier to move forward.

Thanks to all the colleagues at the Eindhoven University of Technology, in the DCT and CST groups, with whom we had chats at the coffee corner during many small breaks. Special thanks to Tom Gommans, Nick Bauer, and Menno Lauret for their friendship in- and outside working hours. You guys made me feel more at home here and exchanging some interesting conversations around drinks has made this journey more enjoyable. Thank you Tom, for the fresh air breaks and talks during the day around shared interests on bikes, road trips, and gadgets; Nick, for all the nice conversations, introducing me to the world of craft breweries, and for your creative touch to the design of the thesis cover; and Menno, for the interesting talks about books, philosopher's, and Istanbul which helped me to refresh my memories of my beloved city every now and then. I would also like to thank Matthijs van Berkel and Bas van Loon, for some off-work enjoyable times and hang-outs in the city.

Next, I would also like to thank my office-mates David Rijlaarsdam, Rick van der Maas, Stan van der Meulen, Alper Denasi, Jonatan Pena Ramirez, Frank Boeren, and Tom Oomen. David, thank you especially for the valuable discussions on designing the experiments which are presented in this thesis. Also thanks to the neighbour office-mates Irmak Aladağlı and Robbert van Herpen.

A Ph.D. study also provides an invaluable opportunity to meet many new people from all around the world. To get to know different cultures, exchanging ideas, appreciating differences, respecting diversity while enjoying common interests and having fun together. I am grateful for the company of many friends with whom I shared memorable moments outside the work environment: Bahadır, Ali Can, Başar, Gözde, Döndü, Bahar, Martin, Sinan, Buket, Camille, Dario, Giulia, Michelle; friends around Netherlands: Akın, Dicle, Yunus, Ezgi, Erman, Ali; and my dear friends back in Turkey: Özgür, Ece, Ekim, Tuğrul, Umut and Volkan. I would also like to thank Tuğrul, Özgül, and İnan Çölmekçi, for their welcoming big heart and being part of my family.

I would like to express my deepest gratitude and love to my parents Sultan and Orhan Öncü. Mom and dad, you have shaped my mind and personality. Without your endless support, love, and encouragement I wouldn't have made this so far. Special thanks also go to my sister Eylem. Sister, you mean the world to me and I will always be there for you as you have been for me. Finally, my dearest, Ceylan, your support and love have been my life energy. I am very lucky for having you by my side while going through this and I hope I can be such a great life companion to you as you are for me.

Sinan Öncü
December 8, 2013
Eindhoven, The Netherlands

Curriculum Vitae

Sinan Öncü was born on April 12, 1981 in Manisa, Turkey. He received his Bachelor of Science degree in Electronics and Telecommunication Engineering at Istanbul Technical University (ITU), Istanbul, Turkey in 2005. His B.Sc. graduation project entitled "Autonomous Parallel Parking of a Car-Like Mobile Robot" was awarded the best graduation project award in both ITU R&D Projects Competition and Chamber of Electrical Engineers (EMO) Graduation Projects Competition, in 2005. Subsequently, he started his Master of Science studies at the same university in the department of Mechatronics Engineering. During his master's study, he worked as research assistant at ITU Mechatronics Research Labs (MEKAR). He received his Master's degree (high honour) in 2008. His master's thesis was entitled "Active Steering Controller Design".

In June 2009, Sinan started his PhD research in the Dynamics and Control group at the department of Mechanical Engineering of Eindhoven University of Technology, working on network-aware modelling and analysis of string stability properties of interconnected vehicles. The results of his PhD research are presented in this dissertation.